Investigating internal variability of surface weather during weather regimes

Master's Thesis in Meteorology
by

Judith Gerighausen

April 2024

INSTITUTE OF METEOROLOGY AND CLIMATE RESEARCH
KARLSRUHE INSTITUTE OF TECHNOLOGY (KIT)

Advisor:	Prof. Dr. Peter Knippertz
Co-Advisor:	Prof. Dr. Joaquim Pinto
Supervisors:	Dr. Joshua Dorrington, Dr. Marisol Osman

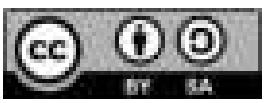

Abstract

Weather regimes are able to describe the large-scale atmospheric circulation in the mid-latitudes by using a few circulation states. Each weather regime has its own specific influence on the surface weather depending on the region and season. This fact can be used to study the influence of weather on renewable energy and which regimes are favorable for power generation and which are not. In addition, weather regimes are used to close the gap between medium-term weather forecasts covering around ten days and seasonal weather forecasts. The previous studies on the Atlantic-European weather regimes use average values for the meteorologically important variables of surface temperature, wind speed, precipitation and solar radiation, which already provide a good overview of the weather to be expected for the individual regimes. However, the average values do not provide any information on how much the meteorological variables vary during an individual weather regime. Unobserved variability means not only a financial risk for users but, in extreme cases, a risk to the health and integrity of infrastructure. In this master's thesis, various methods are used to show the wide range of weather variability during different regimes and times of the year in different regions. Furthermore, it is shown how the atmospheric dynamics change with observed variability and how statements about the variability can be made with the use of the weather regime index.

It's important to note that the relative range of variability is greater in summer than in winter, while the absolute variability is greater in winter. This is due to major differences between regimes characterized by high pressure, which tend to have high variability, especially in summer, and regimes characterized by low pressure, which have regions with low variability in winter, representing windows of opportunities for weather forecasting with weather regimes. However, the reverse can also occur. Yet, for almost every region and variable, there is at least one regime under which the variability is very limited. The variability of a regime can be effectively understood through the changes in atmospheric circulation, which can deviate considerably from its mean value during a regime. The changing parameters in wind direction and, thus, the advected air masses, as well as the radiation balance, provide a clear explanation for the observed, unusual anomalies. The weather regime index, which indicates the strength of the active and all other secondary regimes, shows the unusual weather conditions during a regime in different ways. These are often the result of a combination of temporal shifts of the index, changes in regime strength and influences from secondary regimes. In this case, the changed circulation projects into a secondary regime. How well these influencing factors and, in particular, the secondary regimes explain the changes depends on the season as well as the variable. The influencing factors can well explain temperature variability, while wind speed and precipitation appear less clear, especially in summer.

The knowledge gained here about the general variability of meteorological variables during the regimes represents an important expansion of knowledge about weather regimes. It shows where

the variability is low and, thus, where the average value is likely to occur and where it is not. The knowledge of the influencing factors can be used to better characterize and predict the surface weather during a regime. These results provide a starting point for further research, for example on the temporal correlation of variability between different countries and variables, as well as the influence of weather variability on renewable energies, which can only be estimated based on these results.

Zusammenfassung

Wetterregime sind in der Lage die großskalige atmosphärische Zirkulation in den mittleren Breiten mittels weniger Zirkulationszustände wiederzugeben. Jedes Wetterregime hat dabei seinen eigenen, individuellen Einfluss auf das Bodenwetter je nach Region und Jahreszeit. Diese Tatsache kann dafür genutzt werden, den Einfluss des Wetters auf erneuerbare Energien zu untersuchen und um zu ermitteln, welche Regime günstige Umstände für die Stromerzeugung bergen und welche nicht. Darüber hinaus werden Wetterregime genutzt, um die Lücke zwischen mittelfristiger Wettervorhersage über etwa zehn Tage und saisonaler Wettervorhersage zu schließen. Die bisherigen Studien zu den Atlanto-europäsichen Wetterregime nutzen Durchschnittswerte für die meteorologisch wichtigen Variablen Bodentemperatur, Windgeschwindigkeit, Niederschlagsmenge und Sonneneinstrahlung, die bereits einen guten Überblick über das zu erwartende Wetter für die einzelnen Regime liefern. Aus den Durchschnittswerten gehen jedoch keine Informationen hervor, wie stark die meteorologischen Variablen während eines einzelnes Wetterregime variieren. Unbeachtete Variabilität bedeutet nicht nur ein finanzielles Risiko für Nutzer, sondern im Extremfall ein Risiko für die Gesundheit und Unversehrtheit von Infrastruktur. In dieser Masterarbeit wird mittels verschiedener Methoden gezeigt, wie groß die Spannweite der Variabilität des Wetters während verschiedener Regime, zu verschiedenen Jahreszeiten in unterschiedlichen Regionen ist. Außerdem wird gezeigt, wie sich die Variabilität in Änderungen der atmosphärischen Dynamik wiederspiegelt und wie mittels des Wetterregimeindex Aussagen über die Variabilität gemacht werden können.
Im Allgemeinen ist festzuhalten, dass die relative Spannweite der Variabilität im Sommer größer ist als im Winter, aber die absolute Variabilität im Winter. Hierbei zeigen sich große Unterschiede zwischen hochdruckgeprägten Regimen, die besonders im Sommer zu großer Variabilität neigen und tiefdruckgeprägten Regimen, die im Winter Regionen mit geringer Variabilität aufweisen, welche Gelegenheiten zur besseren Wettervorhersage mit Wetterregimen darstellen. Nichtsdestotrotz gibt es auch die umgekehrten Fälle. Die Variabilität eines Regimes lässt sich gut durch die Veränderungen der atmosphärischen Zirkulation ergründen. Hierbei kann die Zirkulation beträchtlich von ihrem Mittelwert während eines Regimes abweichen. Die sich ändernden Parameter in Windrichtung und somit der adverhierten Luftmassen sowie die Strahlungsbilianz erklären die beobachteten, ungewöhnlichen Anomalien sehr gut. Im Wetterregimeindex, welcher die Stärke des aktiven und aller weiteren, zweitrangingen Regime angibt, stellen sich die ungewöhnlichen Wetterlagen während eines Regimes verschieden dar. Diese sind oft ein Resultat aus einer Kombination aus zeitlicher Verschiebung des Index, Änderungen der Regimestärke sowie Einflüssen von zweitrangigen Regimen (engl. secondary regimes). Dabei projiziert die geänderte Zirkulation in ein zweitrangiges Regime. Wie gut diese Einflussfaktoren und insbesondere die zweitrangigen Regime die Änderungen erklären, ist ebenso von der Jahreszeit abhängig wie von der Variable. So kann festgestellt werden, dass sich Variabilität der Temperatur gut mit den Einflussfaktoren erklären

lassen, während Windgeschwindigkeit und Niederschlag weniger klar erscheinen, besonders im Sommer.
Die hier erlangten Kenntnisse über die allgemeine Variabilität der meteorologischen Variablen während der Regime stellt eine wichtige Erweiterung des Wissens über Wetterregime dar. Es wird gezeigt, wo die Variabilität gering und somit das Eintreffen des Durchschnittswerts wahrscheinlich ist und wo nicht. Die Kenntnisse über die Einflussfaktoren können genutzt werden, um das Bodenwetter während eines Regimes besser zu charakterisieren und vorherzusagen. Diese Ergebnisse stellen einen Anknüpfungspunkt für weitere Forschung dar, beispielsweise zur zeitlichen Korrelation der Variabilität zwischen verschiedenen Ländern und Variablen, ebenso wie der Einfluss der Wettervariabilität auf die Erneuerbaren Energien, der anhand dieser Ergebnisse nur abgeschätzt werden kann.

Contents

1 Introduction

As carbon neutrality becomes increasingly important and is pushed forward with the European Green Deal (Commission, 2019), renewable energy sources (from now on renewables), most notably solar power and wind power, become of increasing importance. Not only do they have to replace conventional power sources such as coal, oil, and power plants fired by natural gas, but renewables also have to cover increasing electricity consumption (Staffell & Pfenninger, 2018). Demand is rising because processes and devices formerly powered by fossil sources are now converted to be electrically driven, such as cars and heating, as well as industrial processes. Steel production or processing of chemicals can be very power-consuming and is still mainly fired by conventional energy sources. Unlike conventional power plants, renewables cannot simply be switched on when needed. Renewables are subject to natural weather variability. Their increasing deployment means that the power grid is not only weather-dependent on the demand side via temperature anymore but also on the production side via wind speed, cloud cover, and, to a lesser extent, precipitation in the case of hydrological power plants. With increasing installations of renewables, the variability of weather conditions will have an increasing impact on the power system (Bloomfield et al., 2016). For example, by 2030, Great Britain's installed capacity of renewables could cover from 0 to 100% of the energy demand, highlighting the large variability (Staffell & Pfenninger, 2018) and Germany's share of renewables reached 52% in 2023 and is planned to reach 80% by 2030 (Bundesregierung, 2024). Weather and climate variability means risks and challenges like over- or underproduction and sudden in- or decrease of energy generation, also called ramps, while operating a power grid (Cannon et al., 2015). To avoid energy shortfall or overproduction, energy is traded across Europe on various time scales, from hours and intra-day trading to trading days and months in advance. Good weather forecasts are needed to keep costs low and ensure the power grid's stability at all times. Like the trading time scales, forecasts must cover these very different time scales. Short- and medium-term forecasts up to several days, driven by initial atmospheric conditions, and seasonal forecasts, driven by initial and boundary conditions, have skillful predictive power (White et al., 2017). The best skill is provided by a forecast covering only very few days and decreasing with the number of forecasted days, and a seasonal forecast has a medium skill. Challenging is the prediction of weather that falls in the gap between the medium-range and seasonal forecast, where fast-changing initial and slowly evolving boundary conditions are essential. This gap is also known as the predictability desert. Here, the forecasting skill is much worse than that of the other two types of forecasts.

One approach to bridge this gap is the use of quasi-stationary, recurrent and persistent flow patterns in the atmosphere, also known as weather regimes (WRs) (Cassou, 2008; Grams et al., 2017; Hertig & Jacobeit, 2014; J. C. K. Lee et al., 2020; Messori & Dorrington, 2023; Michelangeli et al., 1995). Weather regimes are a tool to order the chaotic nature of the mid-latitude troposphere

into a manageable number of discrete states associated with typical weather characteristics for each regime near the surface. When using WRs as a forecasting tool, properly understanding their behavior is especially important. Although there is no unique way to define WRs, they have nevertheless been extensively studied, both as purely dynamical features and in terms of their surface impact on variables such as (extreme) temperature, wind speed or precipitation (e.g. Plaut and Simonnet (2001), Robertson and Ghil (1999), Ullmann et al. (2014), Yiou and Nogaj (2004), and Yiou et al. (2008)). A more detailed description of the impacts of WRs is given in chapter 2. Also studied is how WRs impact renewable energy output. Zonally symmetric regimes cause high wind speeds and above-average wind power production around the North Sea, while regimes that go along with blocking conditions in the atmosphere at the high latitudes in the North Atlantic and western Europe - relocating the mean zonal flow - reduce power production around the North Sea and enhance it around the Mediterranean (Grams et al., 2017; van der Wiel, Bloomfield, et al., 2019). Solar power behaves conversely, with peak production during clear-skied blocking events (Mühlemann et al., 2022). This anti-correlation in energy variables across Europe poses challenges and opportunities for managing the energy output, as it decreases volatility.
WRs have become of interest in recent decades and are well-studied, especially in Europe and North America. It is not only studied how WRs influence surface weather on average and how they impact the energy sector but also by what WRs are influenced. Beerli and Grams (2019), Charlton-Perez et al. (2018), and Domeisen et al. (2020) studied the impact of the stratosphere on the European WRs, Cassou (2008) the influence of the Madden-Julian oscillation and Madonna et al. (2017) the interaction of the jet stream with WRs. Even the preferred transitions between North American and European weather regimes have recently been investigated by Messori and Dorrington (2023).

However, there has been no investigation of the internal variability of surface weather within the regimes. So far, it is only investigated how much of the total atmospheric variance is explained by regimes, varying from 60-90% depending on the regime definition, situation and season (Grams et al., 2020). Observations have been made that the weather during a weather regime does not always match the average values. In fact, sometimes they are very dissimilar, with the opposite surface weather anomalies to the average regime value. Comparable results have been found for explaining certain types of weather with the variability of the North Atlantic Oscillation (NAO) (Beerli & Grams, 2019). This is a potential pitfall for users of weather regimes and weather regime predictions since it poses security and health risks in the case of extreme hot/windy/wet weather conditions or economic risks, especially in agriculture. A wrong forecast can lead to high losses. The energy sector faces special risks such as wrongly forecasted high/low energy production by renewables, which, especially in the latter case, can lead to an overload of power plants if not quickly counteracted. Furthermore, overproduction and unexpectedly low demand can lead to a price drop and substantial financial losses. As a last point, extreme weather can affect and damage the power grid, leading to (regional) power outages. Therefore, a good weather forecast is needed. Since WRs are used to bridge the predictability desert between medium-range and long-term forecasts and WRs show predictability skill (Büeler et al., 2021; Grams et al., 2020), it is essential to gain the missing knowledge of the occurring surface weather variability within the weather regimes. This is what this master's thesis aims to do for the North-Atlantic-European WRs defined

by Grams et al. (2017). Therefore, three questions are addressed:

- How large is intra-regime variability in surface weather?
- How can atmospheric dynamics explain intra-regime variability?
- How can the variability be accounted for within the weather regime framework?

To answer the listed questions, this work is structured as follows. In chapter 2, an overview of the weather regime framework, a summary of weather impacts of regimes, and its importance to energy meteorology will be given. Chapter 3 provides an overview of the data and methods used to obtain the results, discussed in chapter 4 by first addressing the mean anomalies, followed by a view at the variability across Europe and on a country basis. Furthermore, with the help of specific examples, the dynamics behind the variability will be explored, and the variability will be placed within the regime framework. A summary, discussion of the results and research perspectives are presented in the last chapter.

2 Background Information

2.1 Definition of weather regimes

The idea of categorizing the flow patterns of the mid-latitude troposphere into groups that cause comparable weather impacts roots back to the first half of the 20th century when forecasters tried to forecast the upcoming weather by comparing the synoptic situation to flow configurations of the past, as Dorrington (2021) describes. Furthermore, it tries to answer the question of what causes the weather to be persistent, such as blocking flows. The core of mathematically describing the categorized flow patterns or regimes is to find genuinely different dynamics and recurring states that are in preference of other arbitrary flow patterns. Over time, this approach evolved from simple models trying to forecast weather to more and more complex models, and the use of statistical approaches like Empirical orthogonal functions (EOFs) and k-means clustering allowed the filtering of the atmospheric flow for large-scale patterns over areas of interest.

There are two areas where weather regimes are commonly investigated. One area is the North-Pacific-North-American sector, where usually three to four weather regimes are defined, e.g. (S. H. Lee et al., 2023; Messori & Dorrington, 2023; Michelangeli et al., 1995; Robertson & Ghil, 1999). The second region and area of interest of this thesis is the North-Atlantic-European sector. As already mentioned in the chapter 1 and independent of the exact method of defining weather regimes, four regimes are commonly used in winter (Cassou, 2008; Michelangeli et al., 1995; van der Wiel, Bloomfield, et al., 2019; Vautard, 1990). Determining the number of regimes in an area is ambiguous and, in the end, remains a choice of what seems to be the best fit and tradeoff between simplicity and accuracy. The goal is to explain as much of the observed atmospheric variance as possible, with as few regimes as necessary, and the framework of the four "classical" regimes explains 67% of atmospheric variance on average (Grams et al., 2020). In different seasons, weather regimes can be very different, and regimes occurring in winter (DJF) do not necessarily appear in summer (JJA) or vice versa (Cortesi et al., 2019). This is due to weaker air pressure differences in summertime and limits the period of four regimes to a season length of three to five months. Because of that, weather regime sets of a small number need to be defined for each season or month individually. Defining the WRs on a seasonal basis has the advantage of choosing the most frequent flow patterns of a season while keeping the number of WRs low. On the other hand, different flow patterns for each season impede inter-seasonal comparability and continuity in the definition of the weather regime index (which will be explained in chapter 3). To overcome the difficulties of inter-seasonal comparability, Grams et al. (2017) defined the seven weather regimes (7WR). These are defined year-round, explain 77% of the observed atmospheric variance

on average (Grams et al., 2020) and are defined on the 500 hPa geopotential height anomalies and have to be active for at least five days in a row.

Weather regimes can be considered either cyclonic or blocked in nature. This depends on the main geopotential height anomaly. If a negative geopotential height anomaly is dominant, these regimes are called cyclonic regimes, while blocked regimes are associated with a positive geopotential height anomaly. In the definition of the 7WRs are three cyclonic weather regimes as visible in figure 2.1, panels (a)-(c), and four blocked regimes, panels (d)-(g). The first cyclonic regime is the so-called Atlantic trough (AT), with a negative geopotential height anomaly between the British Isles and Greenland. The Zonal regime (ZO) has the negative geopotential height anomaly center over the southern tip of Greenland. ZO resembles the positive phase of the NAO in the framework of the regimes (Beerli & Grams, 2019). The last cyclonic regime is the Scandinavian trough (ScTr), with the negative anomaly shifted to Scandinavia. Since the classical regime definition for winter only defines one cyclonic regime, AT, ZO, and ScTr all fall into the only cyclonic regime usually referred to as NAO+. The first of the four blocked regimes of the 7WR definition is the Atlantic ridge (AR), with the positive geopotential height anomaly between the British Isles and Greenland being opposite to AT. AR is similarly defined in the classical regime framework. The dominating geopotential height anomaly of European blocking (EuBL) spans from the British Isles to Scandinavia. The anomaly of Scandinavian blocking (ScBL), which is the opposite of ScTr, is located over Scandinavia. Both regimes are the "Blocking" regime in the classical framework. The last regime is Greenland blocking (GL), with the leading positive geopotential height anomaly over Greenland. GL resembles the negative phase of the NAO and is similar to NAO- (also called Greenland anticyclone) in the classical regime definition. Opposite, weaker geopotential height anomalies can be found around the leading geopotential height anomaly. The last panel (h) in fig. 2.1 is the "no regime" (NR) situation if the criterion of the weather regime definition is not fulfilled.

2.2 Weather impact of weather regimes

The dominant geopotential height anomaly of a WR drives either low-pressure systems (including storms) near the surface in the case of cyclonic regimes or goes along with a high-pressure system, also referred to as ridge or block. Mid-latitude low-pressure systems are usually connected to the eddy-driven mid-latitude jet since they form beneath the jet caused by a perturbation of the pressure field. They travel with the jet stream, forming the North Atlantic storm track, and depending on the position, they influence different parts of Europe. Low-pressure systems are associated with warm and cold fronts and stormy wind conditions if the low-pressure system is very strong, marked by a strong pressure gradient near the surface and narrowed isobaric lines. At the fronts that are associated with a sudden change in temperature, pressure, and wind direction, precipitation and thunderstorms can occur. For Central Europe, cyclones in wintertime are, in general, associated with warm temperature anomalies due to the westerly wind directions. The warm front of a

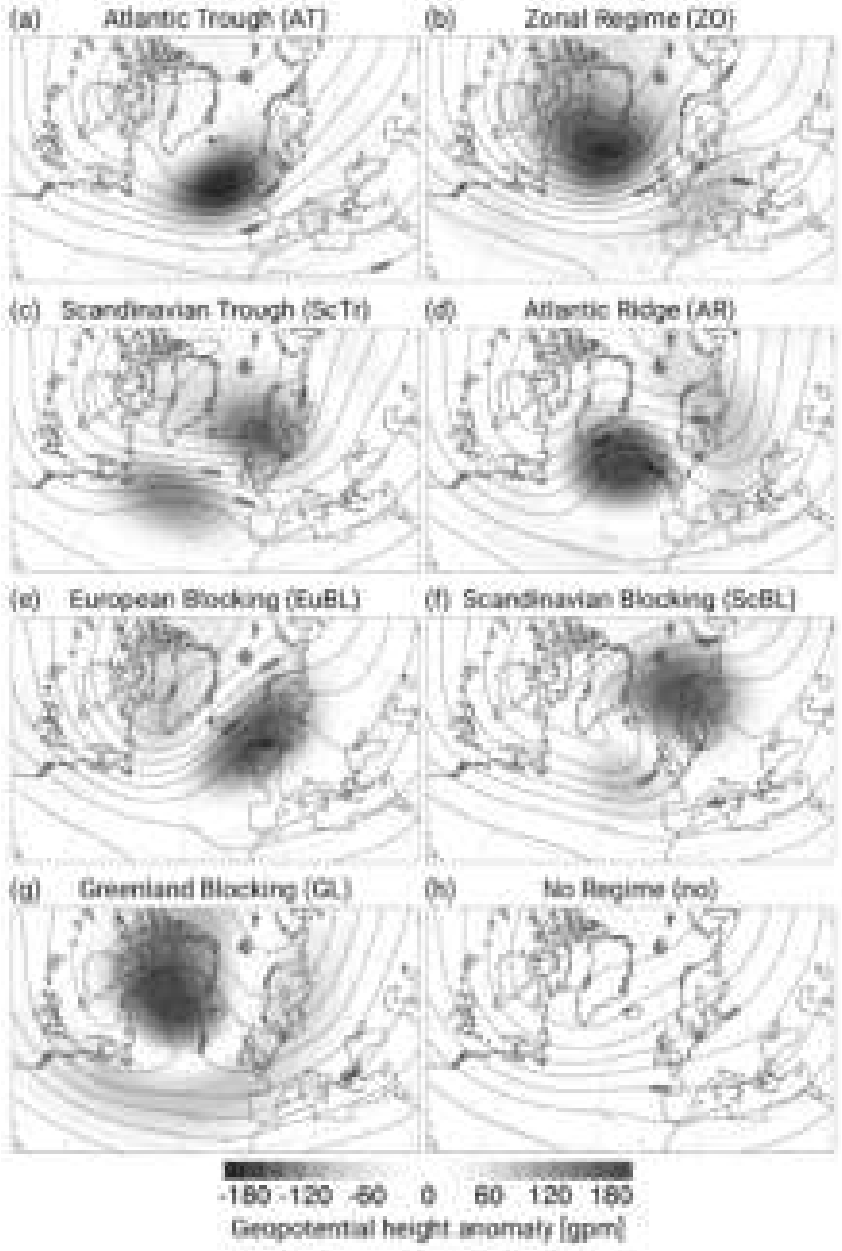

Figure 2.1: The seven Atlantic-European weather regimes (panels a-g) and no regime (h) in the year-round average, with the 500 hPa geopotential height anomaly (shadings), every 20 geopotential meters (gpm), mean absolute Z500 geopotential height as black contours of every 40 geopotential meters and frequency of the regimes. Adapted from Büeler et al. (2021).

cyclone brings warmer than average conditions by (south-) westerly wind conditions together with long-lasting precipitation events. Convective clouds and precipitation events form with the arrival of the cold front, where the wind directions lead to cooler conditions and occasionally snowfall. Note that extremely cold days usually do not occur in the cold sector of a cyclone.

On the other side, the anticyclonic flow of a block favors cold anomalies to the eastern flank of the block in DJF caused by the advection of cold air from (north-)easterly regions (Bieli et al., 2015; Kautz et al., 2022). Heavy precipitation can occur at the system's eastern, western, as well as northern flank of the system. In JJA, blocks are associated with warm temperature anomalies in the center of the block, thunderstorms at the eastern and western flanks, and droughts in the center.

The primary mechanism for heat waves and below-normal precipitation is the adiabatic warming by subsiding air masses, resulting in cloudless skies that allow accumulation of radiatively heated, warm air.

Considering that, the average weather conditions over Europe associated with the 7WR are explainable. The anomalies of a region associated with a WR can change from season to season, and 2 m temperature as well as 100 m wind speed anomalies are more pronounced in DJF than in summertime (JJA) due to the stronger pressure gradients in winter (Cortesi et al., 2019; Grams et al., 2017). Also, the magnitude and area mainly influenced may vary from regime to regime, and regions can see no or opposite temperature anomalies. A detailed view of the anomalies will be provided in the results chapter 4, but cyclonic regimes generally lead to warm temperature anomalies over most parts of Europe in DJF. In contrast, blocked regimes lead to cold ones. Exceptions during blocked regimes can be found in Scandinavia and the Mediterranean during GL. During summer, this distinction between the regime types cannot be made since ScTr goes along with mainly cold anomalies, EuBL and ScBL with warm anomalies, and AT is cold in northwestern Europe and warm in the rest of Europe. All other regimes remain the same. During DJF, the strongest wind speed anomalies can be found at the southern flank of the cyclone, usually resembling the position of the storm track, leading to windy anomalies in Western (AT), Northern (ZO), and Central Europe (ScTr). For JJA, the wind speed anomalies are limited to regions around the North Sea during cyclonic regimes. For blocked conditions, windy anomalies are present in Southeastern Europe during AR and EuBL during DJF, as well as the Mediterranean during GL. The JJA wind speed anomalies are slightly windy for AR and GL. The other blocked regimes are associated with no anomalies or calm anomalies over Europe during JJA. The insolation anomalies anti-correlate with the wind speed anomalies - where it is windy, it is cloudy, and vice versa.

Other studies in the North Atlantic European area use the classical approach with four WRs per season and investigate the impact of WRs on the European weather. Cortesi et al. (2019) uses four monthly defined WRs based on a sea level pressure definition. They find that WRs can alter the wind speed by up to $\pm 50\%$ and different regimes affecting different regions. For example, blocking over Scandinavia leads to below-average wind speeds over Europe, while AR-like situations can lead to higher-than-normal wind speeds. Plaut and Simonnet (2001) and van der Wiel, Bloomfield, et al. (2019) find that blocked regimes lead to increased observations of cold days from November to March, while NAO+ leads to very rare occasions of cold days. A very interesting discovery is that AR leads to fewer cold and warm days, thus being closer to climatology.
Yiou and Nogaj (2004) focus on extreme temperatures during the four classical weather regimes. They find that the blocked regime for northern Scandinavia controls warm temperature extremes in DJF, the NAO+ for all regions from Western Europe to Eastern Europe. At the same time, Southern Europe experiences extremely mild temperatures during the NAO- regime. Cold extremes are due to Blocking in the Mediterranean area and due to Greenland anticyclone in the rest of Europe.

Precipitation is also studied with the classical WRs. It is shown that heavy rain is to be expected during NAO+ around the North and Baltic Seas, while for the southern half of Europe, NAO- brings above average rainfall (Ullmann et al., 2014; Yiou & Nogaj, 2004). Some parts of the

Mediterranean show heavy rainfall during the blocking regime, and in parts of Germany, it is the case during the Atlantic ridge. Less precipitation than usual can be expected during blocking over Scandinavia in Central and Northern Europe and during NAO+ in the Mediterranean area (Plaut & Simonnet, 2001; Yiou & Nogaj, 2004). A study in France revealed that warm summers are usually associated with blocking regimes and extreme hot temperatures. In contrast, cyclonic regimes are present for cold summers and prone to wetter than normal conditions (Yiou et al., 2008). Even in dry summers, heavy convectively-driven precipitation events are not excluded.
Pasquier et al. (2019) showed that the likelihood of precipitation extremes is enhanced in different parts of Europe during autumn (SON). AT and ZO enhance the likelihood in northern parts of Europe, while ScTr and GL are active over many parts of Europe. For EuBL, ScBL, AR, no enhancement of the precipitation extreme likelihood is visible over most parts of Europe except for the Mediterranean during EuBL, southeastern Europe during AR and western Europe for ScBL.

2.3 Energy meteorology in context of weather regimes

With the increasing importance of renewable energies driven by meteorological variability, it becomes increasingly important to understand under which weather conditions renewables provide which amount of energy. The already installed capacities of renewables transformed the European power system from a purely demand-driven and meteorologically influenced by temperature only to a system that is influenced by temperature, wind, and solar radiation on the meteorological side (Bloomfield et al., 2020). The temperature drives the demand in two ways, depending on the county (Bessec & Fouquau, 2008). In colder countries of Northern Europe, the electricity demand decreases when it gets warmer, and the heating of buildings is turned off. In comparison, in more southerly countries, cold and warm temperatures have an effect since, at cold/warm temperatures, the heating/air conditioning is turned on, leading to a non-linear response in energy demand to temperature anomalies. Therefore, it is important to forecast the expected power output and demand to keep the power grid stable and to create appropriate plans to mitigate risks of energy shortages under certain weather conditions with further increasing amounts of renewables.
It has been shown that WRs are an effective tool in discriminating different situations of wind power production (Garrido-Perez et al., 2020). Depending on the WR, the power generation by wind and solar energy is variable for different regimes and regions. A measure of energy generation is the capacity factor (CF). It describes the ratio between the total energy produced and the total installed capacity of either a specific energy source, such as wind, or the total of all energy sources combined in a defined region. Grams et al. (2017) find that countries around the North and Baltic Seas see overproduction by wind energy during DJF if a cyclonic regime is dominant and underproduction for blocked regimes (see figure 2.2). In southeastern Europe, overproduction is the case for blocked regimes and is prone to underproduction during AT and ZO. For the western Mediterranean, energy generation cannot be separated by regime type. Overproduction is observed during AT, ScBL as well as GL, while underproduction of renewables prevails during ZO and EuBL. These observations can also be made in the transition seasons of spring (MAM) and autumn (SON) but with smaller

amplitude. For the summer season, wind power overproduction can be seen during GL as well as AR on a slight scale. At the same time, there is a strong underproduction during ScBL and EuBL in the North Sea region due to low wind speeds centered there in combination with high amounts of wind CF installed in and around the North Sea.

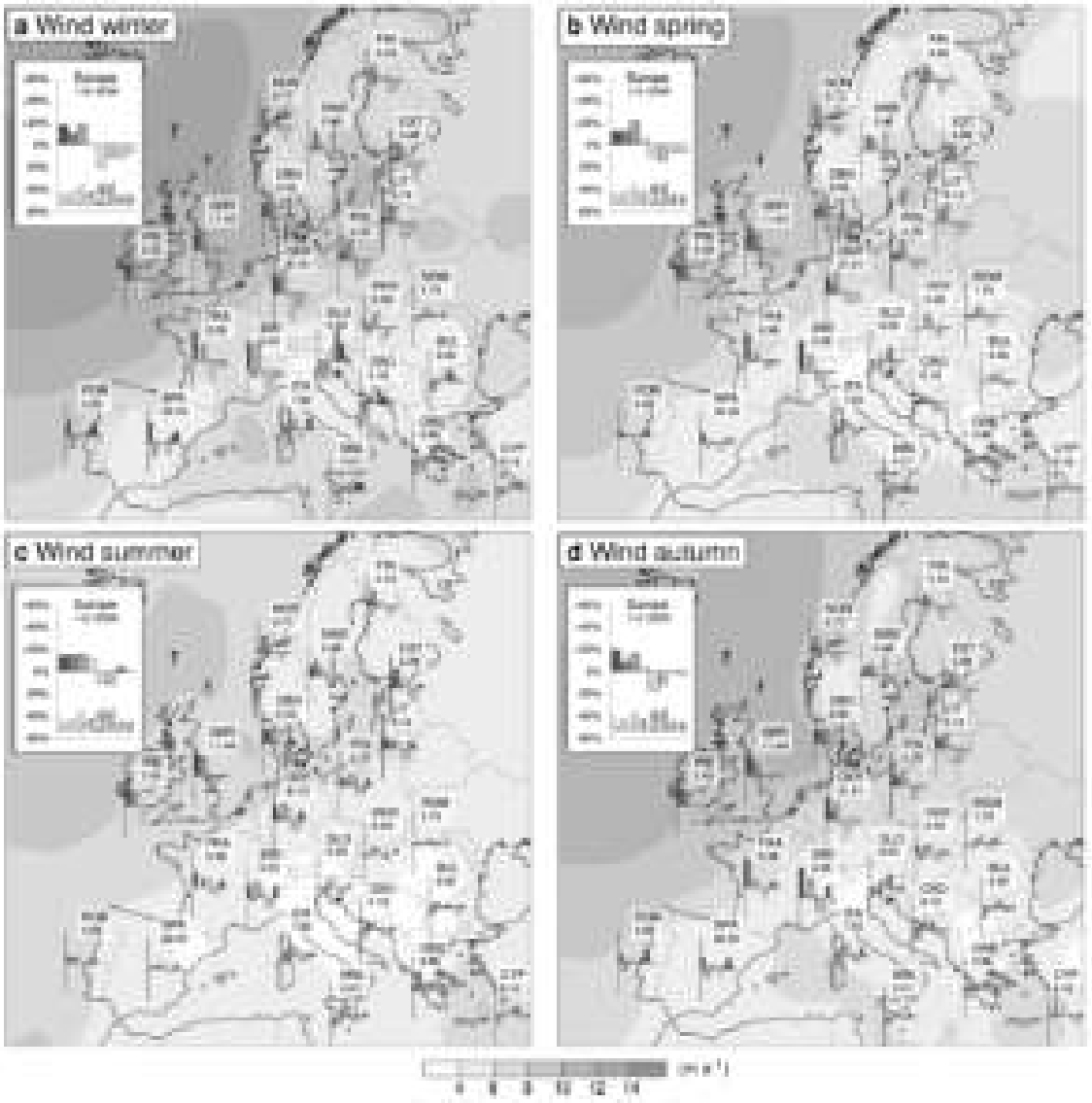

Figure 2.2: The country-based relative change in wind electricity generation depending on the weather regimes normalized against the seasonal mean generation during the cyclonic regimes (red labels), blocked regimes (blue labels) and no regime (grey). Dark/light colors mark over-/underproduction. Above the bar plot is the three-letter country ISO code and the installed capacity in gigawatts as of 2015. The grey shading represents the seasonal mean (1979-2015) of the 100 m wind speed in (ms^{-1}). Adapted from Grams et al. (2017).

While wind power generation peaks in the winter season due to strong winds, solar power production behaves the opposite and peaks during summer mainly because of longer day lengths (Mühlemann et al., 2022; Raynaud et al., 2018; Staffell & Pfenninger, 2018; van der Wiel, Stoop, et al., 2019). In solar power production, there is a strong north-south contrast with higher values to the south of Europe, while in Northern Europe, the seasonal cycle of day length is very dominant (Grams et al.,

2017). This leads to a low impact of WRs on solar power production variability in Southern Europe and summer, while more northerly regions see overproduction during AR, ScBL, and EuBL in DJF (see figure 2.3). In general, it can be said that anticyclones cause positive CFs of solar power due to descending air motion leading to clear sky conditions while cyclones are associated with enhanced cloud cover and thus lower CFs (Mühlemann et al., 2022). Since cyclonic or anticyclonic activity is not dominant over the entire continent at the same time, leading to CFs of the opposite sign in other regions, which might be able to (partly) balance the underproduction in another area if there are enough capacities installed and interconnections between the power grids (Grams et al., 2017; Mühlemann et al., 2022). The largest pan-European overproduction of renewable energy can be observed during AT in DJF, driven by the strong winds over the North Sea region, while solar power has the lowest power output compared to the average (Grams et al., 2017). However, this region's huge wind power capacities make the European power grid volatile. The largest underproduction rates can be seen during EuBL when a large high-pressure system is present in this region, leading to low power generation by the wind. Solar power, which sees the largest overproduction rates during this WR, cannot balance the lack of wind power since the amount of energy generated by solar power is one order of magnitude lower than that of wind.

Managing energy generation by renewables sees mainly three types of challenges: extremely high generation, ramping and extremely low generation, which all see large (inter-)annual variations (Cannon et al., 2015). While power plants can be turned off during high-generation phases, low-generation phases are harder to balance since renewable energies cannot simply turn on when needed. Exceptionally critical to the stability of the power system are situations where the renewables generate low output and the energy demand is increased, for example, due to low temperatures. Events with low solar and wind power generation can be called "Dunkelflauten". Mockert et al. (2023) defines a Dunkelflauten event as lasting at least two days, and the CF drops below a certain threshold. Dunkelflauten are subject to a seasonal cycle, with the peak between SON and DJF and no events in JJA in Germany. On average, four Dunkelflauten occur during a year with an average duration of 3.4 days. Li et al. (2021), which use a slightly different approach to define Dunkelflauten, find comparable results with 5-10 events of one day long Dunkelflauten annually, occurring from October until February. Other authors do not use Dunkelflauten specifically but look at similar events with low generation in combination with high energy demand, leading to effective underproduction of energy, mainly in the winter season. The meteorological conditions are similar in all cases: an extensive high-pressure system is located over Central Europe, leading to weak pressure gradients and ultimately low surface wind speeds (Li et al., 2021; Mockert et al., 2023; Otero et al., 2022; van der Wiel, Stoop, et al., 2019; van der Wiel, Bloomfield, et al., 2019). Often, the high-pressure systems are associated with below-average temperatures, leading to anomalies of -2 to -4 K in the case of Germany and larger than usual variability in the solar radiation towards above-average values in northern countries and below-average values in the Mediterranean. Mockert et al. (2023) and Otero et al. (2022) attribute these events to EuBL and GL, with the formerly mainly responsible in Central Europe and Germany and the latter one more dominant in Scandinavia and being driven by the cold temperatures more than by the lack of energy as for EuBL. Usually, a Dunkelflaute is fully embedded in the life cycle of a well-developed WR since the onset of the Dunkelflaute takes place after the onset of the WR and decays before the disappearance of the WR.

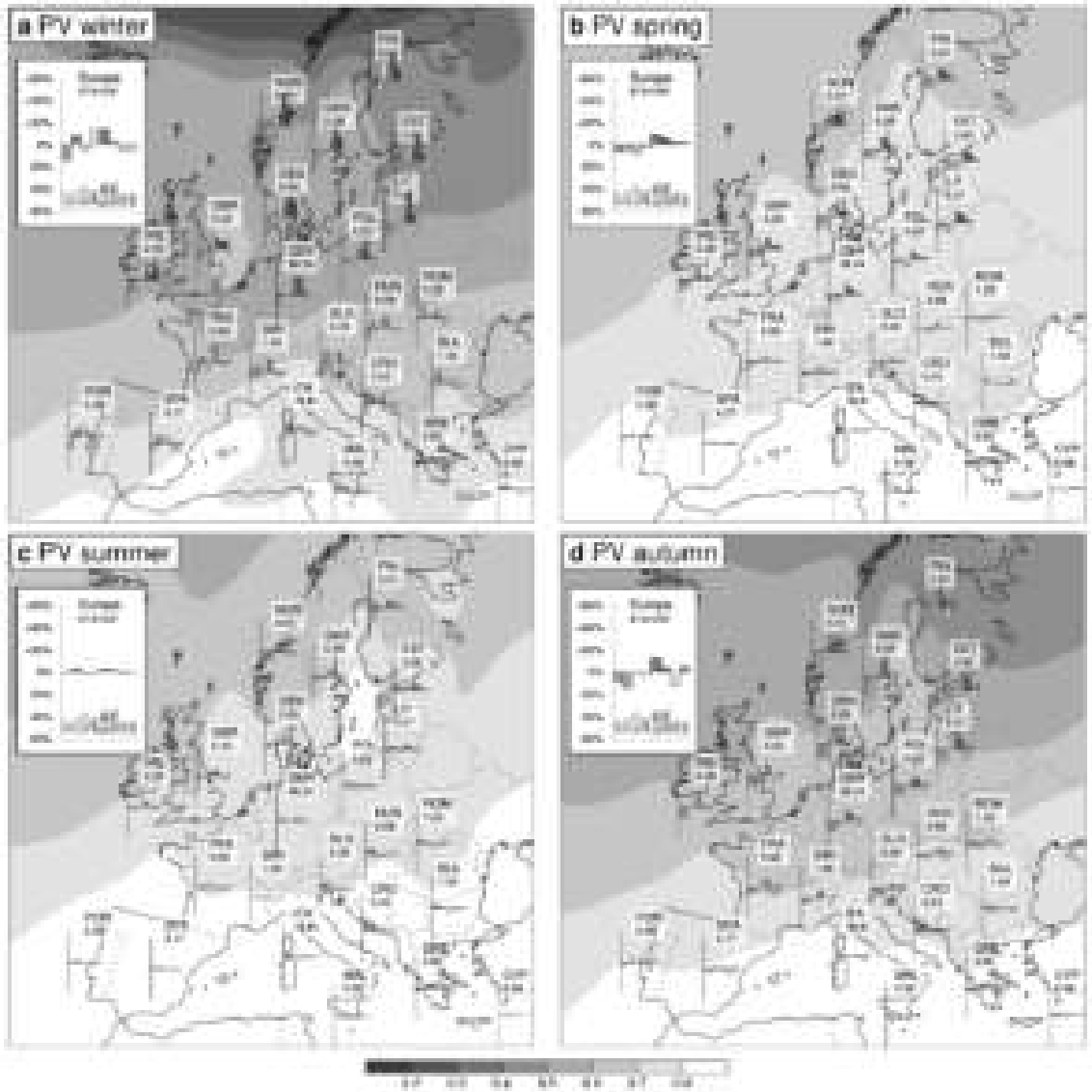

Figure 2.3: As figure 2.2 but for photovoltaic electricity generation with the grey shading representing the seasonal mean (1979-2015) of the daily fraction of insolation and daily potential insolation assuming clear skies. Adapted from Grams et al. (2017).

3 Data and Methods

This chapter provides an overview of the data and methods used in this thesis. First, the database will be presented, followed by an explanation of the weather regime and the definition of the weather regime index. The investigated meteorological variables are presented hereafter, followed by statistical methods to detect weather variability. The last part of this chapter presents methods to learn about the dynamics behind the variability and how to account for them in the regime framework.

3.1 Data

Currently, the past weather is conveniently represented by reanalysis data sets like the ERA5 data set provided by the European Center For Medium Range Weather Forecast (ECMWF). Compared to purely observational-based data sets, reanalyses are globally available and spatial and temporal complete and homogeneous (Hersbach et al., 2020). The massive use of meteorological satellites improved the global coverage of weather variables and can accurately measure certain variables such as surface temperatures or cloud cover. However, they cannot provide good information from cloudy areas, resulting in deficiencies, and satellites are not able to provide a temporally consistent global picture as reanalyses. Inconsistencies of satellites are especially a feature of the high latitudes, where the observation angle of geostationary satellites becomes too bad for adequate measurements, while polar-orbiting satellites measure with time interruptions. Ground and atmospheric-based measurements are even more spatially inconsistent since performing them in densely populated areas is easier than over remote oceans.
Reanalyses are a mixture of observations of many kinds and state-of-the-art weather forecast models to compute the past weather (ECMWF, 2023). The observations are used to set a starting point together with the result of the reanalysis of the previous day and the weather model, which runs on a coarser resolution than the current forecast and then computes the meteorological variables for the following day. However, reanalyses do not represent a perfect picture of past weather since inaccurate and incomplete observations find their way into the data set. Furthermore, the observation techniques changed over time, leading to further errors, and the weather models are not perfect either, making resulting errors nontrivial to understand (NCAR, 2024).
However, due to the homogeneity of the reanalysis data, ECMWFs ERA5 data set is the basis of this work. ERA5 is available from 1940 onward, but synoptic-timescale regime statistics are deeply uncertain in the pre-satellite era. Therefore, the time period used in this study spans over 43 years, from 01/01/1979 to 31/12/2021. ERA5 has a grid resolution of 31 km (0.25°) with hourly data (Hersbach et al., 2020). For data storage reasons, a resolution of 0.5° and 3-hourly data are used.

The domain of the data used spans over the North-Atlantic-European Sector from 80°W to 40°E and 30°N to 90°N.

3.2 Weather regimes

The climatological weather regime patterns are computed analogously to Büeler et al. (2021) and Osman et al. (2023) on the given domain over a 40-year-long sub-period from 1979 to 2019 by first calculating the 500 hPa geopotential height anomaly (Z500') with a 90-day running mean, centered around the calendar date, as reference climatology. Then, Z500' is filtered with a 10-day low-pass filter to remove the synoptic variability. In order to retrieve a set of year-round defined weather regimes, the weaker summer anomalies must be accounted for. Therefore, Z500' is seasonally normalized by dividing it by a 31-day running mean temporal standard deviation over all anomalies of the time range. The temporal standard deviation is cosine-latitude weighted and calendar-day dependent. In the next step, EOF analysis is applied to the anomalies before k-means clustering is performed on the first seven EOFs in phase space, which explains about 70% of the observed variance.
This sequence of methods allows one to categorize the atmospheric flow pattern into the seven regime clusters. More information on the temporal evolution of a weather regime event can be obtained using a weather regime index (IWR). The IWR does not only deliver additional information on the onset, maximum and decay dates but also about the "strength" of a regime. In other words, it is how much the atmospheric flow resembles one of the clusters. The IWR is calculated by following the steps of Büeler et al. (2021), Grams et al. (2017), and Osman et al. (2023). First, a scalar $P_{wr}(t)$ is calculated, measuring the spatial correlation of the instantaneous anomaly field $\phi(\lambda,\phi,t)$ with the cluster mean anomaly field $\phi_{wr}(\lambda,\phi)$:

$$P_{wr}(t) = \frac{1}{\sum \cos\phi} \sum_{(\phi,\lambda)} \phi(\lambda,\phi,t)\phi_{wr}(\lambda,\phi)\cos\phi. \tag{3.1}$$

λ and ϕ denote the latitude and longitude at each grid point of the EOF domain, t the time step and "wr" indicates the regime. Subtracting the climatological mean $\overline{P_{wr}}$ from the anomalies $P_{wr}(t)$ and dividing by the standard deviation of it gives the dimensionless regime index $I_{wr}(t)$:

$$I_{wr}(t) = \frac{P_{wr}(t) - \overline{P_{wr}}}{\sqrt{\frac{1}{N}\sum_{i=1}^{N}[P_{wr}(t) - \overline{P_{wr}}]^2}}. \tag{3.2}$$

To consider a regime active $I_{wr}(t)$ has to be above the threshold of 1.0 for at least five days in a row with a local maximum and a monotonic increase or decrease during the previous or following five days. If several regimes match the criteria, the regime with the highest $I_{wr}(t)$ is considered active; if no regime matches the conditions, the period is labeled with "no regime".
An exemplary evolution of IWRs is given in figure 3.1. At the beginning of the shown time series, no IWR matches the criterion of being active. ScTr crosses the threshold around March 5th but for

too short. Looking at the IWRs also allows to see the evolution of single regimes such as EuBL, which is the regime with the lowest index at the beginning until it starts rising quickly around the same day as ScTr reaches its maximum. Five days later, EuBL reached the status of being active alongside ScBL. In the late stages of the decaying EuBL, around March 15th, AR takes over the active regime role. Combining the knowledge of the active regime with different meteorological variables allows for gathering information on which type of weather occurs under which regime.

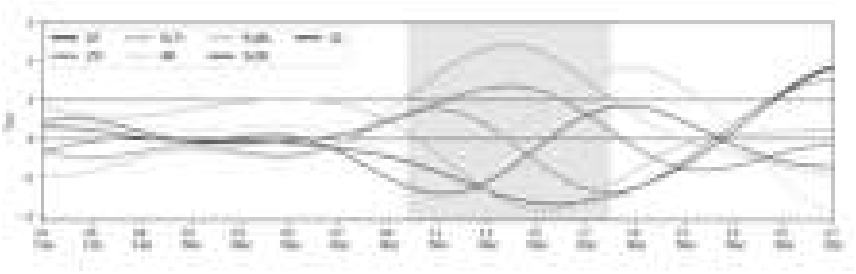

Figure 3.1: IWR evolution in February/March 2016 for all seven weather regimes with thick lines representing the active regime at the corresponding time. Adapted from Hauser et al. (2022)

3.3 Energy-relevant meteorological variables

Four meteorological variables with high socio-economic impact and importance for the energy sector are used: 2 m temperature (T2M), daily total precipitation (TP), 100 m wind speeds. 100 m wind speeds instead of 10 m are used as this is closer to the typical hub height of modern wind turbines. The fourth variable is Solar Daily Insolation (SOLD), computed as the ratio between the daily sums of the net solar radiation and the net solar radiation for clear skies at the surface. The ERA5 datasets for the computation are the surface net solar radiation (SSR) and surface net solar radiation at clear skies (SSRC), respectively. In other words, this computation gives the fraction of the incoming solar radiation of a day compared to what theoretically would be possible on that calendar day, making this metric independent from the varying lengths of days during the year. Note that SOLD is only defined up to the latitude of the Arctic circle at 66°

Anomalies from the climatological mean are computed to gain an overview of the data and filter for interesting regions, regimes and seasons. First, the seasonal cycle is removed from the data by computing the mean value for a given calendar day and smoothing it with a 31-day average for each grid point on each day. Secondly, a linear trend is removed to account for climate change. Together with the regime data, composites are computed for winter, spring, summer and autumn. In the case of precipitation, the first day in the data set was left out due to the model-based fact that precipitation is not available for the whole day. Another date (01/05/2020) had to be eliminated in the precipitation field due to unrealistic values. To further smooth the variables and remove parts of the sub-synoptic variability, a 5-day rolling mean filter is applied. A comparison of T2M anomalies during wintertime AR in figure 3.2 shows slightly smoother distributions of anomalies. For example, the highest anomalies over the North Atlantic are reduced.

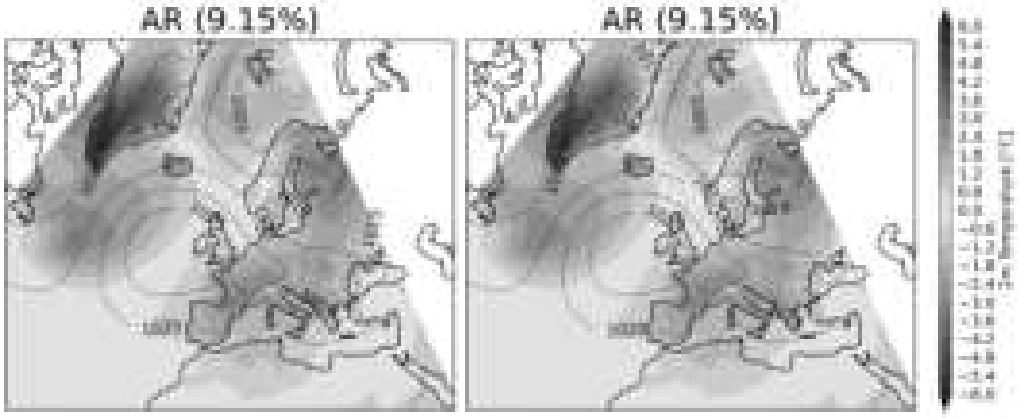

a, daily average b, 5-day-filtered c

Figure 3.2: Comparison of the 2 m temperature anomalies during the AR regime for daily averaged anomalies on the left, averaged over five days in the right, together with the occurrence frequency for the season in brackets and the color bar on the right.

3.4 Methods

3.4.1 Detecting and quantifying variability

Different methods are used to find and visualize the variability within the weather regimes. Box plots are a widely known visualization method. However, with the probability distribution, violin plots contain more information and are preferred. The probability distribution of the violin plot shows how probable the values are by a larger or smaller appearance of the violin. As shown in figure 3.3, the probability distribution in green allows easy detection of multimodalities (as in this example) or a skewed distribution. The calculation of the probability function assumes a steady distribution that leads to the inclusion of values above/below the highest/lowest ever observed anomaly, which can lead to a wrong interpretation and is thus prevented, leading to cut-off edges at the violins. Furthermore, several aspects of variability are shown within the violins used here. The white dot in the middle represents the median of the distribution, indicating the point where 50% of data points are larger or smaller. If a distribution has many but only slightly low/high values and some high/low values, the mean gets shifted compared to the median. The bold black bar indicates the interquartile range where 50% of all data is located, while the thin black line is 1.5 times the interquartile range. Values above or below are considered outliers.

A different method to visualize the variability of one of the variables is the fractional standard deviation (FStD)

$$\sigma_{frac,season} = \frac{\sigma_{regime,season}}{\sigma_{season}} \tag{3.3}$$

that indicates how strong the variability of a weather regime in a region is compared to the climatological variability. FStD can be understood intuitively by considering some exemplary Gaussian distribution, and an FStD of 1 means that the distribution of $\sigma_{regime,season}$ is the same as that of σ_{season}. In a conceptional picture, as figure 3.4 provides, FStD of 1 would be represented by the black curve, which also represents the climatology. In the case of FStD 1, there is no difference.

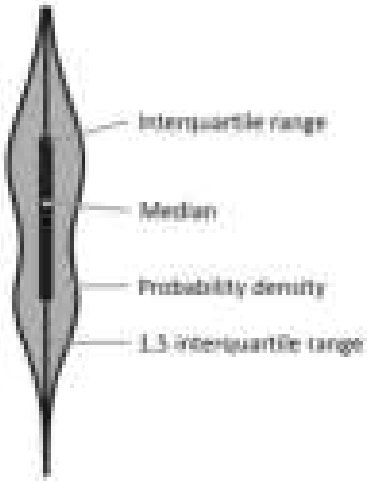

Figure 3.3: Example of a violin plot with labels marking different features of a violin.

This means that the regime does not vary more or less than the climatology, and knowing the WR does not add information about how strong the weather will vary. It will vary depending on the seasonal climatology. An FStD below 1 looks like the blue curve with a smaller distribution driven by the smaller $\sigma_{regime,season}$ value. This shows that knowing the WR reduces the range of possible weather variations but does not entirely rule out variation. On the other hand, a value above 1 (red curve) means a wider distribution, and the FStD shows where much variability in the WR is happening. This means that looking at the WR reveals that the predictability of surface values is lower than normal since the mean hides large proportions of the actual variability.

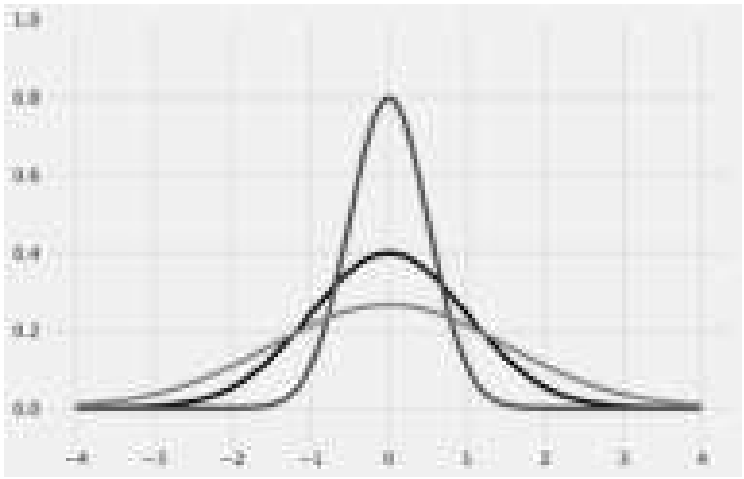

Figure 3.4: Gaussian distributions sharing the same mean but with different standard deviations. The black curve represents a Gaussian distribution with a standard deviation of 1, while the blue has one of 0.5 and the red curve has 1.5.

The signal-to-noise ratio (S2N) is used to evaluate how strong the signal of anomalies is compared to that of climatology. In this study, the equation is as follows with the anomalies of the variables:

$$S2N = |\frac{anomalies_{regime,season}}{\sigma_{season}}|. \tag{3.4}$$

In general, a high S2N means that the anomalies are large, the signal of the anomalies is strong compared to the variability, and thus, it is likely that the anomalies will occur. If the S2N is low, it is either due to small anomalies or because the anomalies are not more/less likely than one would expect from climatology. This also means that in this region for that variable, there is only little to no impact by a WR.
S2N is proportional to:

$$S2N \propto |\frac{anomalies_{regime,season}}{\sigma_{frac,season}}|. \tag{3.5}$$

This leads to four different combinations of high/low absolute values for anomalies and FStD as listed in table 3.1.

Table 3.1: Table of different combinations between high and low absolute values for the anomalies and FStD. The resulting value of S2N depends on the exact values of the anomalies and FStD, especially for the first and last scenario.

scenario	anomalies	FStD	S2N
uncertain extremes	high	high	high
unlikely variability	high	low	high
certain variability	low	high	low
certain climatology	low	low	around 1

These scenarios can be interpreted as follows: the first scenario "uncertain variability" with high values for the anomalies, FStD and S2N mean that a regime has a strong impact on the region, leading to large anomalies that are likely to occur, given by the high anomalies and S2N. However, there is some sort of strong variability, that could include very high or low values, indicated by the high FStD. In scenario "unlikely variability", the high anomalies lead to high S2N. In this case, together with low FStD, the anomalies are likely to occur without large variability. The certainty of the weather impact of a regime is increased compared to climatology. In the "certain variability" scenario, the S2N is very low due to a high FStD. This points towards much variability and increased uncertainty regarding the weather. The climatology underestimates the risks for extremes in this case. In the last scenario, "certain climatology", the exact value of S2N is as in the first scenario, depending on the anomalies and FStD. However, small anomalies and FStD reveal areas where little to no impact of the active WR is expected, and the climatology can be expected. Examples for each of the scenarios can be found in chapter 4

3.4.2 Dynamics behind the variability

Quantifying the variability is already a step further than any other previous study focusing on regime impact. However, it is not only the goal to see the weather variability in different regions but also to understand better where the differences come from. To see the atmospheric flow differences between an average regime impact and how the flow pattern looks in the distribution's upper/lower tails, a variable's upper/lower third of values (also terciles) is selected. To obtain the terciles, the variable is sorted from its highest to its lowest anomaly and divided evenly into three parts. The terciles and the 500 hPa geopotential height field (Z500) reveal the differences in the flow pattern. Since the flow configuration over the North-Atlantic-European region projects into all IWRs at all times, they can be used to obtain more information about the exact configuration. To see the averaged temporal evolution of the different indices, a 10-day lagged analysis is performed. Here, certain dates (test dates) during an active regime are given, and all IWRs, including the IWR of the active regime, are shown ten days before and after the given dates in 3-hourly time steps. For example, the test dates are the 15 coldest days of the observed time period during a regime, and seasons are given for analysis. The analysis will then provide not only the IWRs of all regimes during these 15 test days but will also give back the IWRs for each of the ten previous and following days. By that, it is easily visible if other regimes frequently play a role during a regime event.
In order to better examine the data for significance, a two-sided Kolmogorov-Smirnov test is carried out. The test uses random samples to test whether two random variables X and Y - here, the test data and the remaining data from the lagged analysis - have an identical distribution. There are two possible hypotheses:

$$H_0 : F_X(x) = F_Y(x) \text{ and } H_1 : F_X(x) \neq F_Y(x) \tag{3.6}$$

The null hypothesis H_0 describes the case that both random variables have the same probability distribution, and under the alternative hypothesis H_1, they have different ones. The comparison between the distribution functions $F_{X,m}$ and $F_{Y,m}$ is determined using the following test statistic:

$$d_{n,m} = \sup |F_{X,n}(x) - F_{Y,m}(x)| \tag{3.7}$$

with n and m being the number of observation values of X and Y and d the difference. The null hypothesis is rejected if $d_{n,m}$ exceeds the critical value K_α:

$$K_\alpha < \sqrt{\frac{n*m}{n+m}} d_{n,m} \tag{3.8}$$

where α describes the significance level, which is set here at 1%. The Kolmogorov-Smirnov test is carried out individually for each individual time lag, looking at a distribution over all independent regime events. The test allows the identification of a regime behaving significantly different from its normal behavior during the active regime. This is why this metric can identify when other regimes contribute to the outcome of the test dates.

4 Results

This chapter is structured as follows: first, the mean anomalies during the regimes are discussed again, although they are well-studied (Grams et al., 2017). This provides a solid basis for the following analysis of internal regime variability. Furthermore, the latest reanalysis, ERA5, is used, providing validation against previous work based on ERA Interim. Secondly, in section 4.2, areas with high and low variability are identified across Europe and in further detail in Germany. In the third section 4.3, the dynamics behind the variability of T2M anomalies are explored in wintertime GL. Furthermore, it is shown how the variability projects into the IWRs to gain an indicator that makes it easier to predict the outcome of a regime. Afterward, in section 4.4, the analysis is extended to other countries and variables of the same regime. In sections 4.5 and 4.6, further examples are discussed, where the exemplary analysis of GL provides results that behave similarly and allow a better understanding of the dynamics behind the variability and examples where the whole analysis reaches its limits, especially that of IWRs. In the last section 4.7, guidelines on using the IWRs to capture weather variability are presented.

4.1 Mean anomalies during weather regimes

4.1.1 Wintertime anomalies

The wintertime T2M anomalies over the European continent in ERA5 show the same features as the analysis in ERA-Interim, but with greater detail, as can be seen in figure 4.1. The cyclonic regimes show warm temperature anomalies in DJF over Europe. The areas with the strongest warm anomalies can be found to the south, southeast, and east of the surface low-pressure system, which advects mild, oceanic air. The black mean sea level pressure (MSLP) lines can identify the pressure systems. Depending on the exact location of the cyclone, the main affected area is shifted. AT brings modest warm anomalies across Europe with its trough between Iceland and the British Isles. The anomalies are strongest during ZO and can be found further north around the Baltic Sea due to the more northerly position of the cyclone. ScTr's warm anomalies are of a smaller spatial extent and are located mainly in Eastern Europe.
In contrast, blocked regimes are predominantly associated with cold anomalies. These occur due to the anticyclonic advection of cold polar and continental air from the north and east to the southeast of the high-pressure system. The strongest cold anomalies of $-5\,\mathrm{K}$ and below can be observed during GL and ScBL in Northern and Eastern Europe, respectively. AR and EuBL bring more moderate cold anomalies but are more spatially extended. EuBL and partially ScBL show cold anomalies in the center of the anticyclone, leading to the assumption that not only cold air advection

is a driver of the anomalies, but radiative cooling is also a driver.
Although cyclonic regimes are mainly warm in DJF and blocked regimes are cold, some areas on the European continent see different anomalies. The main exceptions are the Mediterranean, which sees no (warm) anomalies during ZO and ScTr (GL), and Scandinavia, which sees warm anomalies during EuBL and ScBL. In both regions, the anomalies can be explained by the position of the storm track. The warm anomalies in Scandinavia during EuBL and ScBL, as well as the warm anomalies in the Mediterranean during GL, occur due to the relocation of the storm track to those areas forced by the dominating anticyclone. During the cyclonic regimes, the Mediterranean is too far away from the cyclones and comes under the influence of subtropic high pressure.
Over the North Atlantic and Greenland, temperature anomalies are also visible, often opposite to the one described on the European continent. For example, Greenland experiences colder than normal conditions during cyclonic regimes and warmer than normal conditions during blocked regimes, especially during ScBL and GL when mild air gets advected at the northwestern flank of the anticyclone. Also, Northern Africa is partially influenced during the regimes, but these areas are not the focus of this study.

As for the T2M anomalies, the position of high and low-pressure systems plays a crucial role in the occurrence of 100 m wind speed anomalies (see fig. 4.2). Compared to the temperature anomalies, the strongest wind speed anomalies are located at the entire southern flank of a cyclone, while calm anomalies occur in the core of an anticyclone. Very low wind speeds in the core of the anticyclone are visible for AR and EuBL. The core of AR upstream of the European coastline affects Western Europe with below-average wind speeds, while Scandinavia, as well as the Western Mediterranean, see windy anomalies. ERA5 allows the visibility of local wind systems, in this case of the Mistral wind in Southern France.
For EuBL, the calm anomalies are pronounced in the North Sea region, where the calm anomalies are the strongest for all DJF regimes, while windy ones are strong over Scandinavia. Calm wind speed anomalies for the North Sea and Scandinavia can be found during GL, where the anomalies do not occur in the regime's center. The anomalies are caused by low-pressure gradients between several pressure systems, as Mockert et al. (2023) already reported. By knowing that the largest capacities of wind power are installed around the North Sea, it is easy to understand why EuBL and GL are prone to energy shortages by renewables, especially in combination with the very cold anomalies possible for GL (Otero et al., 2022). On the other hand, in the Mediterranean area and the southern North Atlantic, where the storm track gets shifted during GL, higher than-normal wind speeds occur. ScBL shows calmer than normal conditions over Europe except Southern Europe. Slightly higher than normal wind speeds occur locally in the Mediterranean area, while Northern, Eastern and Central Europe experience lower than usual winds but more locally differing than during GL.
The three cyclonic regimes are all associated with strong windy anomalies but affect different regions. AT causes strong windy anomalies, mainly in Western Europe, and some slight windy anomalies towards the Baltics. During ZO, the band with the strongest windy anomalies spans from the British Isles across the North Sea towards the Baltic Sea and also affects the surrounding countries. The extended Mediterranean area experiences calm wind speeds during ZO-phases. ScTr leads to windy anomalies in many parts of Europe, but not as strong as during AT or ZO. The

British Isles and Central Europe are the main ones affected. Calm anomalies during ScTr can be found in Scandinavia and the Iberian Peninsula.
Precipitation (fig. 4.3) and solar radiation anomalies (fig. 4.4) are somewhat correlated to the wind speed anomalies. In regions affected by strong, windy anomalies, precipitation rates are usually above average, and SOLD is below seasonal climatology. The low-pressure systems of cyclonic regimes are loaded with humidity and rain out in Western Europe (AT) and Northern Europe (ZO). Wet anomalies spread throughout Europe for ScTr, except for the western Mediterranean. Orography plays a bigger role for TP and SOLD than for wind and T2M. For example, during ZO, highly wet anomalies are visible on Great Britain's and southern Norway's coasts, where the MSLP lines are almost perpendicular to the coastline. ZO shows a strong dipole between wetter areas in the north and drier-than-normal areas in the south. This is also visible in SOLD, where the rainy northern half of Europe is cloudier than average, and the extended Mediterranean sees strongly above-normal sunshine rates. SOLD in AT and ScTr follows the example of ZO.
The dipole of ZO is reversed for GL, even though the contrast is not as strong. For AR, precipitation is reduced strongly in the core over the North Atlantic and expanding into Western Europe, while Eastern Europe is slightly wetter than usual. However, SOLD anomalies are mostly above average. During EuBL, nearly all of Europe sees below-average precipitation but also above normal SOLD. ScBL also shows expanded areas of suppressed rainfall, especially in Northern and Eastern Europe, while the Mediterranean region is wetter than average. The SOLD anomalies during ScBL are pretty sharp and strong. Cloudy anomalies are visible in the Mediterranean and North Sea area and opposite anomalies of the same magnitude are positioned in between.

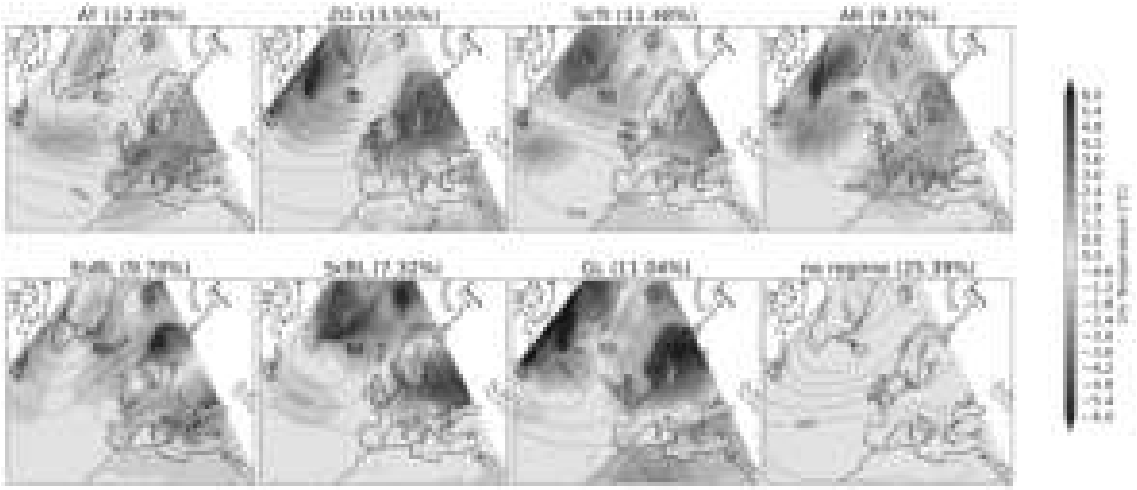

Figure 4.1: T2M anomalies in [°C] during the seven weather regimes and the no regime in shadings during DJF over Europe and the North Atlantic together with mean sea level pressure lines in black and units in hectopascal. The occurrence frequency of the regimes is given in brackets.

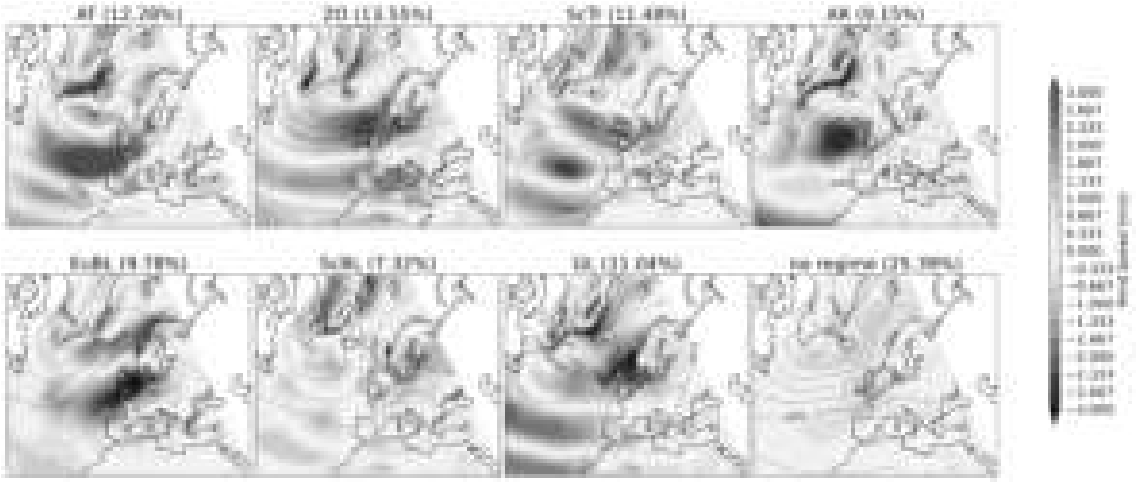

Figure 4.2: 100 m wind speed anomalies in [m/s] during the seven weather regimes and the no regime in shadings during DJF over Europe and the North Atlantic together with mean sea level pressure lines in black and units in hectopascal. The occurrence frequency of the regimes is given in brackets.

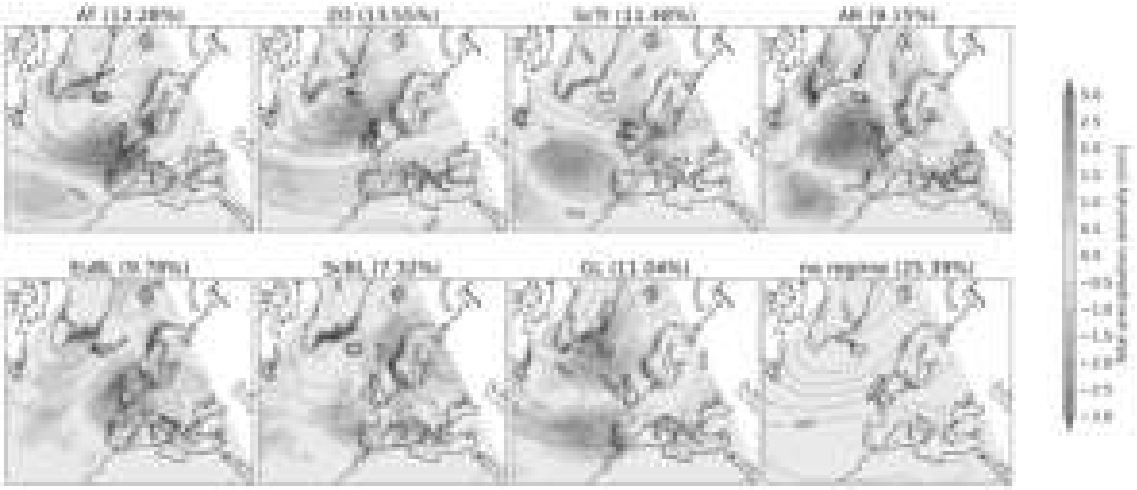

Figure 4.3: Anomalies in TP in [mm] during the seven weather regimes and the no regime in shadings during DJF over Europe and the North Atlantic together with mean sea level pressure lines in black and units in hectopascal. The occurrence frequency of the regimes is given in brackets.

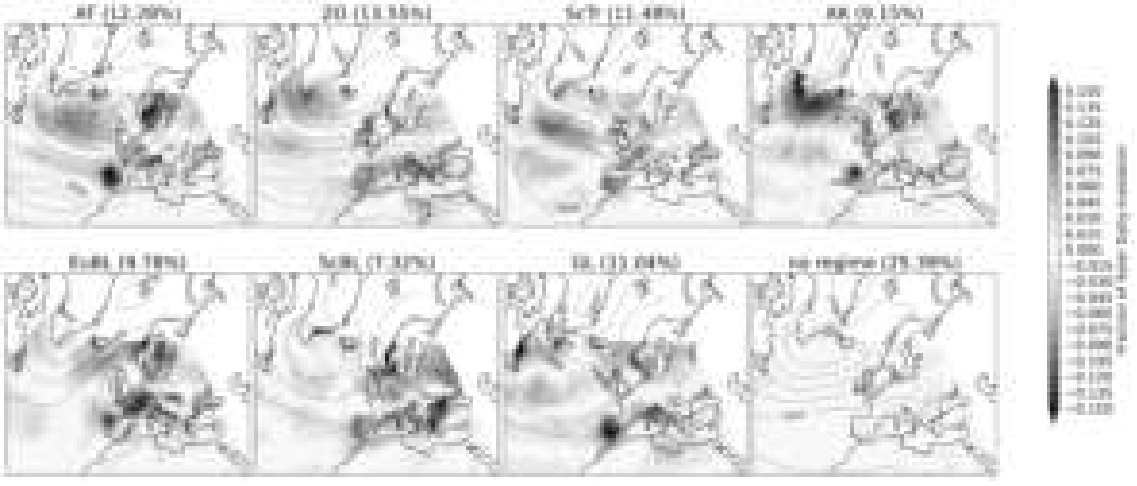

Figure 4.4: Fraction of SOLD anomalies during the seven weather regimes and the no regime in shadings during DJF over Europe and the North Atlantic together with mean sea level pressure lines in black and units in hectopascal. The occurrence frequency of the regimes is given in brackets.

4.1.2 Summertime anomalies

The atmospheric circulation of the Northern Hemisphere differs in summer compared to winter. The main differences are the weaker pressure and temperature gradient and, thus, a reduced baroclinicity compared to winter. This difference is driven by the changes in solar radiation that is enhanced in JJA. The temperature differences between the North Pole and the Equator decrease the pressure gradient. The lower baroclinicity leads to a lower formation frequency of cyclones and less intense cyclones. The blocking events in summer also change. While DJF blocking events are associated with radiative cooling in their core and cold air advection causing cold spells, the hot extremes frequently observed during summer are due to radiative and adiabatic warming.
Furthermore, JJA goes along with more convective precipitation events than DJF due to the increased heating of lower air masses by radiation, leading to more unstable atmospheric conditions. Moreover, the generally warmer air can carry more moisture according to the Clausius-Clapeyron-Equation.
Compared to the DJF anomalies, as expected, all variables show weaker amplitudes in JJA (see figures 4.5, 4.6, 4.7, 4.8). To a lesser extent, this is also true for the transition seasons (Appendix figures 1 to 8). In JJA, the separation between the blocked regime type being cold and the cyclonic regime type being warm cannot be made. AR is the regime that stays the most similar to its winter conditions during JJA. Cold and slightly windier anomalies cover large parts of the European continent, while the center of dry anomalies is now confined to the British Isles, and the remainder of Europe is wetter than average. Sunny SOLD anomalies can only be found there as well. The other regimes appear with more or less pronounced differences. EuBL and ScBL are now regimes that are associated with warm anomalies in Central and Northern Europe due to warm air advection from the Mediterranean as well as the formation of hot air in the center of the high-pressure system (Bieli et al., 2015; Pfahl & Wernli, 2012). The surface high-pressure system goes along with below-average wind speeds as well as sunny but very dry conditions, especially during EuBL. Cold T2M anomalies during GL now capture the entire continental Europe to some modest degree. The area with enhanced precipitation shifts from the Mediterranean in DJF to Central and Northern Europe and is accompanied by a slight enhancement of wind speeds and cloud cover. This can be explained by the northerly shift of the weak storm track caused by the expansion of the subtropical high-pressure belt.
For the zonal regimes, AT sees warm anomalies in Southern Europe and slightly cold anomalies in Scandinavia. ZO goes along with warm and sunny anomalies and ScTr with cold and cloudy anomalies. For ZO, the JJA low occurrence frequency of about 4% needs to be noted, strongly reducing the length of the already limited data set which is divided into four seasons with seven regimes each. An occurrence frequency of 4% equals about 3.8 ZO-days per year in JJA, thus a low relevance. As for all cyclonic regimes, the area with higher than usual wind speeds at the southern flank of the cyclone is more restricted and weaker but, overall, affects the same regions as in DJF. Wet anomalies are located more northward during AT and ZO, while for ScTr, they can be found more to the east.

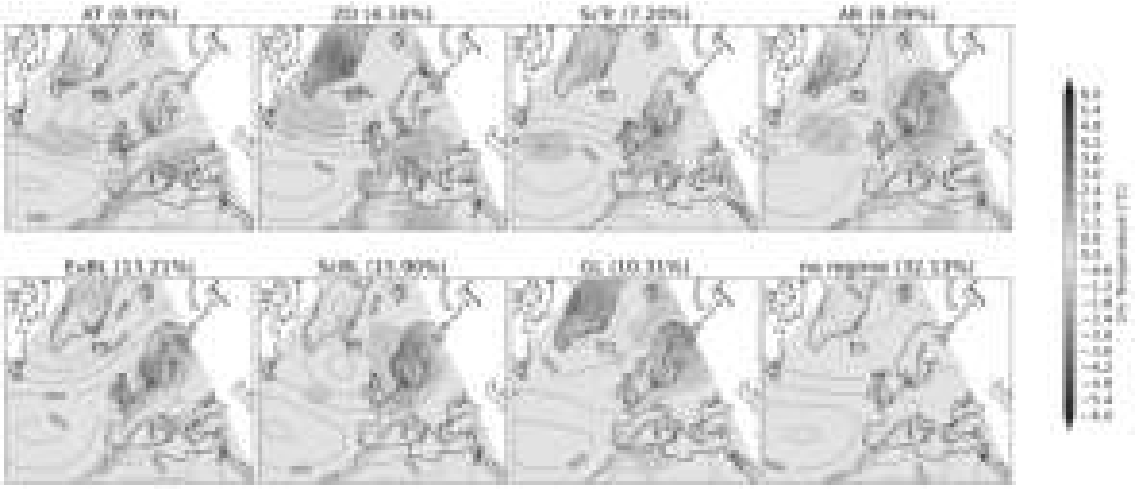

Figure 4.5: T2M anomalies in [°C] during the seven weather regimes and the no regime in shadings during JJA over Europe and the North Atlantic together with mean sea level pressure lines in black and units in hectopascal. The occurrence frequency of the regimes is given in brackets.

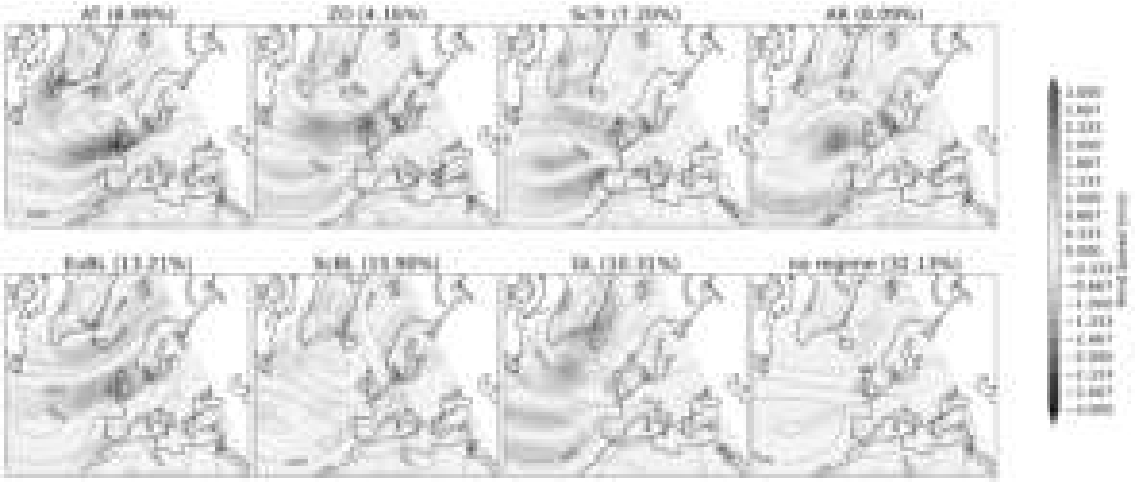

Figure 4.6: 100 m wind speed anomalies in [m/s] during the seven weather regimes and the no regime in shadings during JJA over Europe and the North Atlantic together with mean sea level pressure lines in black and units in hectopascal. The occurrence frequency of the regimes is given in brackets.

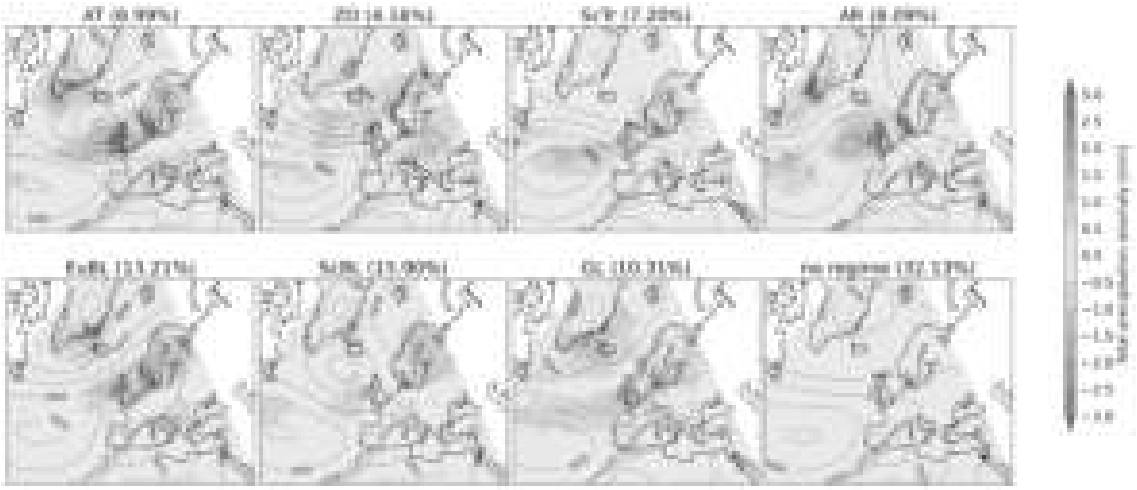

Figure 4.7: Anomalies in TP in [mm] during the seven weather regimes and the no regime in shadings during JJA over Europe and the North Atlantic together with mean sea level pressure lines in black and units in hectopascal. The occurrence frequency of the regimes is given in brackets.

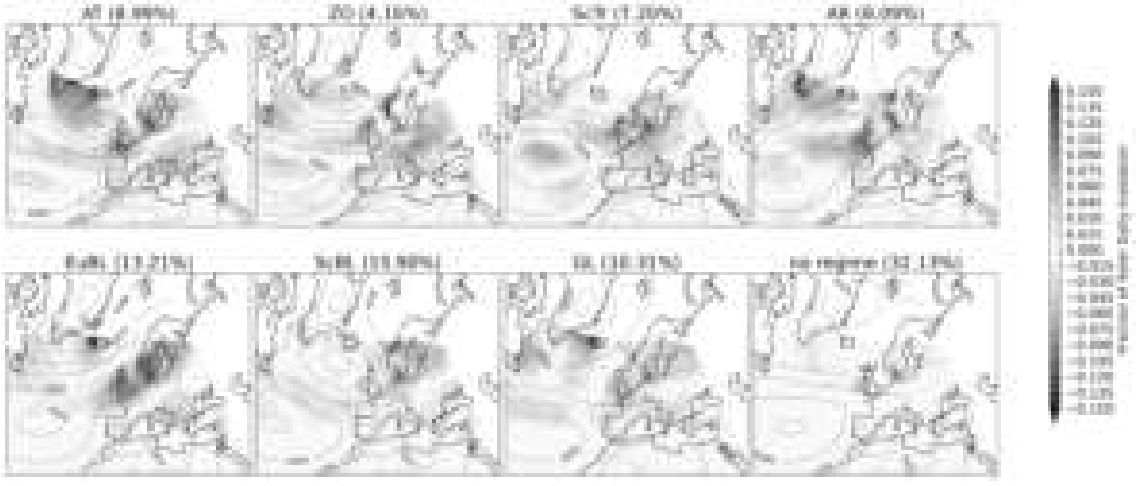

Figure 4.8: Fraction of SOLD anomalies during the seven weather regimes and the no regime in shadings during JJA over Europe and the North Atlantic together with mean sea level pressure lines in black and units in hectopascal. The occurrence frequency of the regimes is given in brackets.

4.2 Detecting weather variability during weather regimes

4.2.1 Overall picture in Europe

The mean anomalies allow an estimation of the upcoming weather, which is likely happening during a WR. However, using the concept of WRs in weather forecast applications, it is also very important to know when (strong) deviations from the mean occur and, furthermore, what is leading to the unexpected type of weather. In this section, the first step is taken to evaluate how strong the mean anomalies can vary across Europe by using the S2N and FStD. This combination of metrics increases the knowledge of occurring weather during a weather regime in comparison to the climatology and the mean anomalies alone. It is shown that some regimes vary more than others, and variability can not be neglected. While some regimes vary only for a certain variable, others vary for many at the same time and place, while still others do not vary that much at all. The variations strongly depend on region and season, but all contain some variability. Situations like the "unlikely variability" scenario presented in chapter 3 are windows of opportunity for regime-based weather forecasting at longer lead times. At these times, the link between the large-scale atmospheric flow and the surface is particularly strong. The scenario of "unlikely variability" means that the average impact of the regime is very likely and does not include large variations. This makes the situations more predictable than situations with high variability, such as "uncertain extremes," where the anomaly is likely but with variations, and "certain variability," where large variability is to be expected. Knowing that a regime impact is reliable increases the value of a weather regime forecast used to bridge the sub-seasonal forecasting gap. The enhanced reliability of the impact of the regime on a region allows better ahead planning, for example, of energy suppliers that can use this knowledge to assume energy consumption and production or plan maintenance. On the other hand, if S2N is low and FStD high, a situation is interesting for scientists seeking to explore variability, but for users, these situations are challenging due to the less reliability of the weather impact. Ahead-planning times are reduced, and it might suggest to users to hedge against both positive and negative extreme outcomes.

In winter, windows of opportunity with high absolute values of T2M (fig. 4.1), low values of FStD (fig. 4.9) resulting in high values of S2N (fig. 4.10) can be found for example during ZO around the North Sea, where the likelihood of warmer than normal weather is high or during AR in southern France, where it is likely to experience colder than normal weather, without large variations. In general, regions with a strong S2N signal are visible over the North Atlantic and encircled with a red line. In these areas, the anomaly, which is not necessarily the strongest, is very likely to occur. For example, this is the case for warm anomalies in AR, EuBL, ScBL and GL, as well as for the cold anomalies over the ocean for cyclonic regimes. The FStD can also have a strong co-located reduction, but the reduction in variability does not necessarily co-locate or constrain these areas. The lowest variability of surface weather can often be detected over the ocean, caused by the oceans being more homogeneous and isotropic than the land surfaces. In these "unlikely variability" cases, the regimes function how users might automatically assume they do. They can be relied upon to guide decision-making without further consideration.

The more interesting areas from a scientific standpoint are those where the mean of the anomalies hide variability or even mask the impact of the regime. No impact of a specific regime on a specific region is detectable (certain climatology), e.g., for wintertime T2M anomalies during ScBL or ScTr on the Iberian Peninsula.
Hints for variability in surface temperature are visible for EuBL and ScBL in Central Europe. The FStD is around 1, and S2N is below 1 but not 0. This points towards some variability but also to the frequent occurrence of anomalies close to the mean, as in the scenario "uncertain extremes". The scale of the actual range of variability is not apparent with this methods and further investigations are necessary, as done in the following section. Large variability is visible over northern Africa during AR and temperature anomalies of some degree are visible over northern Africa for many regimes. Since Africa is not the focus of this thesis, no further investigations are carried out in this region, but the results imply that the European WRs also have an effect on northern Africa, which could be a starting point for further research.
In this study, by far the most prominent example of increased variability, as scenario "certain variability" suggests, is GL over Western Europe and the Mediterranean. The FStD is well above 1 in large areas. The area co-locates with the area where the T2M anomalies switch from cold anomalies in France and Germany first to no anomalies from the Pyrenees to the Alps and eventually turn into warm anomalies over the Iberian Peninsula. The high FStD indicates that there is a large variability of the surface temperature, and the low S2N indicates that the signal of the mean anomalies is very low. This allows speculations that some GL events bring cold/warm anomalies much further southward/northward than expected by looking at the mean anomalies alone.

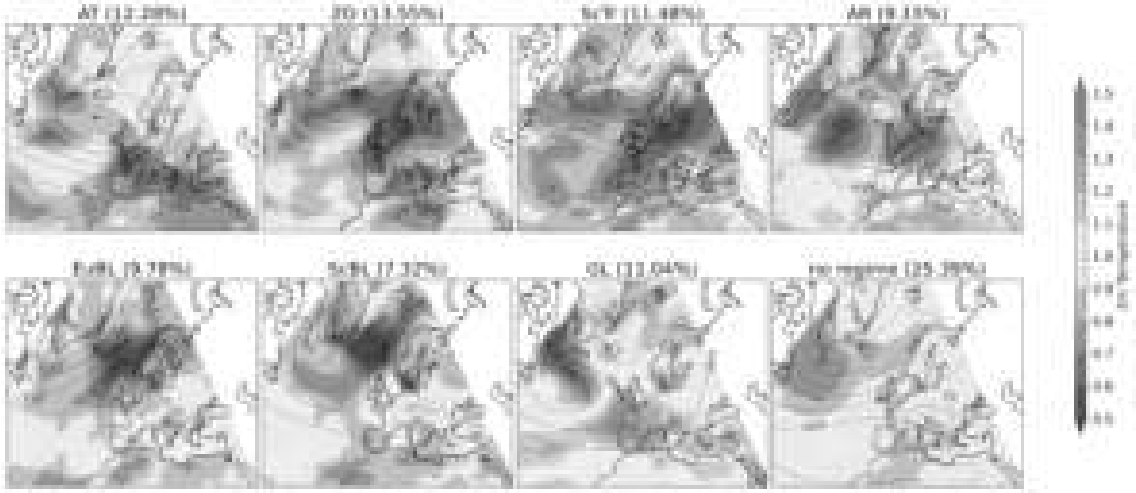

Figure 4.9: Fractional standard deviation of T2M anomalies during the seven weather regimes and the no regime in shadings during DJF over Europe and the North Atlantic together with mean sea level pressure lines in black and units in hectopascal.

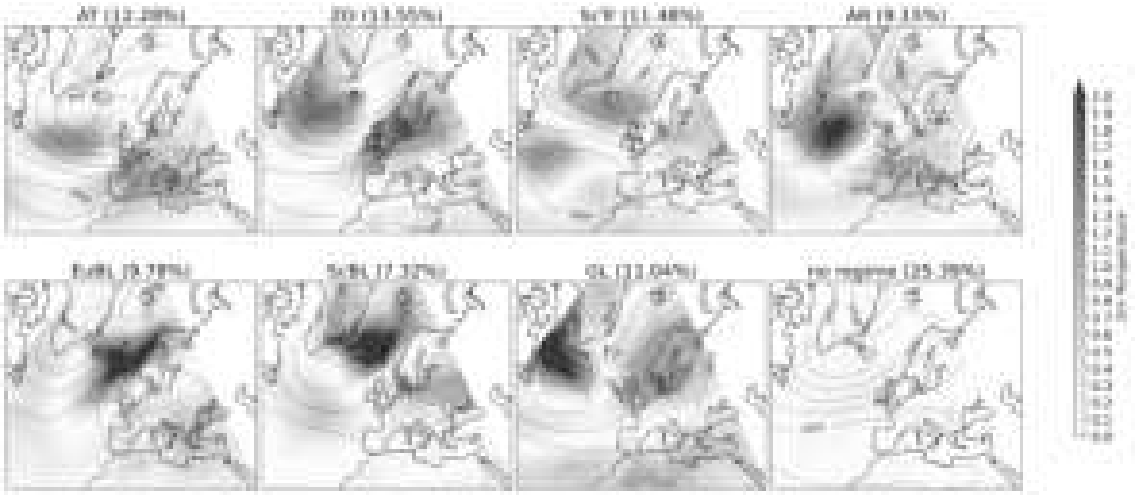

Figure 4.10: Absolute values of the signal to noise ratio of T2M anomalies during the seven weather regimes and the no regime in shadings during DJF over Europe and the North Atlantic together with mean sea level pressure lines in black and units in hectopascal. The red line indicates values above 1.

During summer, the signals into FStD fig. 4.11 and S2N fig. 4.12 for T2M are much weaker than during DJF due to weaker anomalies and a less variable climatology. The low signals cause less clear observations of variability in JJA. The FStD is mainly around 1, indicating that there is neither stronger nor weaker variability than climatology suggests. Lower values of FStD can be seen during the cyclonic regimes, while the blocked regimes are mostly around 1. Even over the oceans, where the lowest signals of FStD can be observed during DJF, the values are around 1 during JJA. This means more variability over the oceans during summertime blocked regimes.
The clearest signal in FStD is observable during ZO, where the low FStD values span from west to east over the North Atlantic, ultimately reaching the British Isles and Norway. There, the S2N is low. Together with the very low magnitude of the anomalies, this means little impact by the ZO regime compared to the climatological mean. Over the European mainland, where the anomalies are stronger during ZO, the variability is stronger than over the British Isles but reduced compared to climatology. The enhanced S2N supports this. Furthermore, high values of S2N can be observed to the south of Greenland alongside low (but not the lowest) FStD values and slightly cold anomalies. The warm anomalies over Central Europe are higher, but the S2N is lower, together with only a slightly reduced FStD. This means good predictability over the North Atlantic region and more variability over Central Europe. But again, ZO needs to be treated with caution .
AT and ScTr are more trustworthy, as both show slightly reduced values in FStD over large parts of Europe and regionally increased S2N, pointing towards lower variability. The main area of reduced variability is around the North Sea, giving a window of opportunity for predictability. For the blocked regimes, the temperature anomalies are more pronounced in the north of Europe than in the south, projecting into slightly higher S2N values. However, the apparent anomalies do not project into less variability. In fact, the variability is increased for most regions, compared to DJF, especially over the seas. Over the landmasses, AR and GL see the most notable changes. While GL sees slightly reduced variability compared to climatology (and strongly reduced variability compared to DJF), AR sees enhanced variability compared to climatology and DJF, making the mean anomalies less trustworthy.

As the anomalies, the S2N and FStD during the transition seasons are a mix between summer and winter signal (see Appendix figures 9 to 24). While the cyclonic regimes show low variability, EuBL and ScBL have medium variability, AR shows high variability in the Mediterranean, and the strong variability of GL is shifted northward to the coastline of the Atlantic and North Sea with the European continent.

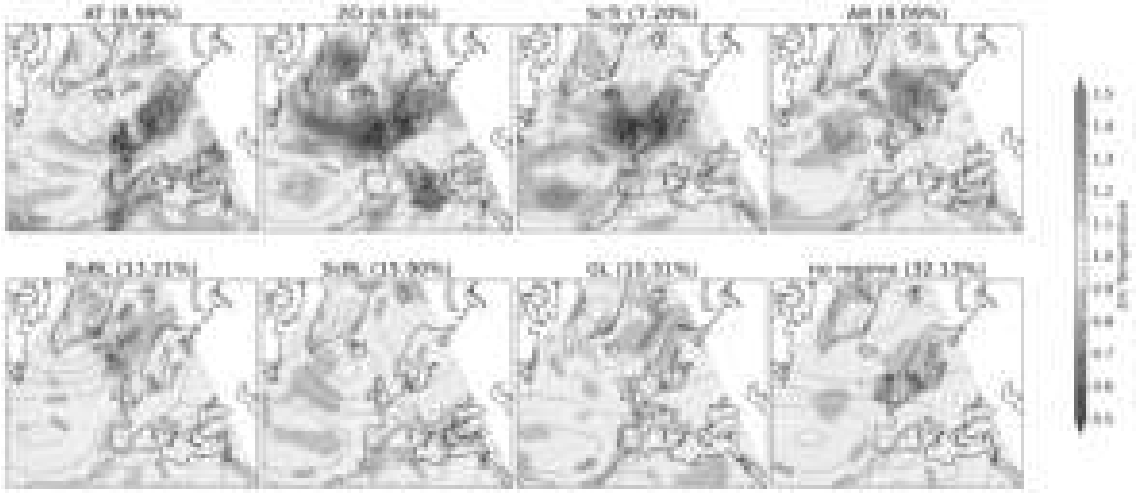

Figure 4.11: Fractional standard deviation of T2M anomalies during the seven weather regimes and the no regime in shadings during JJA over Europe and the North Atlantic together with mean sea level pressure lines in black and units in hectopascal.

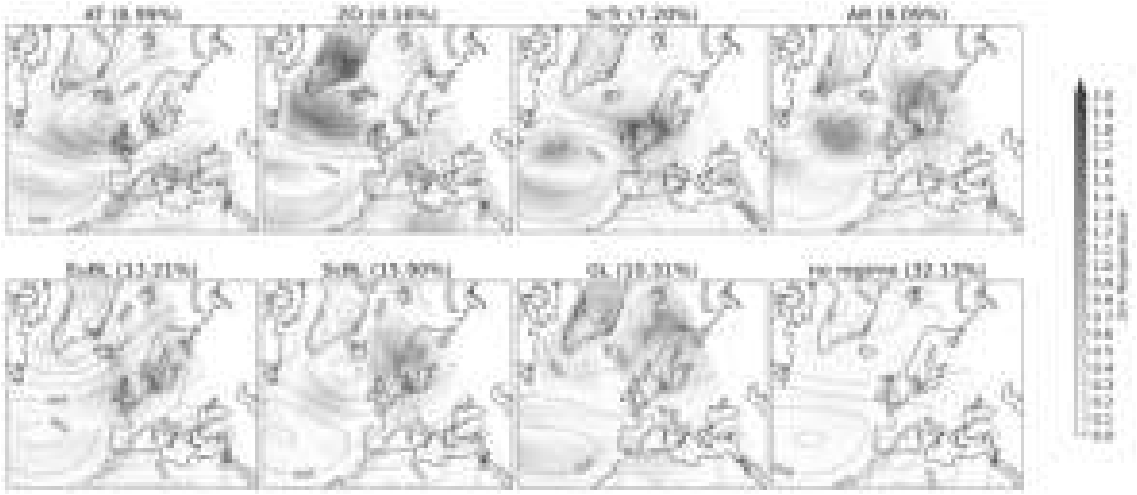

Figure 4.12: Absolute values of the signal to noise ratio of T2M anomalies during the seven weather regimes and the no regime in shadings during JJA over Europe and the North Atlantic together with mean sea level pressure lines in black and units in hectopascal. The red line indicates values above 1.

FStD for wind and SOLD is less pronounced and spatially more variable than T2M during DJF (figures 4.13, 4.15). Locally confined but strong FStD, as for example, for wind anomalies during AR, ScBL and EuBL around the Alps, shows very local effects on the variability within the weather. The local enhancement is also better visible than changes in the mean anomalies, revealing areas where the mean needs to be used with more caution than in other areas. To some degree, the local enhancement of FStD projects into S2N (figures 4.14, 4.16) but not as well, making FStD the more powerful tool to detect variability. The best window of opportunity for wind is given during EuBL in Western and Central Europe with low FStD, high S2N values and very calm anomalies, making it a perfect example of scenario B. GL and AR show larger areas with reduced variability as well, while the other regimes show more local differences. For SOLD in DJF, less variability can be expected during AT and ScTr over the entire Europe and more during ScBL and EuBL in Eastern and Central Europe, respectively. For ZO, AR and GL, the variability is moderately reduced, with enhanced variability over Northern Africa for ZO and AR and over the British Isles for GL.
The FStD for wind in JJA fig. 4.17 is more variable than during winter, and the S2N is weaker fig. 4.18. Areas with reduced and enhanced variability are much more local. While AT is the regime with the lowest variability for wind in JJA, the picture for EuBL and AR changes compared to winter. Both are more variable over Europe, and ScBL, GL, and ScTr also show increased variability.
SOLD during JJA shows less dramatic changes between the seasons than wind. AT shows a strong S2N signal fig. 4.20 and low FStD fig. 4.19, making it a regime with low variability. GL also shows a stronger S2N and lower FStD during JJA compared to DJF. SOLD during GL is less variable in JJA than in DJF. The same is true for the rare ZO over the continent, while over the Mediterranean Sea, the variability is strongly increased. Increased variability is also detectable for ScTr, AR, EuBL and ScBL. The former two change from a regime with decreased SOLD anomalies to a regime with anomalies, while during the latter two, the area with increased variability gets enlarged.
TP's FStD (fig. 4.21) is more variable than the one other the other variables (note the extended color bar). The large variations in Northern Africa are eye-catching, especially during DJF. Since precipitation rates are very low over the Sahara, even small amounts of rainfall can lead to a large variability. The above 1 values of FStD during DJF over Europe can be detected for AT in Western Europe, ScTr in Central Europe and GL in the same region as for T2M. During JJA, AT becomes a less variable regime in terms of TP, supported by S2N (fig. 4.22), while the variability during ScTr is relocated to Eastern and Northern Europe (figures 4.23 4.24). For GL, the area with enhanced variability moves further to the north with the area of enhanced precipitation, compared to DJF. Interesting changes are visible in AR over the western Mediterranean and during EuBL. While the British Isles and Scandinavia are certainly seen to be drier than normal, the Mediterranean and Central Europe see high FStD and low S2N signals alongside rather weak anomalies, indicating increased variability.
The results of TP need to be treated with caution, since hydrological data in a reanalysis tend to be more flawed than other variables. It is shown by Dulière et al. (2011) and Lavers et al. (2022) that ERA5 is capable of representing the spatial extent and temporal evolution of precipitation well but fails in a good representation of extreme precipitation. The reasons for that are related to convective precipitation with high precipitation rates but on a smaller scale than the grid and orographic effects. Other variables, mainly temperature and wind speed, are found to be represented well by ERA5 in

many regions (Molina et al., 2021; Velikou et al., 2022).

The novel approach of FStD and S2N detects areas with variability over Europe in different seasons and variables. It also shows how variability differs from region to region and highlights that some regimes are less variable across all variables, like AT in JJA. In contrast, other ones are more variable across all variables, like AR in JJA, and for many, it is dependent on the variable, e.g., ScBL in JJA or EuBL in DJF. The approach also shows that the variability is dependent on the relative position to the centers of action of a WR. Temperature and wind speed anomalies see low variability close to the southern flank in the case of cyclonic events, while for blocked regimes, it is regime-dependent. Variability in TP during winter behaves oppositely during cyclonic events, with increased variability at the southern flank. During blocked regimes, the variability is decreased close to the core of the high-pressure system for EuBL, ScBL and AR. During JJA, variability relative to the centers of action becomes very regime-dependent. SOLD in DJF and JJA behaves as T2M for the cyclonic regimes, while the blocked regimes see increased variability related to their core.

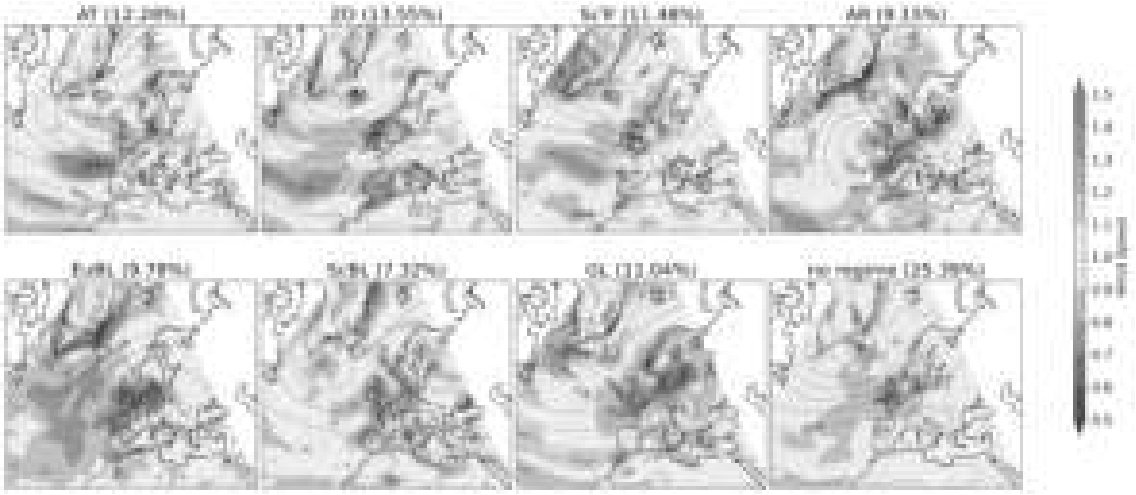

Figure 4.13: Fractional standard deviation of 100 m wind speed anomalies during the seven weather regimes and the no regime in shadings during DJF over Europe and the North Atlantic together with mean sea level pressure lines in black and units in hectopascal.

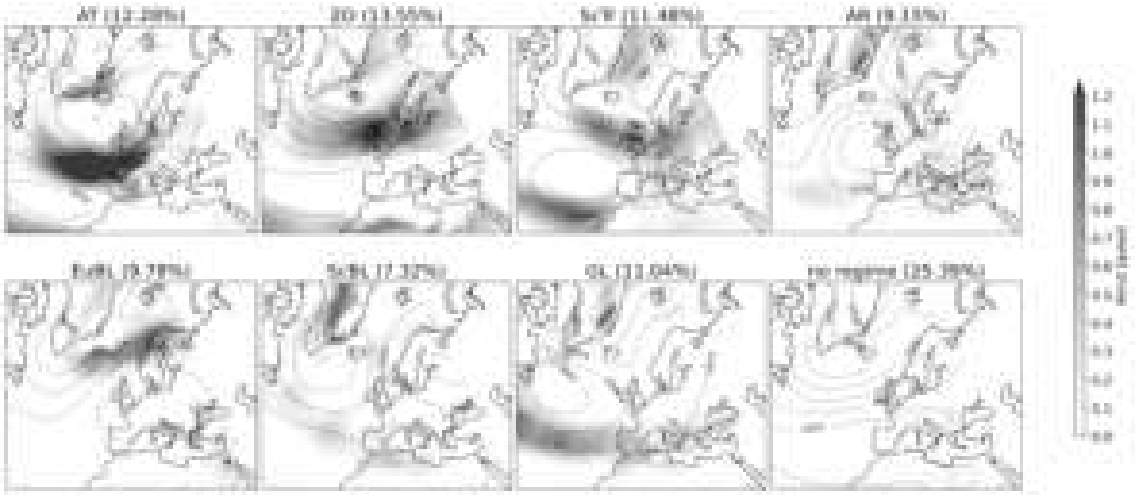

Figure 4.14: Absolute values of the signal to noise ratio of 100 m wind speed anomalies during the seven weather regimes and the no regime in shadings during DJF over Europe and the North Atlantic together with mean sea level pressure lines in black and units in hectopascal. The red line indicates values above 1.

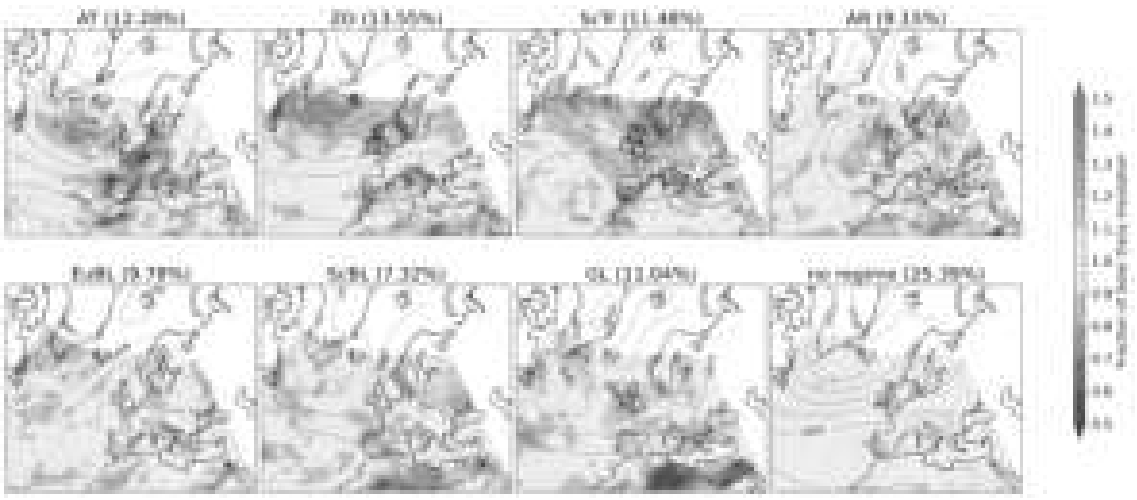

Figure 4.15: Fractional standard deviation of SOLD anomalies during the seven weather regimes and the no regime in shadings during DJF over Europe and the North Atlantic together with mean sea level pressure lines in black and units in hectopascal.

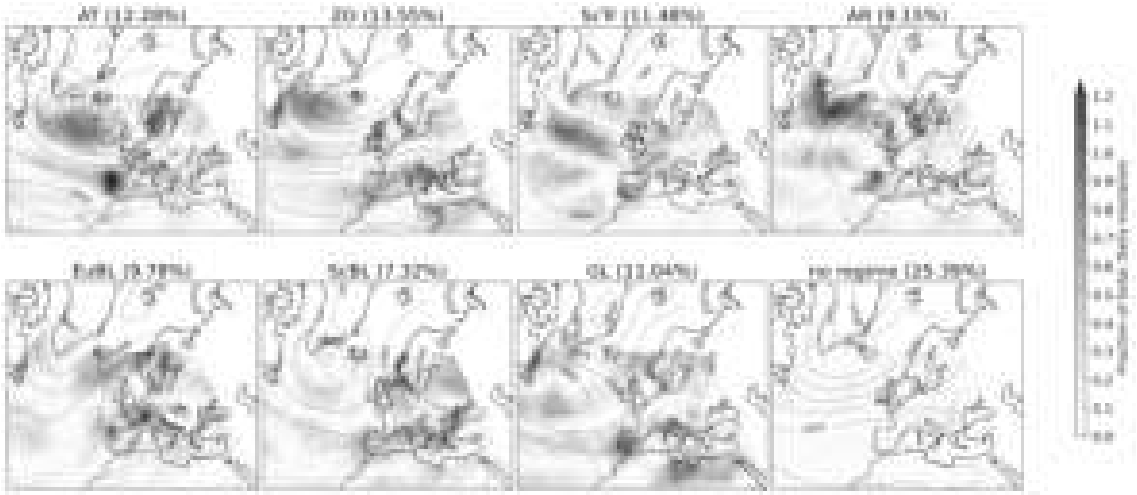

Figure 4.16: Absolute values of the signal to noise ratio of SOLD anomalies during the seven weather regimes and the no regime in shadings during DJF over Europe and the North Atlantic together with mean sea level pressure lines in black and units in hectopascal. The red line indicates values above 1.

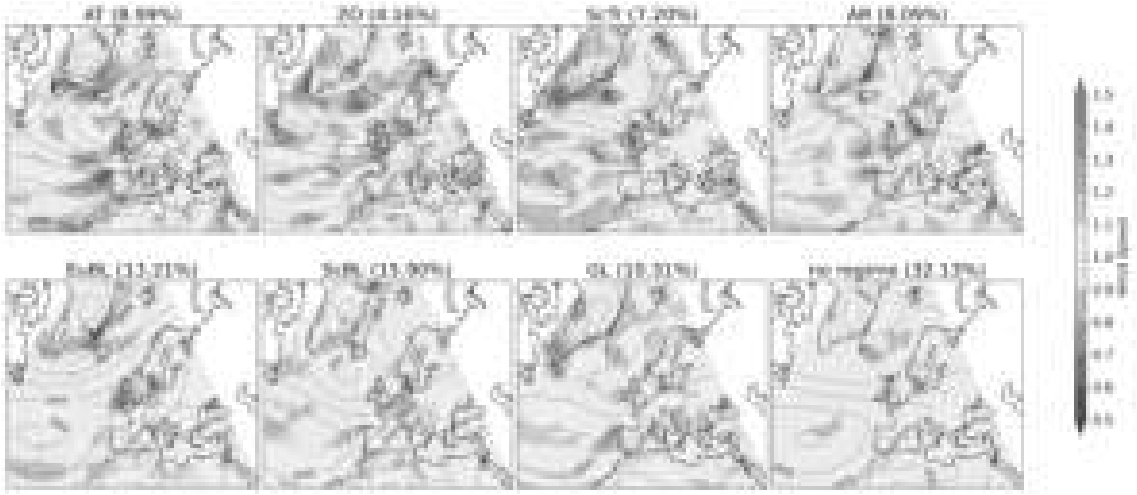

Figure 4.17: Fractional standard deviation of 100 m wind speed anomalies during the seven weather regimes and the no regime in shadings during JJA over Europe and the North Atlantic together with mean sea level pressure lines in black and units in hectopascal.

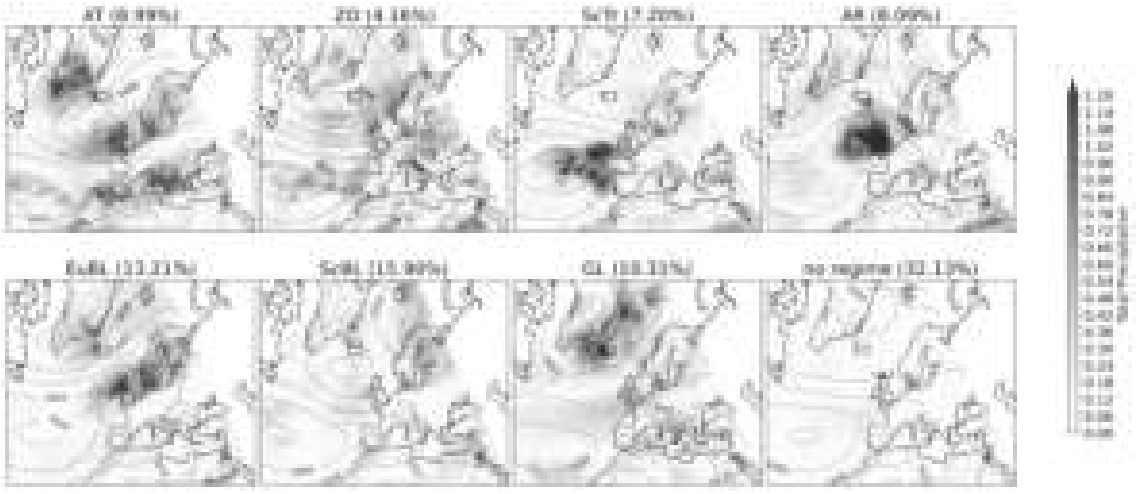

Figure 4.24: Absolute values of the signal to noise ratio of TP anomalies during the seven weather regimes and the no regime in shadings during JJA over Europe and the North Atlantic together with mean sea level pressure lines in black and units in hectopascal. The red line indicates values above 1.

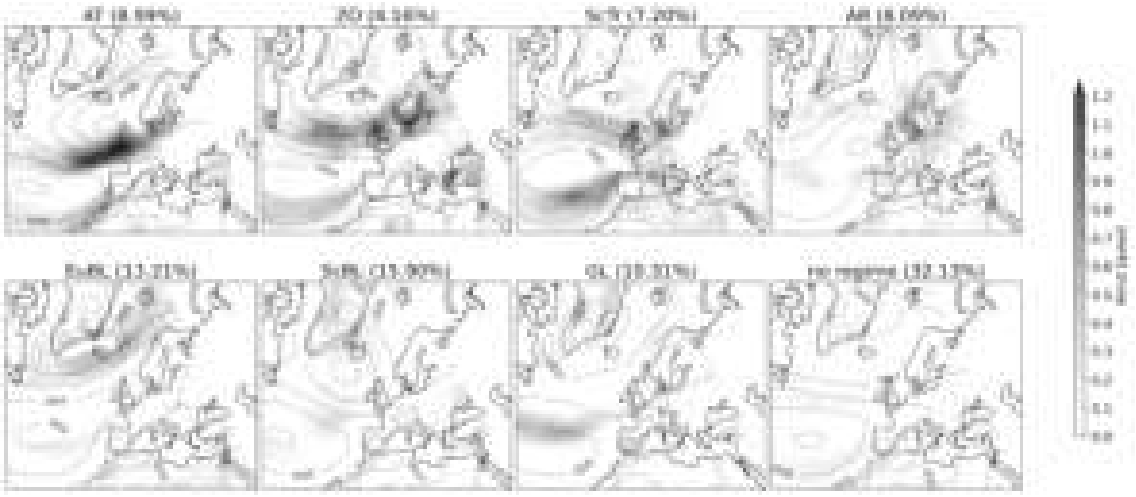

Figure 4.18: Absolute values of the signal to noise ratio of 100 m wind speed anomalies during the seven weather regimes and the no regime in shadings during JJA over Europe and the North Atlantic together with mean sea level pressure lines in black and units in hectopascal. The red line indicates values above 1.

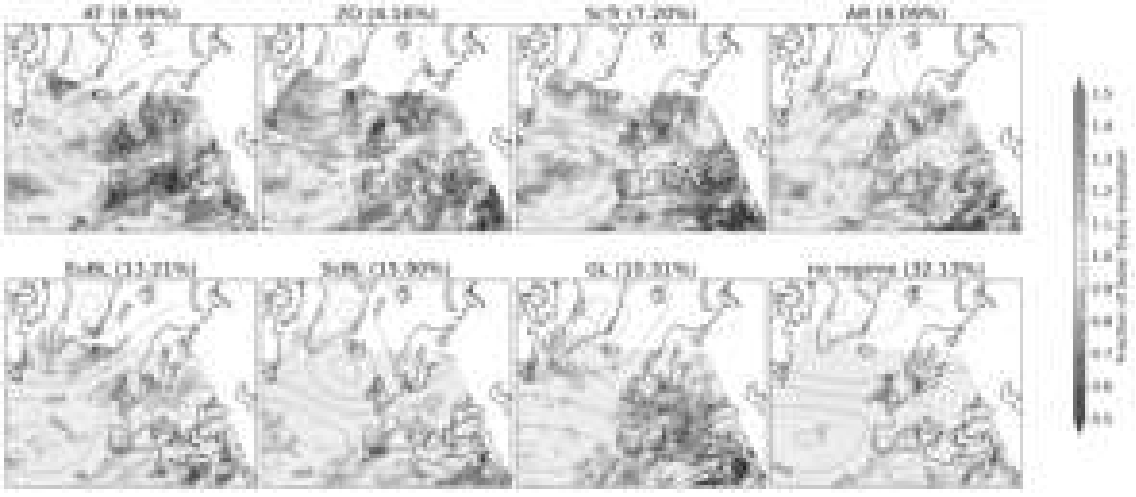

Figure 4.19: Fractional standard deviation of SOLD anomalies during the seven weather regimes and the no regime in shadings during JJA over Europe and the North Atlantic together with mean sea level pressure lines in black and units in hectopascal.

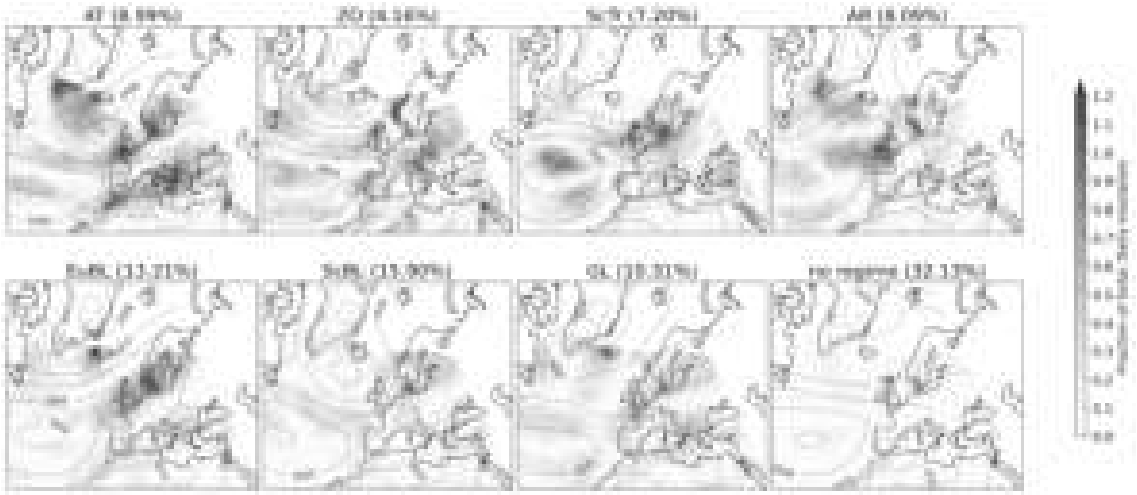

Figure 4.20: Absolute values of the signal to noise ratio of SOLD anomalies during the seven weather regimes and the no regime in shadings during JJA over Europe and the North Atlantic together with mean sea level pressure lines in black and units in hectopascal. The red line indicates values above 1.

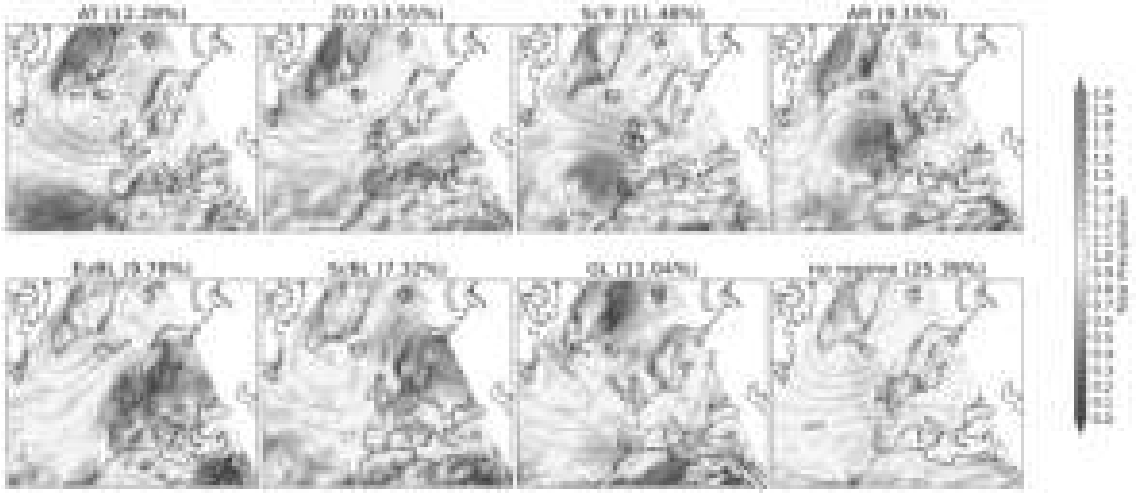

Figure 4.21: Fractional standard deviation of TP anomalies during the seven weather regimes and the no regime in shadings during DJF over Europe and the North Atlantic together with mean sea level pressure lines in black and units in hectopascal.

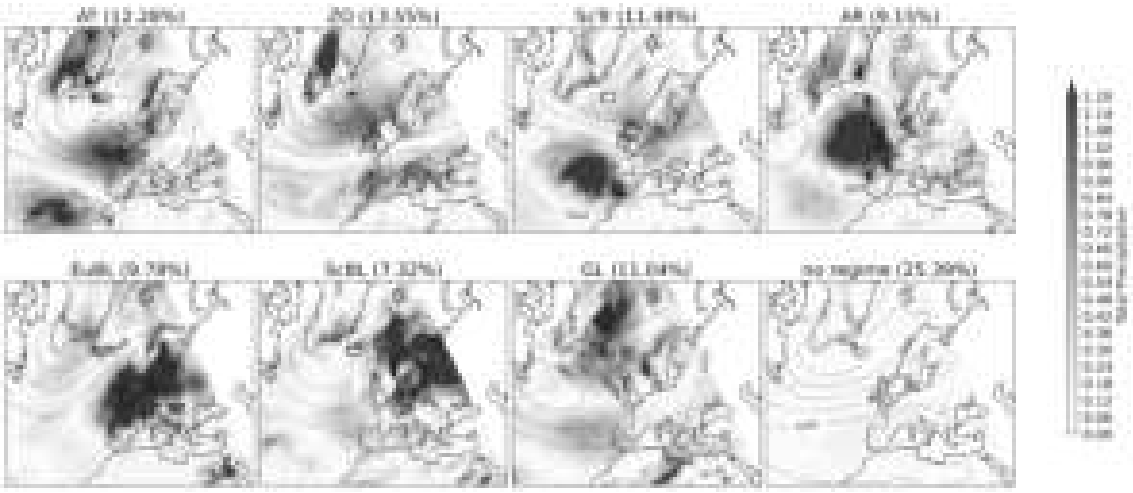

Figure 4.22: Absolute values of the signal to noise ratio of TP anomalies during the seven weather regimes and the no regime in shadings during DJF over Europe and the North Atlantic together with mean sea level pressure lines in black and units in hectopascal. The red line indicates values above 1.

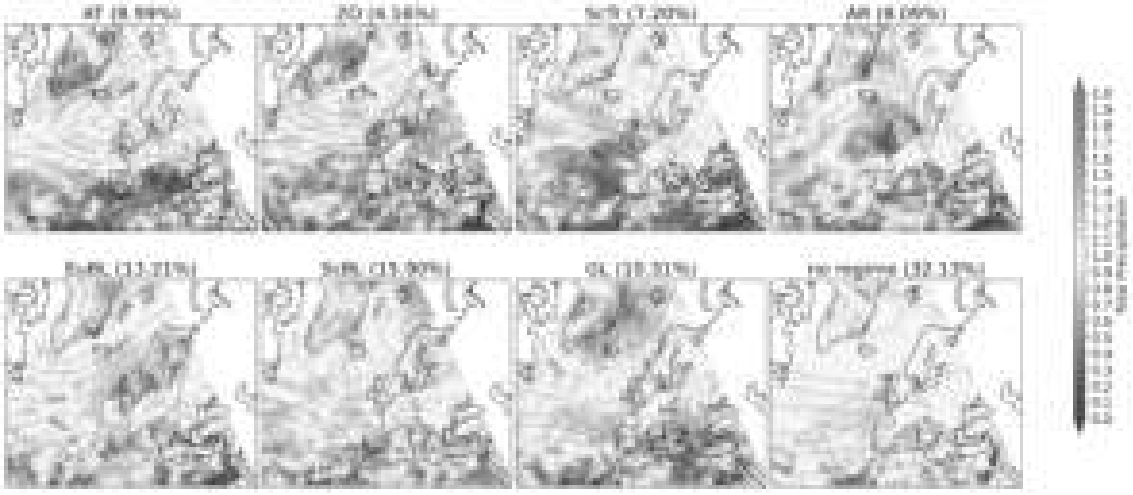

Figure 4.23: Fractional standard deviation of TP anomalies during the seven weather regimes and the no regime in shadings during JJA over Europe and the North Atlantic together with mean sea level pressure lines in black and units in hectopascal.

4.2.2 Country-based intra-regime variability

The FStD and S2N analysis already delivers a broad picture of where to expect variability and how it is varying between seasons, regions and variables. This is already an increased amount of knowledge compared to previous studies and shows that the mean can hide variability necessary to keep in mind if a precise forecast is desired. However, these methods measure the anomalies relative to the climatology and do not tell the absolute values of the anomalies. Therefore, in the second step, country-based violin plots of the anomalies are used. To get an easily understandable, eye-catching picture of the variability, all violins of the 7WRs of a season and variable are placed next to each other, alongside no regime and climatology.
The violins show the internal variability of weather during weather regimes very well on a country basis and also indicate how probable the occurrence of extreme values is. The violins further show how the variability changes from season to season and how regimes can reduce variability for one variable. Germany is chosen as the main focus of this study due to collaboration with German industry partners and its central location in Europe, leading to weather impacts from many directions. However, the analysis could be performed for any other country in Europe, which is not included here as it would go beyond the scope of this thesis.

Generally, the violin plots show that the absolute variability of values is larger in winter than in summer for all variables (see tables 1 and 2). The percentage by which a regime reduces variability compared to climatology is greater in DJF than in JJA and can strongly vary between the regimes. The violin plot of the T2M anomalies in Germany for DJF (fig. 4.25) shows large variability both between and within the regimes. It shows that every regime can produce values of above and below-average anomalies, even if considered a warm or cold regime. No matter how large the mean anomaly of either sign is, each regime contains days of the opposite sign. Yet their spread is smaller than that of climatology, especially when leaving out very extreme regime values located in the thin tails. With their small range of values, ScTr and AR are the least variable regimes in temperature in Germany. The violins of both regimes have a small spread of 13 K compared to approximately 25 K of the climatology. This is equal to a reduction of about 43%. Neither regime contains very extreme values of either sign in Germany and both bring anomalies of a medium scale. The difference between both regimes is - as already discovered in section section 4.1 - that ScTr is among the warm regimes, and AR is a cold one in DJF for Germany. As can be seen with the interquartile range, about three-quarters of the values of ScTr are above average, while the same amount of values is below average for AR, indicating that the opposite anomalies are not infrequent. If the opposite anomalies occur, the magnitude is with -6 K and 4 K not very large.

The cyclonic regimes of AT and ZO are, on average, much warmer than ScTr but also have a larger range of observed values and reduce the variability by 27% and 30 %, respectively. AT and ZO have their majority of values in the warm range, with the interquartile range being well above 0 K. Both regimes are the two warmest during DJF in Germany and make warm anomalies very likely, with the bulk of values gathering around 4 K. However, their coldest ever observed values are at -9 K and -8 K, increasing the variability to about 17 K for both. AT and ZO's most extreme cold

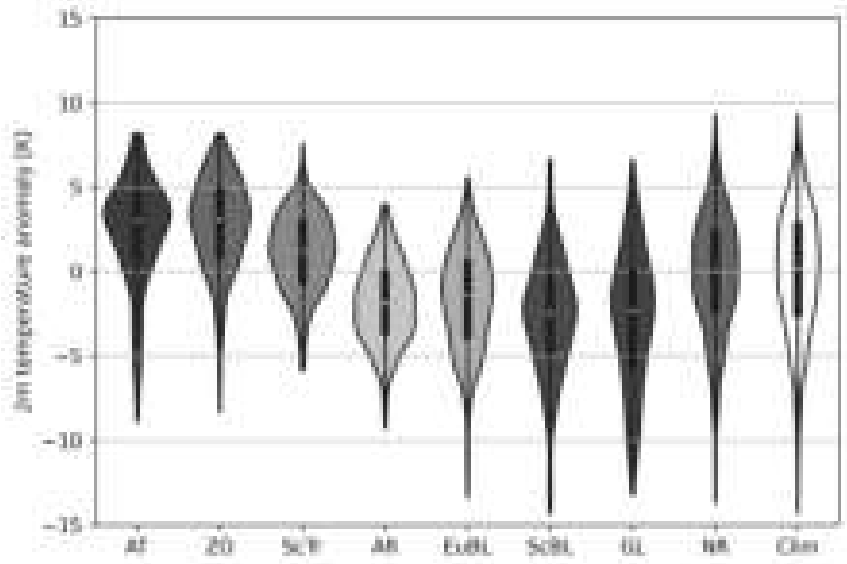

Figure 4.25: Violins showing the T2M anomalies in Germany for the seven weather regimes as well as the no regime (NR) and the climatology (Clim) during DJF. The white dot marks the mean of the anomaly for the regime, the bold black bar marks the interquartile range, and the thin black bar marks the 1.5 interquartile range.

values are outside the 1.5 interquartile range, making them outliers. The very low values shift the median slightly below the value where the largest probability is observed. In the case of AT, the extended probability is not driven by one single outlier, but several since the lower tail still shows some width. If considering that the lower ends of the distribution of both regimes are very narrow below -2 K, AT and ZO are also regimes that reduce the variability in the T2M range to approximately 10 K.

The blocked regimes EuBL, ScBL and GL share a large variability of 18, 21 and 20 K. Compared to climatology and no regime, this is only a small reduction in variability by 20, 11 and 16% and highlights the importance of knowing about the large variabilities. EuBL is the warmest of these three coldest regimes, with almost the same median temperature as AR. The difference between AR and EuBL is the spread of values, which also projects into the larger interquartile range of EuBL. The interquartile range of EuBL reaches the positive area, meaning that more than a quarter of EuBL days see warm temperature anomalies, which can reach values up to 5.5 K. But EuBL also sees more days below -5 K compared to AR and extreme values up to -13 K. The very cold days of EuBL are rare and probably driven by outliers represented by the narrow, small tail. Considering the low probability of extremely cold days during EuBL, it makes AR and EuBL interesting for applications. Both are considered cold regimes and likely to bring cold anomalies but unlikely to bring extremely cold anomalies. For Germany, very cold values are more likely to occur with ScBL and especially GL. ScBL has the widest spread of T2M anomalies of all regimes, and more than three-quarters of values are below the 0 K anomaly. The tails at the upper and lower end are wider for a larger range of values. An even flatter distribution with a large spread, spanning a total range of approximately 20 K is the case for GL, making it the most variable regime in terms of variability in DJF in Germany for T2M. While the coldest anomaly occurs under ScBL, almost equally cold anomalies are more likely under GL. GL has a wide distribution that shows some width above 5 K and below -10 K. This very wide distribution of anomalies corroborates the hypothesis that the

mainly cold regime GL in Germany, with the highest probability for the coldest anomalies, can also be associated with very warm anomalies.
It can be stated that the mean anomaly already gives a good estimation of the most likely anomaly. Still, it also hides the large variability possible within the regimes. Thus, the full distributions should be kept in mind when using the mean anomalies to consider the variability within the regimes. It is important to know that cold anomalies can occur during regimes considered warm during winter, and warm extremes can happen during cold regimes and are not limited to a few outliers, but their risk is strongly reduced. The full overview of the value ranges and percentage that a regime reduces the variability, including the variables of wind speed, TP and SOLD, is provided in table 1.

For summer, the picture of the variability within the WRs gets less clear for T2M (see figure 4.26 and table 2). Although the absolute variability is reduced, the relative variability is larger. The reduced weather variability expected when using WRs instead of the climatology is with 21% worse than in DJF (28%). The highest reduction in variability during winter is reached during AR and ScTr. During summer, ScTr is still the regime that reduces the variability the most, with 33%, and the worst regime is EuBL, with only 6%. Furthermore, the extreme values are not as strong outliers as the ones during DJF, meaning they must be considered more than during DJF. In absolute terms, the variability of climatology is 14 K, and for ScTr, the variability is 10 K, and for EuBL, it is almost 14 K. However, there is explanatory power within the regimes when using probability distributions. EuBL and ScBL, one could expect the hottest anomalies during JJA due to heat accumulation beneath the long-lasting high-pressure situation. This is true for the main proportion of days, as ScBL and EuBL are among the warmest regimes by their median values in JJA, with the largest part of the distribution above 0 K. But cold anomalies must be considered since more than a quarter of days are beneath the 0 K anomaly line. ZO also needs to be considered to bring anomalies of the same range as ScBL and EuBL if occurring. AT can get nearly as warm as the two blocked regimes with a maximum warm anomaly of about 6 K. However, the distribution is much different, with the median at around 0 K. GL is more on the cold side than AT but can also lead to warm and cold anomalies of a large range, almost as large as climatology. The remaining two regimes of ScTr and AR are the ones that are very likely to experience cold anomalies in Germany during DJF, and ScTr is the only regime where the distribution is clearly smaller than that of climatology.
For the other variables, wind, TP, and SOLD, pictures similar to those of T2M are given. In winter, some regimes lead to a strong reduction in the range of variability compared to climatology (figures 25, 27, 29), while in summer, this is not the case (figures 26, 28, 30). For wind and TP, these are EuBL and ScBL, which lead to very calm and dry anomalies with a decreased range. ScTr, on the other hand, is likely to be windy and wet in DJF but also in JJA. However, the reduction in the variability range is not as large. EuBL and ScBL, on the other hand, see large variations in wind and are among the most variable regimes for TP in JJA. For SOLD, no such seasonal variation is visible.
Placing the results in the view of energy meteorology means that the picture is more complex than just looking at the means and the capacity factors and deciding how the impact of a WR on renewables will be. For Germany, the cyclonic/blocked regimes show overproduction/underproduction in

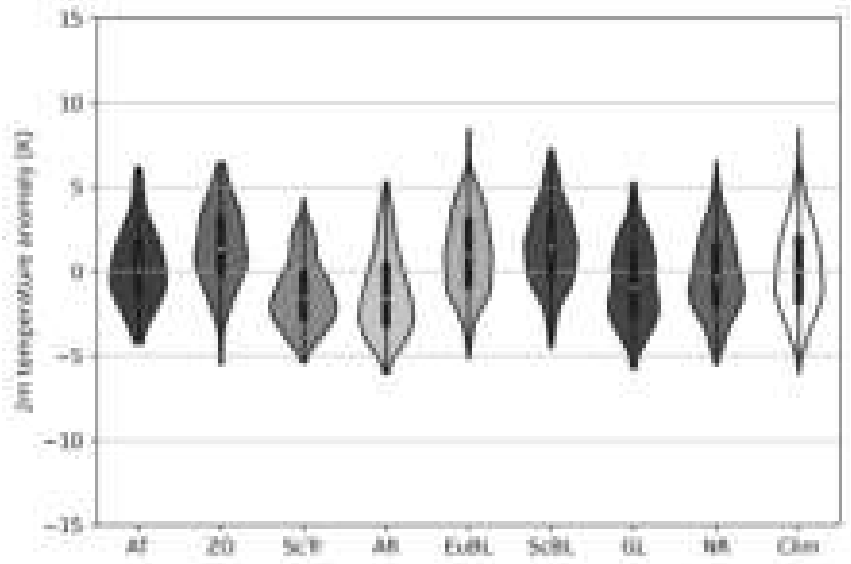

Figure 4.26: Violins showing the T2M anomalies in Germany for the seven weather regimes as well as the no regime (NR) and the climatology (Clim) during JJA. The white dot marks the mean of the anomaly for the regime, the bold black bar marks the interquartile range, and the thin black bar marks the 1.5 interquartile range.

the CFs for wind power during DJF on average (Grams et al., 2017). However, considering the variability in the wind, about a quarter of all days of the cyclonic regimes show less than normal wind speed, which affects the power output negatively and eventually leads to below-average CFs on certain days. On the other hand, the blocked regimes EuBL and ScBL (to a lesser degree GL and AR as well) show large reductions in variability, allowing assumptions that the underproduction of energy by wind is very likely.

Since the energy system based on renewables is not only dependent on wind speed variability, the possible partial balance by solar power (Mühlemann et al., 2022) and demand changes due to temperature changes and their probabilities need to be taken into account when evaluating the whole picture. Then, one can say that for winter in Germany, EuBL is one of the most reliable regimes with low wind speeds and cold, but unlikely extremely cold, conditions. But for solar power, which is less important during DJF, EuBL sees strong variability.

Regimes carrying low information about the variability for energy meteorology are ZO and ScTr. They vary less on the temperature side than the blocked regimes but very much on the wind speed side. Their wide distribution of wind speed anomalies, from clearly negative to extremely windy, leads to higher uncertainties in energy output. Therefore, wind energy can see overproduction during ZO and ScTr and also underproduction due to calm anomalies or the switching off of wind turbines due to too strong winds.

During JJA, when solar power is much more important, the picture becomes more heterogeneous, making AT the regime that seems to be most reliable across the relevant variables T2M, wind speed and SOLD due to low variability. It also shows that it is best to individually evaluate each regime, variable, season, and region since the methods used here only allow suggestions for the temporal and spatial correlation between them. Grams et al. (2017) mentions that stronger interconnections between power grids of different regions of Europe can reduce the susceptibility to energy shortages by renewables. In this scenario, one region can (partially) balance the power shortage of another

region. One example is the overproduction during ZO around the North and Baltic Seas, while the Mediterranean sees large underproduction rates. Considering the probability of low wind speeds during ZO around the North Sea, it is conceivable that the power exchange could fail due to the fact that there are too few amounts. This example shows the importance of further investigating the spatial and temporal correlation. Similarly, the methods do not allow a concrete statement of how the meteorological variability impacts the CFs. For energy applications, research on this specific question would complete the picture of the variability, but it is beyond the scope of this study.

4.3 Reasons for weather variability during Greenland blocking

4.3.1 Atmospheric flow and temperature distribution during warm and cold Greenland blocking days

To explore the differences between the average atmospheric flow and situations when the weather is far off from the average or "unusual", a comparison is made between them. As the T2M anomalies during GL in DJF seem to be a very interesting example due to the large spread, the dataset of the anomalies over Germany is first sorted by strength of anomaly from highest to lowest values and then divided into three parts, hereafter called terciles. The upper tercile contains the warmest third of data, the lower tercile contains the coldest third of data, and the middle tercile contains the remainder of the data with values in between. Using terciles instead of a certain number of extreme days makes the results more robust for evaluation without losing too much information on changed circulation/anomaly patterns. As can be seen in the comparison between figures 4.27 and 4.28, there are differences in the magnitude of the anomaly as well as slight changes in the circulation pattern, but overall, in terms of the distribution of the anomalies and the greater circulation pattern, the terciles and extremes are the same.

To provide consistency and due to the reasons already mentioned in the previous section, the flow pattern over Germany is analyzed during wintertime GL, although neighboring countries might seem more interesting. Since GL is a seemingly very interesting example due to the large distribution and variability across Europe indicated by the FStD, other European regions will be investigated later in this study in the following section 4.4. During GL in DJF over Germany, clear differences in the Z500 pattern are visible in figure 4.27 between the warmest tercile and the coldest tercile. The coldest days are much colder than the average anomalies. Although the cold anomalies are centered over Germany in this case, the extremely cold anomalies do not exclusively exist in Germany. They span wide areas in Europe, from northern France to Finland. Also, the British Isles are colder than normal, and the cold air masses reach the northwestern part of the Mediterranean as well, but the strength of the anomalies is getting weaker. Over northern Scandinavia, the cold anomalies are less pronounced than the average, while in the south, they are more pronounced. During these cold GL days, the temperatures over Greenland and the southeastern part of the Mediterranean are higher than during the average GL event.

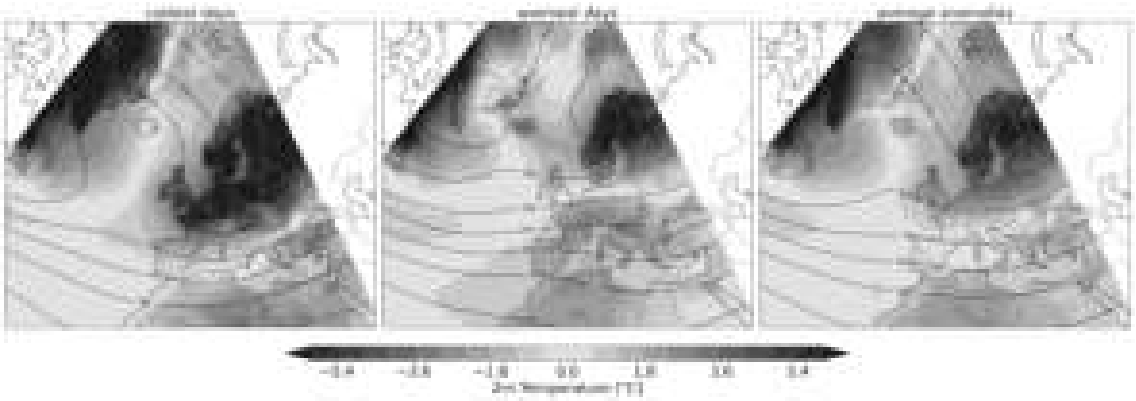

Figure 4.27: Coldest, warmest third of T2M anomalies centered over Germany during DJF during GL in shadings on the left and the middle. The average anomalies are on the right for comparison. The 500 hPa geopotential height during these dates is shown as black lines.

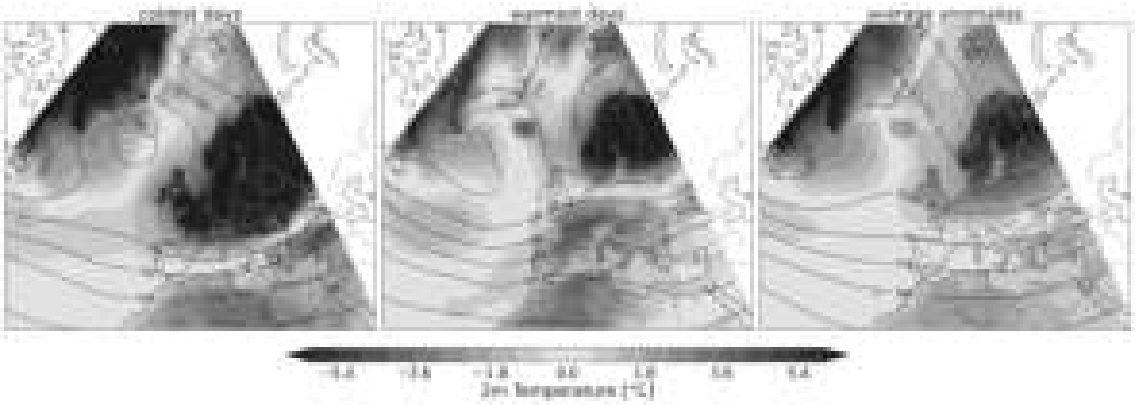

Figure 4.28: The 10 coldest and warmest days of GL taken from 10 different events over Germany during DJF in shadings on the left and the middle. The average anomalies are on the right for comparison. The 500 hPa geopotential height during these dates is shown as black lines.

By looking at the Z500 isobars for the cold tercile, it is visible that the ridge over the North Atlantic is wider, while the trough over northeastern Europe is deeper and more easterly tilted. According to literature, it is known that the advection of cold air masses from Russia and the Arctic is the main reason for cold spells in DJF over Germany (Bieli et al., 2015). Co-located blocking and nighttime cooling are not crucial for forming cold extremes over Germany (Kautz et al., 2022; Pfahl & Wernli, 2012). The enhanced easterly tilt of the trough over Scandinavia during cold GL days opens the passage for more and colder air from the north into central Europe. The ridge over the Atlantic blocks central and northern Europe from the inflow of mild air from the North Atlantic. The intense ridge causes the storm track to be displaced to the south, which can be detected when comparing the positions of the 540 hPa isobar, which is shifted south during the coldest days.
The position of the storm track is also the reason for warm anomalies during the warmest third of dates during GL over Germany. The exemplary 540 hPa isobar is located far further north and supplemented by the 525 hPa isobar, which does not describe the (intensified) ridge during the coldest/average anomalies. In fact, no ridge over the Atlantic is visible at all, giving way to the mild, oceanic air. If comparing the most extreme circulation patterns of figure 4.28, a decaying ridge is visible, pointing towards wave breaking at the end of a regime life cycle. The wave breaking

can result in regime transition and could mean GL's late stages favor warm anomalies. This deeper comparison between the circulation patterns of the terciles and extremes shows that when using the terciles, information can get lost due to the averaging. However, the main points are still visible and more robust. The extremes can be used as a supporting tool to clarify unclear situations. However, in both ways of investigating the warm circulation pattern of GL, above-average anomalies are present over most of Germany, being more intense to the south and slightly below average over the most northerly parts of Germany. France and the entire Mediterranean show warm temperature anomalies as well. Scandinavia, on the other hand, is showing cold anomalies that are intensified in the north compared to the average anomalies.
Looking at figure 4.27, the dynamics behind the temperature anomalies during GL in DJF seem to be clear, but it does not explain why GL in the one case is very intense, while in the other case, GL does not look like a GL event at all. In fact, over Europe, it looks more like a cyclonic event. In the next section, the reasons for this will be explored. However, these differences between the very intense and cold GL and the warm, cyclonic GL can explain the near-zero mean anomalies in parts of Europe as well as the very widespread distributions visible in the violin plots.

4.3.2 Flow pattern projections in the weather regime index

To see if and how the altered flow pattern is captured by the IWR, the lagged analysis of the upper and lower terciles of wintertime T2M anomalies of Germany during GL is performed. In the case of the lower tercile analysis, the dates contained in this tercile are the test dates and, thus, the point to where everything else refers. In the resulting figure 4.29, panel a, these dates can be found at time lag 0. The corresponding IWR is the blue, solid line of GL. The IWR represents the average IWR of these test dates. Further, the lagged analysis averages the IWR 3 hours before the test dates. By doing so in 3-hourly time steps for ten days before and after the test dates, the solid line forms and displays the evolution of GL events relative to the test dates, similar to the evolution of a single event explained in chapter 3. It allows to see if the test dates occur at the beginning of a regime life cycle, in the middle or at the end. This has further implications for interpreting the anomalies, as demonstrated later. The dashed line always contains the other two terciles of a regime and is added for comparison. In the case of testing the lower tercile of GL, the other two terciles are the upper and the middle one. To better see, when there is a significant difference between one tercile (solid line) and the other two (dashed line), the Kolmogorov-Smirnov test adds a bold dot to the solid line if the level is smaller or equal to the test level of 1%. Setting the significance level to the low value of 1% is more rigorous, making the results less likely to occur by chance and thus more robust. For all other regimes, the approach is performed while testing cold GL days in reference to the test dates. For example, the solid line of AR contains the IWR of AR during the cold GL test dates, while the yellow, dashed AR line holds the AR-IWR during the other two terciles of GL.

The analysis of the lower (cold) tercile of GL (fig. 4.29, panel a) shows that the GL-IWR reaches the peak already before the occurrence of the cold days and persists until after the occurrence of the cold days. It is known that the evolution of cold spells takes some time after the onset of blocking (Kautz et al., 2022). Compared to the dashed line, the IWR during the cold days is not significantly

stronger for the majority of time steps. This means that a cold GL event cannot be explained (fully) by an unusually strong GL in general. Instead, changes in the IWR of other secondary regimes contribute to a cold outcome of GL. The prime example of a contributing IWR is AR, which crosses the threshold to be considered an active regime about five days before the dates of interest on day 0 and continues to be active until 2 to 3 days after the cold GL days. AR peaks two days before the cold GL days and already declines during these days.
The AR-IWR differs significantly from its normal behavior during a GL event by rising above the threshold instead of slowly declining. This combination of GL and AR means that the circulation pattern of the Z500 level projects strongest into GL, but there is also a projection into AR that would be strong enough to be considered an AR if GL were not present. The strong ridge over the North Atlantic observed during cold GL days is captured within the regime framework by the strong IWR of AR. The stronger AR activity leads to a substantial reduction of the ZO-IWR. The ZO-IWR is significantly lower over almost the entire observed time period, starting about a week before the occurrence of the GL cold days. Around this time, the other cyclonic IWRs of AT and ScTr also start to become significantly lower than usual. At the same time, EuBL and ScBL are more active but not thought to be of the most importance for explaining the unusual GL appearances. The lowering in the cyclonic IWRs, especially of ZO, shows that changes in the flow can project into the regime with an almost opposite geopotential height anomaly signature, and this can be of significant importance. It also shows that a regime does not have to be "co-active". Positive or negative changes in an IWR very far below the threshold can be of importance in showing the "sub-flavor" of a regime.

In the case of the warm GL days, the situation is different, as expected by the different flow and temperature distributions during these days. The GL-IWR is considerably weaker than usual, and the warm days occur in the late, decaying stages of a GL cycle (fig. 4.29, panel b). The latter supports the hypothesis of the previous section about warm GL events. The temporal evolution of GL is not as rapid as the other GL events since the IWR is active already before this analysis starts at -10 days, and the end is at the same time as usual, pointing towards long-lasting GL events. Almost the entire IWR of GL is significantly different from the other two terciles, except for the region where the lines cross. The non-significant IWR is caused by the testing algorithm of the Kolmogorov-Smirnov test, which tests each step individually. The lines are too close in this area to be considered significantly different.
In the decaying stages of GL, AT becomes increasingly important by behaving completely differently to its normal behavior with a steep increase and crossing the threshold line of 1 by -4 days and lasting until +2 days. AT is much stronger than usual, especially before the warm GL days. The atmosphere projects more into ScTr and ZO as well and less into AR and EuBL, while for ScBL, there is no significant change. The prominent changes in AT and AR can explain the untypical warm appearance of GL. A weaker, longer-than-normal lasting GL and stronger than normal AT in the late stages of GL are the keys to understanding why a GL event can become warmer than average. The co-occurring AT opens the pathway to the advection of mild air from the Atlantic Ocean into Central Europe.
This means that changes in the IWR represent changes in temperature well and are a good indicator of the exact character of GL. Based on secondary IWR indices and the temporal structure of the event in IWR space, it is easy to distinguish between a cold and warm GL. The exact findings are

only valid for Germany and DJF. Other countries and seasons need separate investigations, but they show the possibilities of this approach.

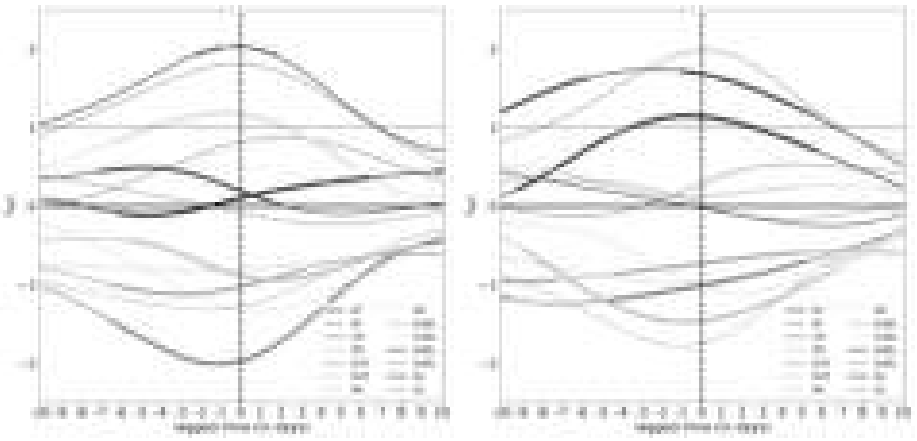

a b

Figure 4.29: 10-day lagged analysis previously and following the lower tercile days of GL over Germany during DJF (a) and the upper tercile days (b) of T2M. The dashed line of a regime represents the timely evolution of the other two terciles. Bold dots on the solid line indicate the significance of the particular regime at this time step compared to the dashed line.

4.4 The wider view of Greenland blocking

4.4.1 Wintertime Greenland Blocking across Europe

The FStD analysis for GL temperature anomalies during DJF in section 4.2 showed increasing variability from Scandinavia to the Iberian Peninsula. Germany is located in between, where the variability is already increased, but not as much as in the western Mediterranean. This makes it interesting to see if the enhancement of the variability in the western Mediterranean is driven by the same features and how the reduced variability of Scandinavia projects into the IWR analysis performed for Germany.

As an example of the Scandinavian region, Norway, is chosen. On average, GL is a very cold regime throughout Scandinavia. In the case of Norway GLs, the median anomaly is with almost -5 K by far the coldest of all regimes fig. 4.30. Furthermore, GL reduces the variability of the temperature anomalies compared to the climatology. Although EuBL reduces the variability the most, GL still reduces the variability range from 22 K (climatology) to approximately 14 K. This is a stronger reduction than observed in Germany, where GL varies in a range of 20 K compared to climatological variability of 25 K. This aligns with the observations in FStD and S2N, which point towards a low variability of anomalies. The anomalies during wintertime GL can reach warm anomalies up to 2.9 K but are much lower than in every other regime. For the coldest anomalies, only AT is in the range of GL for the coldest GL anomalies at -11.4 K.

The very cold nature of GL in Scandinavia also appears when comparing the coldest and warmest tercile to the average anomalies, as can be seen in figure 4.31. On average, the warmest days in Norway show only a slight cold T2M anomaly - in some regions, the anomaly is near 0 - indicating

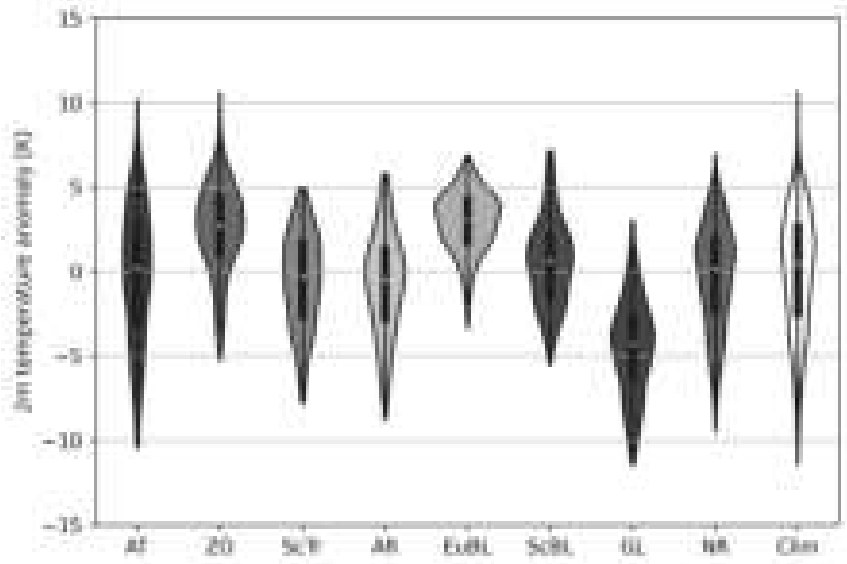

Figure 4.30: Violins showing the T2M anomalies in Norway for the seven weather regimes as well as the no regime (NR) and the climatology (Clim) during DJF. The white dot marks the mean of the anomaly for the regime, the bold black bar marks the interquartile range, and the thin black bar marks the 1.5 interquartile range.

that only a very small fraction of GL days see warm anomalies. The rest of Europe during this time is moderately cold, including the Mediterranean. The atmospheric flow pattern shows a strongly west-east tilted ridge over the Atlantic and Greenland, while the flow pattern over Europe is generally widened. The coldest anomalies during the warm days in Norway can be found in the Baltic countries and Russia.

During the coldest tercile of GL days, the anomalies are below -6 K in entire Scandinavia. They also spread into the surrounding countries of Central and Eastern Europe but with lower magnitude. In the Mediterranean, warm anomalies prevail, and the ridge over the North Atlantic is wider than on average, while the flow over Southern Europe is very zonally. The trough over Scandinavia is much deeper than on average. Overall, the coldest GL days in Norway look like a very intense version of the average.

The very intense GL for the coldest days is also visible in the lagged analysis of Norway figure 4.32, panel a. The IWR is significantly higher than the other two terciles, and the cold days appear at a very late stage of GL. GL is already decaying when the coldest anomalies occur, indicating that radiatively driven processes like nighttime cooling under clear skies play a more important role in the formation process of cold anomalies than it does further to the south. This makes the Scandinavian cold anomalies different from the Central European ones like the German GL, where the advection of cold air is considered more important (Bieli et al., 2015). Nevertheless, when exploring the details of the Norwegian cold days, one can see the significant enhancement of AR at around day -6, which is previous to the peak of GL at day -4, together with the strong decrease of the ZO-IWR. This is a parallel to the German example and could hint at some similarities in the formation process. However, at the time of the Norwegian cold days, AR is significantly below its comparison line, and AT is very active instead. ScTr is also significantly more active and - although being in the negative range of IWR-values - is together with AT the projection into the deeper trough over Scandinavia, intensifying the advection of Arctic air from the north, which seems to be the

second driver of the cold anomalies in Norway. ScTr and AT IWRs are enhanced on the expenses from EuBL and ScBL, which are significantly weaker than average. This is a further difference from the German case when ScBL and EuBL are enhanced during the occurrence of the coldest days.

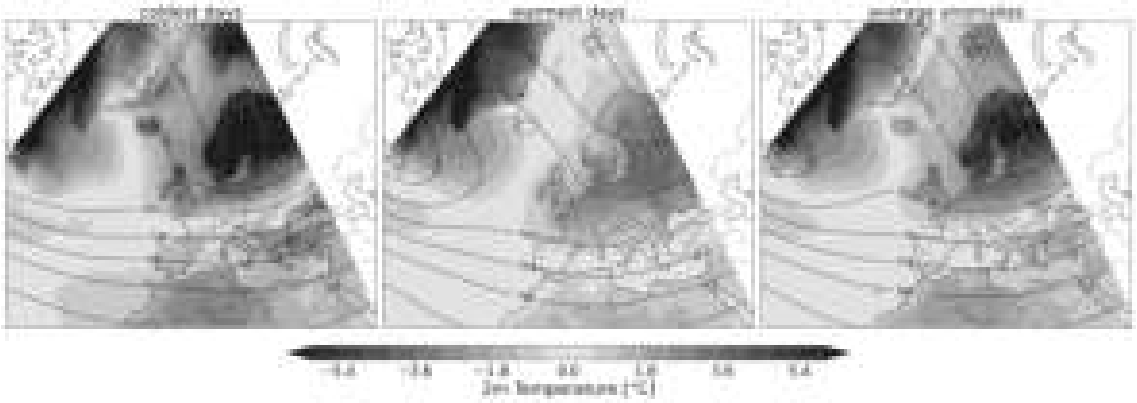

Figure 4.31: Coldest, warmest third of T2M anomalies centered over Norway during DJF during GL in shadings on the left and the middle. The average anomalies are on the right for comparison. The 500 hPa geopotential height during these dates is shown as black lines.

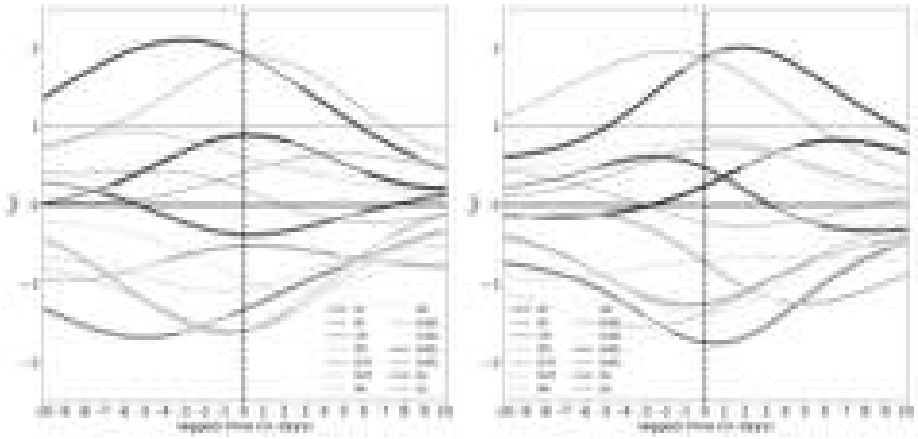

a b

Figure 4.32: 10-day lagged analysis previously and following the lower tercile days of GL over Norway during DJF (a) and the upper tercile days (b) of T2M. The dashed line of a regime represents the timely evolution of the other two terciles. Bold dots on the solid line indicate the significance of the particular regime at this time step in comparison to the dashed line.

As for the cold days, the warm days in Norway differ from the German example. Again, the temporal component of the GL life cycle seems to play the most important role. The warmest days of GL in Norway occur about five days after the onset of GL and two days before the peak of GL-IWR. During these days, GL is not significantly weaker than during the other two terciles. The wider flow pattern projects into the significant enhancement of the IWRs of EuBL and ScBL while the cyclonic regimes are all significantly lower. Together, this leads to a more shallow trough over Scandinavia, impeding the inflow of the very cold Arctic air from the north. While Norway sees reduced variability during GL in winter for T2M and experiences very cold anomalies in an already cold country, different drivers for the coldest and warmest anomalies during GL could be identified compared to Germany, where temperature variability during GL is much larger. Spain, which is identified to see the strongest variability during GL in T2M anomalies, follows the German case as presented in the following.

On average, the temperature anomalies over Spain are slightly warm during GL (see 4.1 again). The anomalies are stronger in southern Spain than in northern Spain, where there are no anomalies of either sign visible. Spain is identified as the area where there is the most variability to be expected by looking at the high FStD in figure 4.9 and low S2N in figure 4.10 during DJF. The widest distribution of temperature anomalies in Spain is observed during GL with 13.6 K (fig. 4.33. The distribution is only a bit smaller than climatology (15 K). It is also visible that GL is, on average, the second warmest regime in Spain during DJF, only exceeded by AT. Looking at the interquartile range of GL, it reveals that more than 50% of GL days are on the warm side, and the median is not located in the middle of the interquartile range but above, pointing towards the wide range of possible temperatures. Cold anomalies are not unlikely in Spain during GL either, as can be seen by the strongly skewed distribution. The coldest anomalies reach about -7 K, which is surprisingly cold for one of the warmest regimes in Spain. If users rely only on the average values, they will be right in most GL days. However, one can be caught up in unexpected cold anomalies, as shown here. This can, for example, lead to increased electricity consumption due to increased heating, leading to unplanned electricity demand and thus to increased costs. Someone aware of this possibility of extremely cold anomalies can better estimate such weather situations and thus reduce costs, especially if there are indications, as shown for the German GL days and will be shown for the Spanish days in the following.

The tercile and lagged analyses reveal a quite similar picture as to the situation over Germany. When comparing the cold tercile days, the T2M anomalies are overall somewhat weaker over the northern half of Europe but reach south into the Western Mediterranean, where the anomalies are well below 0 K (see figures 4.34 and fig. 4.27). The overall flow pattern almost looks like during the cold days in Germany. The strong ridge visible during the cold days in Germany is almost in the same position during the cold days over Spain. The differences are the slightly more expanded trough over central Europe where the 530 hPa line reaches the Spanish-French border instead of crossing France in its center. Also, the 540 hPa isobaric line shows a difference with a curvature to the north over the Atlantic and to the south over Spain. Together, this leads to the advection of cold air towards Spain, which explains the cold anomalies there. The lagged analysis for the lower tercile shows a strong, significant enhancement of AR and a strong, significant

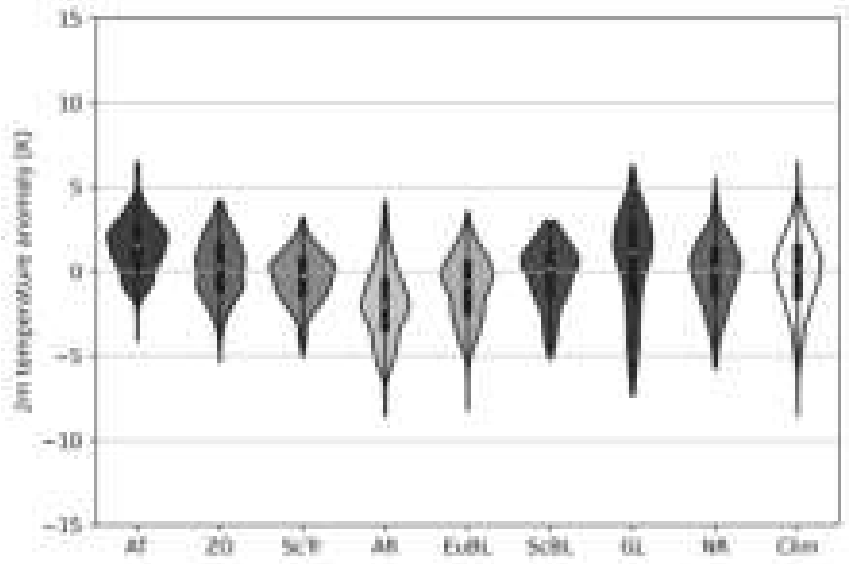

Figure 4.33: Violins showing the T2M anomalies in Spain for the seven weather regimes as well as the no regime (NR) and the climatology (Clim) during DJF. The white dot marks the mean of the anomaly for the regime, the bold black bar marks the interquartile range, and the thin black bar marks the 1.5 interquartile range.

reduction of ZO. The AR-IWR becomes very much pronounced during the six days before the cold days and lasts until two days after the peak. At the same time, AT is suppressed compared to the other two terciles and gets stronger as AR-IWR begins to lower. ZO is lowest between -2 and -1 days before the cold days and lower during the whole analysis. The IWR of GL itself is not significantly different from the other two terciles before the cold days. Still, after day 0, the differences become significant since the GL-IWR remains at a higher level for longer periods. Compared to the peak, the cold days occur around the beginning of the peak GL-IWR, where AR plays a role in the early days of the GL event, leading to the ridge over the North Atlantic, blocking the inflow of mild air and allowing the advection of cold air across the European continent. This suggests that the cold anomalies over Spain depend more on cold air advection than on radiative cooling during the duration of GL since this process takes time to evolve cold anomalies.

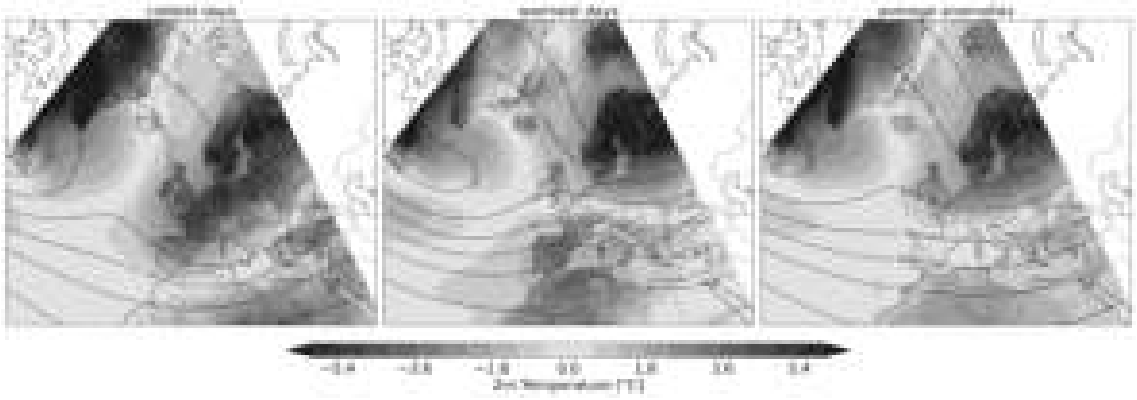

Figure 4.34: Coldest, warmest third of T2M anomalies centered over Spain during DJF during GL in shadings on the left and the middle. The average anomalies are on the right for comparison. The 500 hPa geopotential height during these dates is shown as black lines.

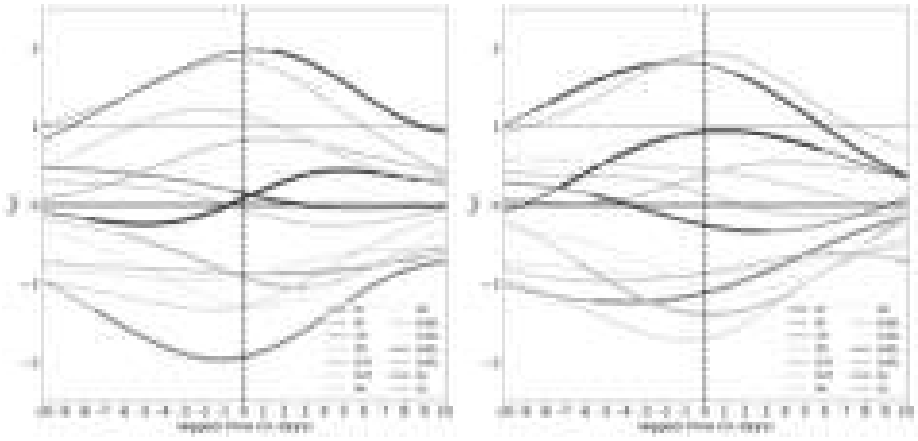

a b

Figure 4.35: 10-day lagged analysis previously and following the lower tercile days of GL over Spain during DJF (a) and the upper tercile days (b) of T2M. The dashed line of a regime represents the timely evolution of the other two terciles. Bold dots on the solid line indicate the significance of the particular regime at this time step in comparison to the dashed line.

The warm tercile days over Spain are much warmer than during the average GL days (fig. 4.34). Above-average T2M anomalies also occur over the entire Mediterranean area and France. The border between warm and cold anomalies reaches from the English Channel across Germany and Hungary to the Black Sea. On both sides, strong T2M anomalies can be found. Compared to the German warm terciles, the warm anomalies are stronger and located further south. During German warm terciles, the cold anomalies are restricted to Scandinavia, while during the Spanish warm terciles, Eastern Europe and the British Isles experience cold days. Compared to the cold terciles, where the flow pattern for Germany and Spain looked about similar, the differences for the warm terciles are larger. The high-pressure zone over Greenland is still visible on the Z500 level, although being more west-east-tilted as in a decaying state of a GL. The isobaric lines over Southern Europe are closely together and show a northerly curvature over the Iberian Peninsula. In the lagged analysis, the warm days occur in the late stages of a GL, with a rapidly decaying GL afterward. As for the German warm days, during the Spanish warm days, the activity in AR is reduced and enhanced in AT and ZO during the decaying GL. This means after the peak of cold days, the breakdowns of GL are often warmer than the average. During the other blocked regimes, the warm anomalies are mainly observed during the beginning of the life cycle when the cold air advection has not yet reached the area of cold anomalies and the outgoing radiation has not had enough time to cool the area. During GL, the cold air is replaced by warmer air from the Atlantic Ocean transported by the more northerly positioned storm track when the high-pressure system over Greenland does not have the power to redirect the storm track, which leads to the projection in the secondary IWRs. Whether this is simply due to the reformation of the atmospheric flow pattern or if further contribution factors are the driver behind the increased/decreased projection into AT+ZO/AR is not clear at this stage. In literature, it is shown that the stratospheric polar vortex and, ultimately, the frequency of Rossby wave-breaking events play a role in modifying the odds of certain weather regimes occurring that are closely related to the phases of the NAO (GL with NAO-, ZO and ScTr with NAO+) (Beerli & Grams, 2019; Osman et al., 2023). They showed that ZO and ScTr are twice as frequent if the polar vortex is strong and the number of Rossby wave

breaking is low. Since AR and AT are known to be less influenced by that, it is unclear if these findings can easily be transferred and show that more research on the influence of the Stratosphere, Rossby waves and other contributing factors on secondary regimes would be beneficial.

4.4.2 Behavior of other variables in wintertime Greenland blocking

The same analysis can be repeated for the other variables, with the example of wintertime GL over Germany. On average, the wind speed anomalies are below average over Germany, with the stronger winds in the north (fig. 4.2). The S2N shows intermediate values (fig. 4.14), also with the higher values in the north and FStD is below one (fig. 4.13). Together with the violin plot of wind (fig. 4.36), it becomes apparent that below-average wind speeds can be expected in Germany most of the time, but there can be some variability with above-average wind speeds, especially in southern Germany where the anomalies, the S2N signal and the FStD point towards slightly more variability. Looking at the calm third of the anomalies (fig. 4.37), the ridge over the Atlantic is stronger than average, increasing the magnitude of the anomalies more than the spatial extent. In the corresponding lagged analysis (fig. 4.38, panel a), the GL events of calm days tend to be shorter, and the strong ridge does not project into a stronger GL but into strong, significant AR, as in the temperature example. A small proportion goes into the stronger projection of EuBL, while all other IWRs are reduced or unchanged.
During the windy days of GL in Germany, above-normal wind speeds occur, especially in the southern part. The Z500 flow pattern shows a northward-shifted storm track. The ridge over the Atlantic is not as visibly reduced as during the warm days of GL since the 520 hPa isobaric line still shows the bend towards Greenland. The shift of the storm track projects mainly into the lagged analysis by significant enhancement of AT and reduction of AR and EuBL (fig. 4.38, panel b). AT peaks on day 1 after the windiest anomalies in the late stages of a long GL event.
For precipitation anomalies, the analysis is almost the same as for wind. But there are some minor differences. First of all, the average anomaly is around 0 (fig. 4.3), no S2N signal (fig. 4.22) and a slight tendency towards increased variability indicated by the FStD (fig. 4.21). In the violin plot, GL is the most variable blocked regime (fig. 4.39). However, it is still less variable than the cyclonic regimes and climatology. The dry anomalies are associated with a more than normal pronounced ridge that projects mostly in AR (fig. 4.41, panel a). Since the isobaric lines over Europe are a bit further spatially spread across the continent, there is also a stronger projection into EuBL, although the value is still very negative. ZO and AT are again reduced. GL-IWR is lower in the beginning but only partially significant, and the dry days occur more toward the onset of GL. The partial significance could mean that some dry GL events are actually significantly lower than the wet and middle ones but are balanced by others that behave more like the average GL. This underlines the importance of the secondary regimes. The wet GL days occur with a narrower trough over the Atlantic, projecting into less AR and leaving space for stronger cyclonic regimes (fig. 4.41, panel b). As in all examples before, this is mainly due to AT.
Although SOLD is not highly relevant to the production of renewable energies by solar power due to the short duration of sunshine in DJF, it is noteworthy to consider this in order to complete the

picture of GL. SOLD also has an around 0 anomaly in Germany and is the least variable regime for it (fig. 4.42). As one would suspect, the cloudiest GL days occur together with a significant enhancement of AT and ZO, while AR and EuBL are reduced (fig. 4.44, panel a). GL is already decaying as the anomalies occur well beyond the peak, also visible in the Z500 pattern (fig. 4.43). The pattern resembles a wave-breaking event in the atmosphere. On the other side, the sunniest day with enhanced SOLD occurs together with a well-established AR, more EuBL and less than normal projection in all cyclonic regimes (fig. 4.44, panel b).

In summary, this means for wintertime GL over Germany that if the IWR of AR is significantly higher than usual and the cyclonic IWRs are significantly lower, GL will be colder than usual, less windy, direr and sunnier. This is no surprise since high-pressure systems are associated with these conditions in DJF. All these anomalies occur close to the peak of the GL, and the GL-IWR remains mostly unchanged. For some variables like SOLD, the GL-IWR is weaker in the beginning. AR reaches its peak activity closely before the GL peak and has a value above 1. Furthermore, AR seems to be the primary driver of these anomalies since the Z500 flow pattern shows a pronounced ridge over the North Atlantic. However, the other significantly changed IWRs can not be ignored. On the other hand, low-pressure systems are associated with rain and wind, which occasionally are severe winter storms. Rainy conditions accompany more clouds than normal, reducing sunshine length and low-pressure systems in DJF, which means warmer than normal conditions. This happens during GL if AT-IWR is enhanced (almost) to the activity threshold of 1. Alongside the AT enhancement, ZO and ScTr are also enhanced in most cases. IWRs of AR and EuBL are significantly lower than usual, while ScBL remains unchanged in any situation, also when AR is enhanced. The timely evolution of GL-IWR shows that warmer, cloudier, windier and wetter conditions appear in the late stages of GL, when the IWR is beyond its peak, thus weaker, and AT is peaking. GL is an example of the secondary regime approach working very well, delivering a well-rounded picture across all variables.

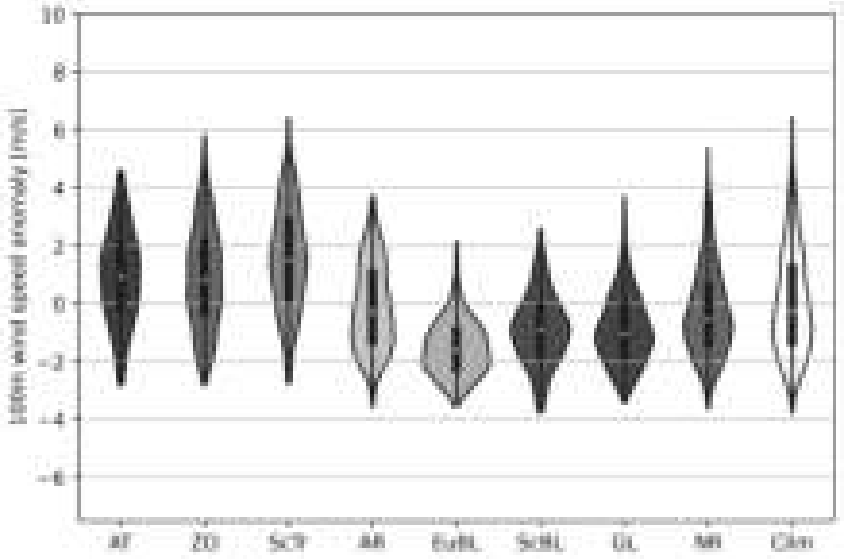

Figure 4.36: Violins showing the wind speed anomalies in Germany for the seven weather regimes as well as the no regime (NR) and the climatology (Clim) during DJF. The white dot marks the mean of the anomaly for the regime, the bold black bar marks the interquartile range and the thin black bar marks the 1.5 interquartile range.

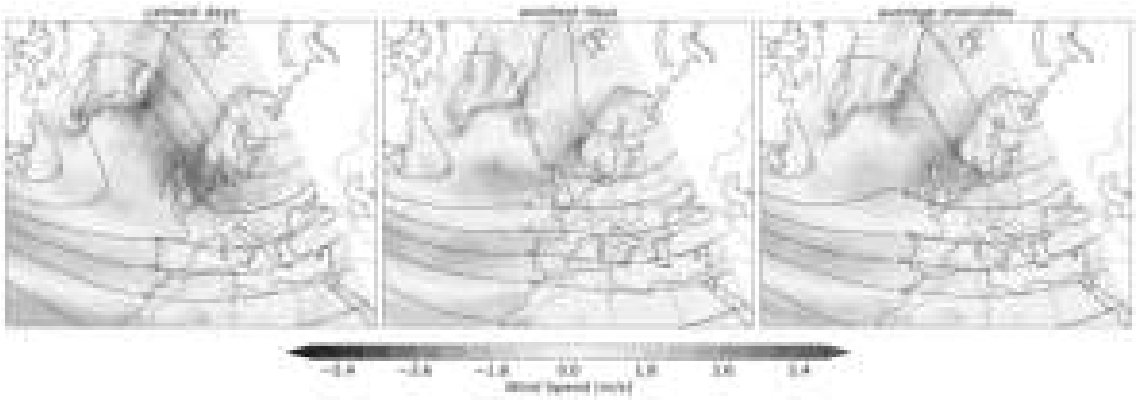

Figure 4.37: Calmest, windiest third of wind speed anomalies centered over Germany during DJF during GL in shadings on the left and the middle. The average anomalies are on the right for comparison. The 500 hPa geopotential height during these dates is shown as black lines.

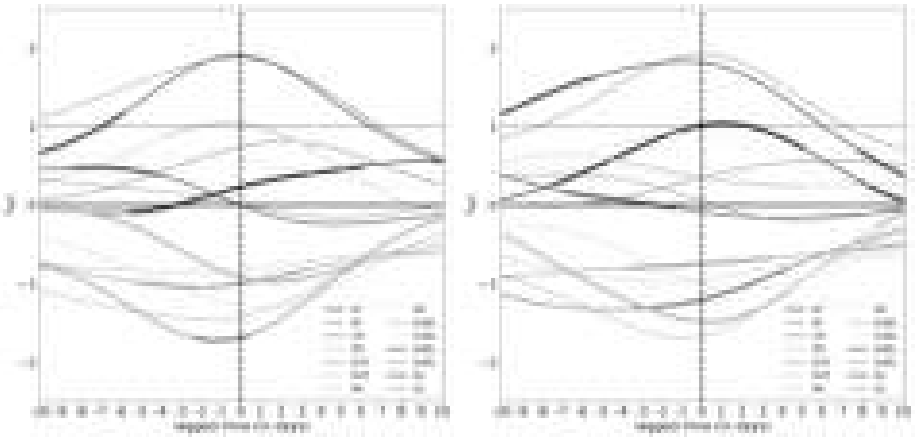

a b

Figure 4.38: 10-day lagged analysis previously and following the lower tercile days of GL over Germany during DJF (a) and the upper tercile days (b) of Wind. The dashed line of a regime represents the timely evolution of the other two terciles. Bold dots on the solid line indicate the significance of the particular regime at this time step in comparison to the dashed line.

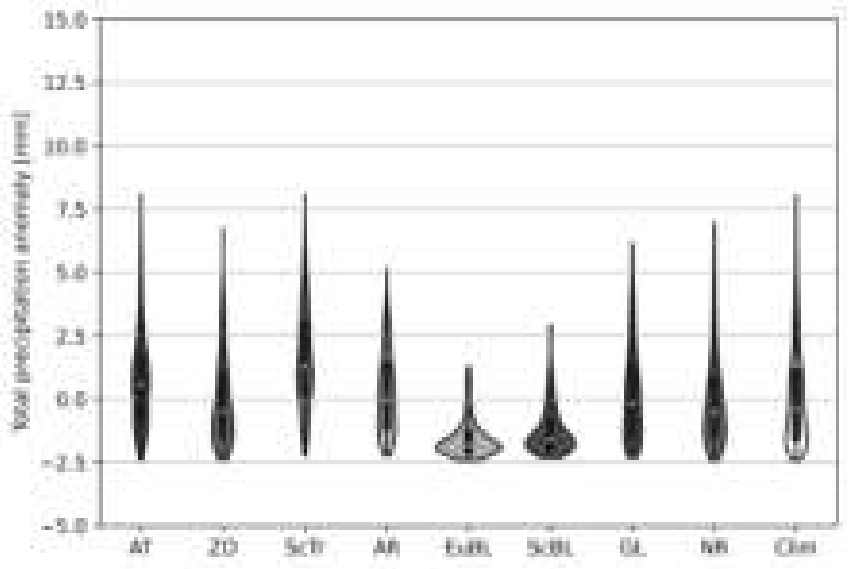

Figure 4.39: Violins showing the TP anomalies in Germany for the seven weather regimes as well as the no regime (NR) and the climatology (Clim) during DJF. The white dot marks the mean of the anomaly for the regime, the bold black bar marks the interquartile range and the thin black bar marks the 1.5 interquartile range.

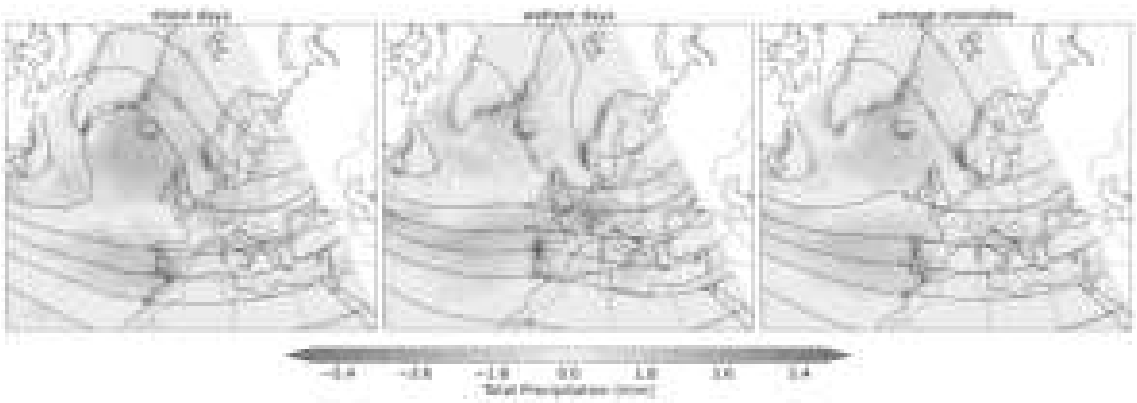

Figure 4.40: Driest, wettest third of TP anomalies centered over Germany during DJF during GL in shadings on the left and the middle. The average anomalies are on the right for comparison. The 500 hPa geopotential height during these dates is shown as black lines.

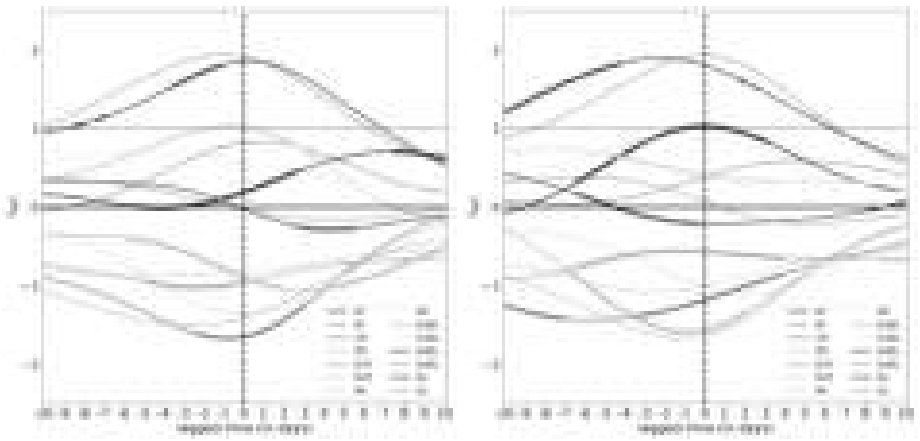

a b

Figure 4.41: 10-day lagged analysis previously and following the lower tercile days of GL over Germany during DJF (a) and the upper tercile days (b) of TP. The dashed line of a regime represents the timely evolution of the other two terciles. Bold dots on the solid line indicate the significance of the particular regime at this time step in comparison to the dashed line.

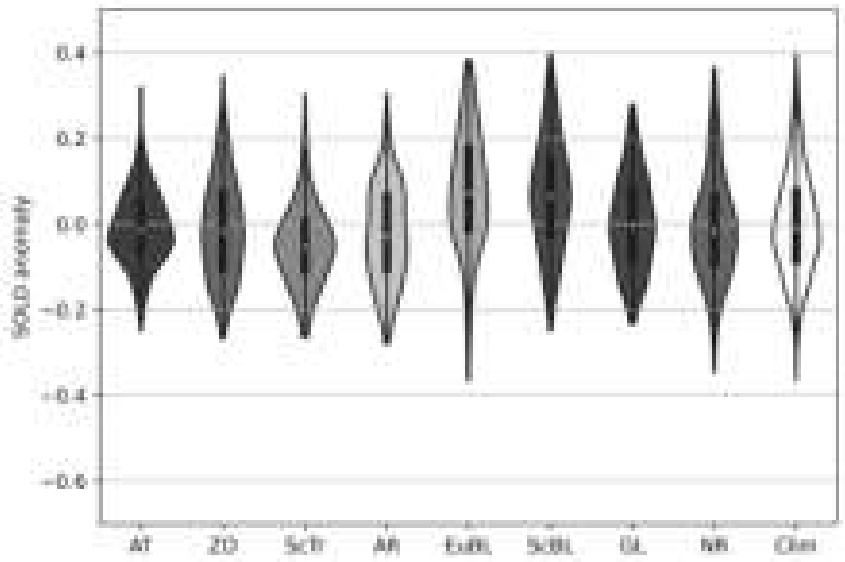

Figure 4.42: Violins showing the SOLD anomalies in Germany for the seven weather regimes as well as the no regime (NR) and the climatology (Clim) during DJF. The white dot marks the mean of the anomaly for the regime, the bold black bar marks the interquartile range and the thin black bar marks the 1.5 interquartile range.

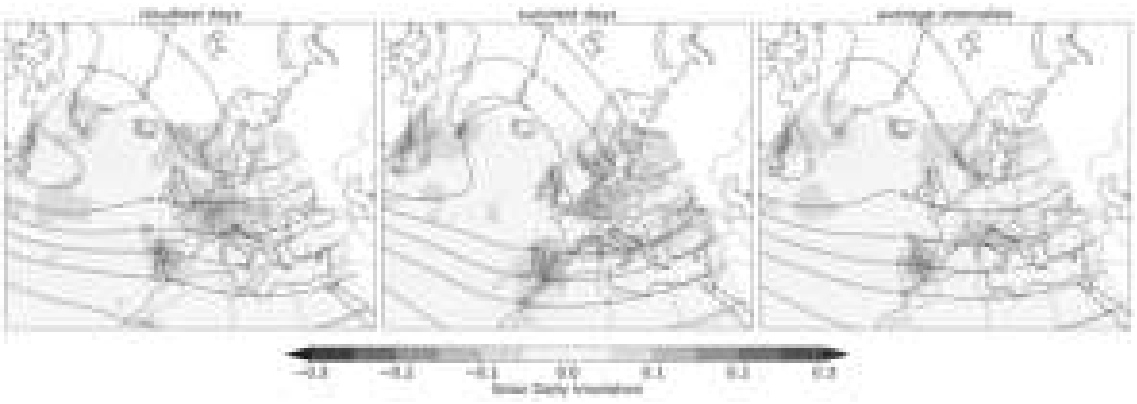

Figure 4.43: Cloudiest, sunniest third of SOLD anomalies centered over Germany during DJF during GL in shadings on the left and the middle. The average anomalies are on the right for comparison. The 500 hPa geopotential height during these dates is shown as black lines.

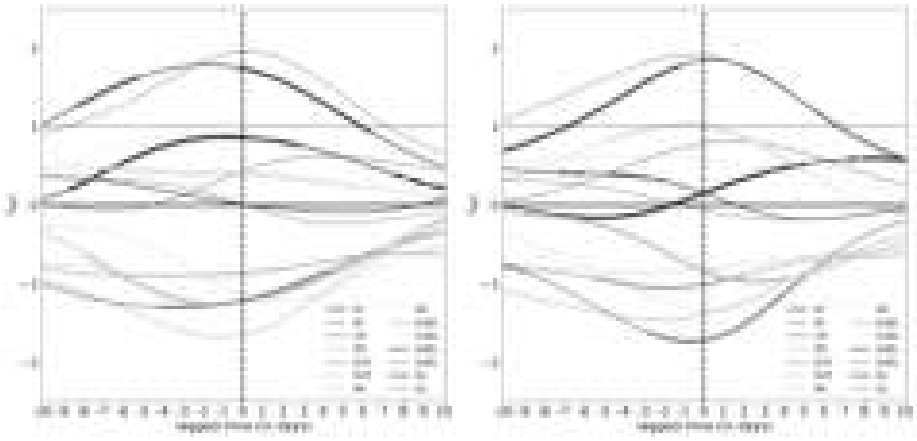

a b

Figure 4.44: 10-day lagged analysis previously and following the lower tercile days of GL over Germany during DJF (a) and the upper tercile days (b) of SOLD. The dashed line of a regime represents the timely evolution of the other two terciles. Bold dots on the solid line indicate the significance of the particular regime at this time step in comparison to the dashed line.

4.5 Where the secondary regimes also perform

As shown above, the IWRs of the regimes not active during a regime are often relevant and carry important information on the precise appearance of the flow pattern. Differences in the atmospheric flow pattern that do not necessarily change the active regime but project into the IWRs of the non-active regimes can have large impacts on the outcome of the regime and thus have the power to explain the impacts. This addition of information comes without adding too much complexity. That secondary regimes are a powerful tool to understand better and predict weather variability can also be demonstrated with other regimes. Note that the variability cannot be easily explained by the secondary regime approach for every regime, as in the previous example of GL over Germany, Norway, and Spain. In other regimes, other processes might be more relevant for certain variables, thus changing the leading secondary IWR as presented in section 4.6. Nonetheless, the following examples of well-working IWR processes are presented. All examples are centered on Germany.

4.5.1 A mix of several regimes determines the outcome

Total precipitation anomalies during ScBL in the summertime are an example of a case in which several secondary IWRs modify a regime's outcome. On most occasions, ScBL is a slightly dry regime, but several of the wettest events occurred during ScBL (fig. 4.45). The view at S2N and FStD supports that ScBL is a very variable regime (fig. 4.24 and fig. 4.23). S2N is very low, mainly due to the weak anomalies, and FStD is above 1, indicating increased variability. The variability in TP during ScBL is the largest of all regimes in JJA, almost fitting the size of climatology. Knowing ScBL as an active regime does not increase the knowledge of possible precipitation anomalies. Two points that can be made with the distributions are: firstly, that ScBL is more likely to be drier than the average, but secondly if ScBL is wetter than usual, the wet anomalies can be high. If looking

at the wettest days, it is visible that the Z500 flow pattern is more amplified than during average (fig. 4.46). The trough over the British Isles is deeper, and the ScBL ridge over Scandinavia is higher. This does not significantly project into the IWR of ScBL, which is slightly weaker than during other times (fig. 4.47, panel b). Especially the stronger bend of the 560 hPa line from the British Isles into Europe does not change anything in the IWR projection, as one could expect. Instead, it projects into significantly more AR and ScTr by smoothing the trough over the Atlantic (AR) and shifting it towards Scandinavia (ScTr), leading to wet anomalies in France, Germany, the British Isles and especially on the northern face of the Alps. Here, the impact of orography on variables such as TP becomes visible as the atmospheric flow pushes clouds against the Alps, leading to increased precipitation rates.

During the dry days of ScBL, the trough identified over the British Isles during the wet days is shifted to the Atlantic Ocean. Again, there is no substantial change in ScBL-IWR (fig. 4.47, panel a). The enhanced trough projects into a less negative ZO-IWR at the expense of AR. Over the European continent, a stronger projection into EuBL evolves in the later stages of ScBL, explaining the extended high-pressure area over Western Europe. The cause of precipitation during ScBL is the trough over the North Atlantic, carrying rain at its southeastern flank. During the dry situations, the high pressure over Central Europe blocks the trough from reaching the land masses. In contrast, during the wettest days, the southeastern flank reaches the continent and drives precipitation in combination with orography.

The example of TP during ScBL underlines the importance of using secondary regimes, as the change in the active regime is not strong enough to explain the variability.

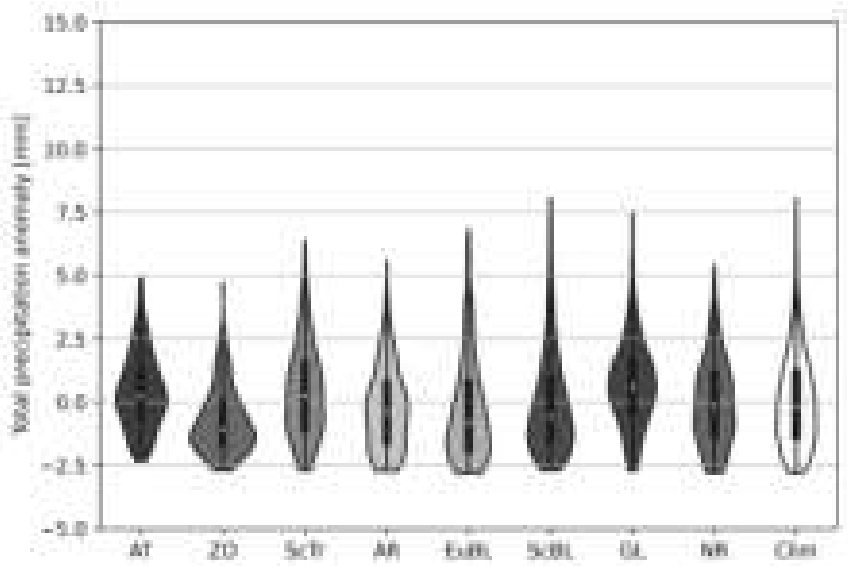

Figure 4.45: Violins showing the TP anomalies in Germany for the seven weather regimes as well as the no regime (NR) and the climatology (Clim) during JJA. The white dot marks the mean of the anomaly for the regime, the bold black bar marks the interquartile range, and the thin black bar marks the 1.5 interquartile range.

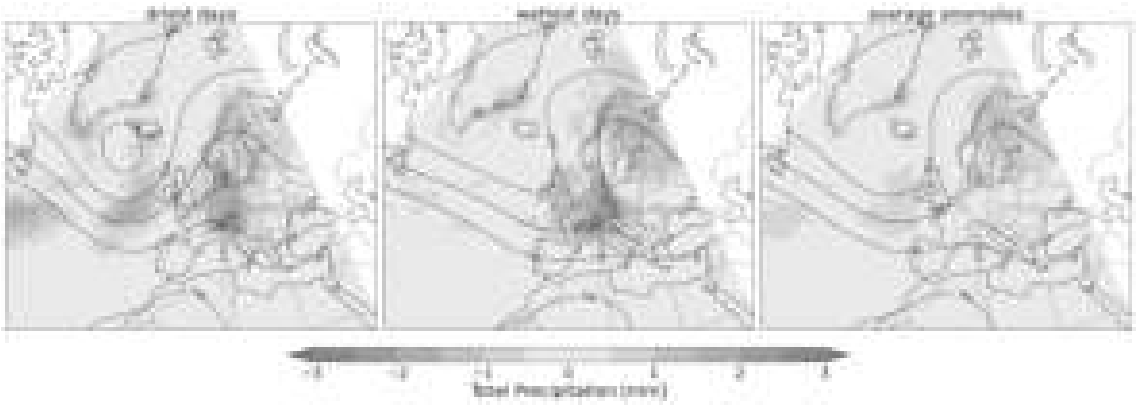

Figure 4.46: Driest, wettest third of TP anomalies centered over Germany during JJA during ScBL in shadings on the left and the middle. The average anomalies are on the right for comparison. The 500 hPa geopotential height during these dates is shown as black lines.

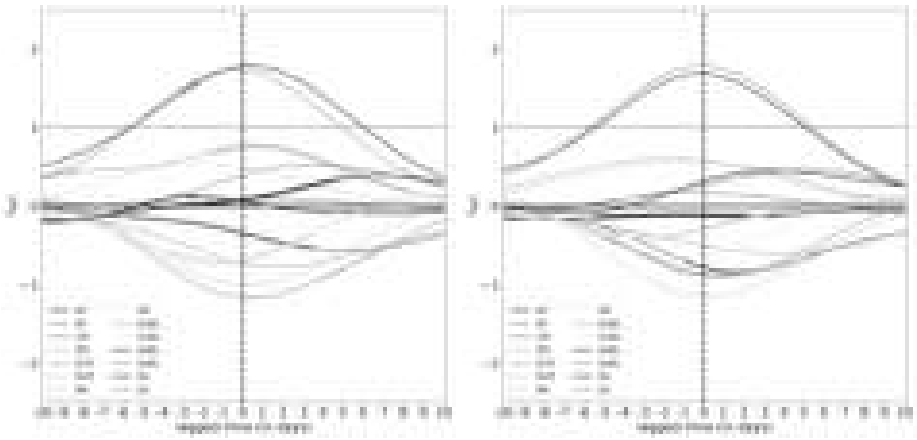

a b

Figure 4.47: 10-day lagged analysis previously and following the lower tercile days of ScBL over Germany during JJA (a) and the upper tercile days (b) of precipitation. The dashed line of a regime represents the timely evolution of the other two terciles. Bold dots on the solid line indicate the significance of the particular regime at this time step in comparison to the dashed line.

4.5.2 The enhancement and suppression of the main weather regime index

Like the T2M anomalies of Norway during GL, the anomalies of ZO over Germany are driven by the main IWR, and the secondary regimes are of secondary importance in explaining the variability. As already noted in section 4.1, ZO is among the warmest regimes in DJF but can, rarely, contain surprisingly cold anomalies (fig. 4.1). Over Germany, warmer anomalies are observed in the north rather than in the south. Northern Germany shows a strong S2N signal and a low FStD (fig. 4.9 and fig. 4.10). For southern Germany, the signal is weaker but has the same sign. Scenario B allows to suggest that a ZO event leads to warm anomalies without large variability. The degree of the anomaly might vary but will be well above 0 K for a large majority of cases (fig. 4.25). Because of that, ZO can be seen as a window of opportunity where knowing the regime enhances the likelihood of a more precise weather forecast. A look at the tercile analysis reveals that the warm tercile of ZO is ≥ 5 K for Germany and even higher in regions further east (fig. 4.48). On the other hand, the cold tercile barely shows cold anomalies, clarifying the warm character of ZO. The warm days

of ZO are associated with a stronger than usual ZO index and occur around the same time as the peak-IWR in a well-established ZO environment (fig. 4.50, panel b).
The cool anomalies of ZO can only be expected at the beginning of a ZO event, significantly shifting the entire ZO life cycle to later days (fig. 4.50, panel a). A high projection in EuBL and ScBL is visible with the shifted ZO for the entire period. The low-pressure gradient over southern Europe causes this projection.
The method of using the terciles to explore the distribution of anomalies and flow patterns can be refined by considering the ten coldest, independent days ever observed during ZO. As shown in chapter 3, the general results are similar to the tercile but allows to gain extra insights, especially in situations where rare but large anomalies occur. It is revealed that very cold anomalies of $\leq -3\,\mathrm{K}$ can occur during days that are considered a ZO fig. 4.49, explaining the extended lower tail of the ZO-distribution. The lagged analysis, where the solid line now contains the ten coldest days and the dashed line is the middle and upper tercile, underlines how early in the life cycle of ZO the cold days appear (fig. 4.51, panel a). The lagged analysis also underlines the importance of the preceding EuBL with an IWR just below the activity threshold. EuBL-IWR starts to decline as ZO-IWR is rising.
The example of ZO shows that not only secondary regimes such as EuBL for ZO are important but also when anomalies occur in a regime's life cycle, and in some cases, the anomalies are accompanied by an enhancement in the main regime IWR.

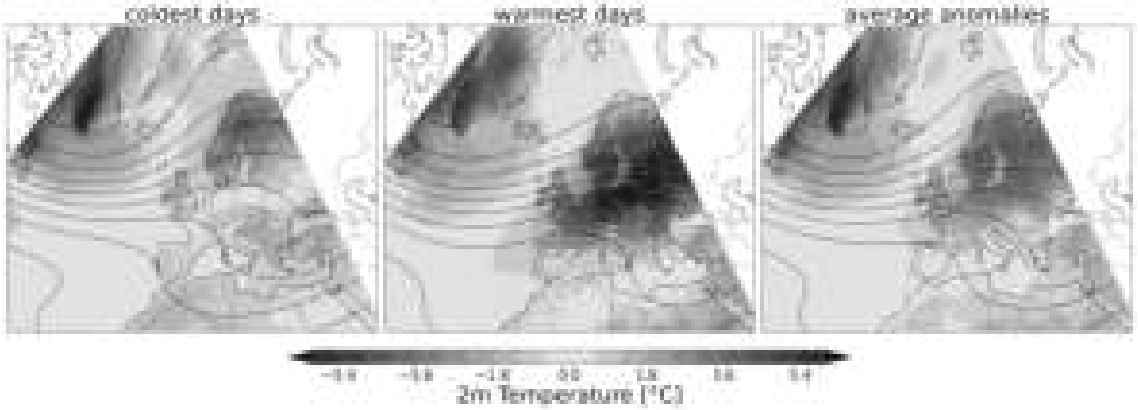

Figure 4.48: Coldest, warmest third of T2M anomalies centered over Germany during DJF during ZO in shadings on the left and the middle. The average anomalies are on the right for comparison. The 500 hPa geopotential height during these dates is shown as black lines.

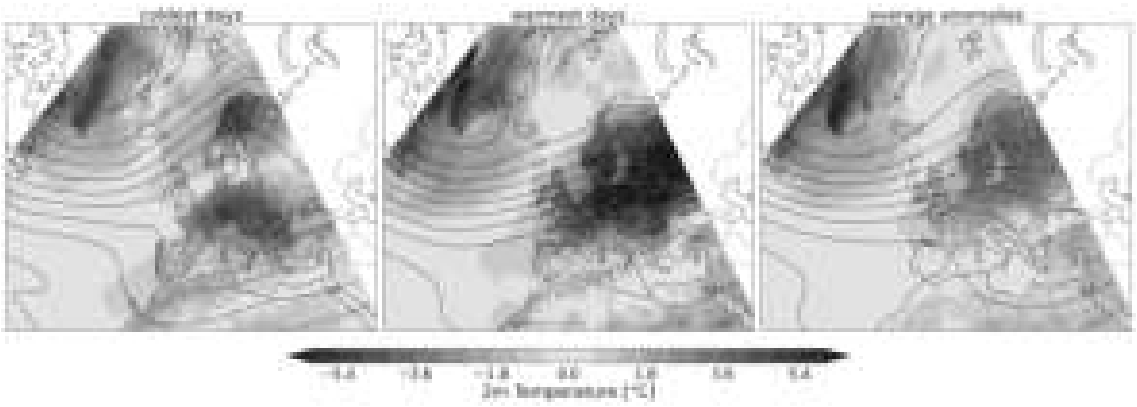

Figure 4.49: 10 coldest and warmest independent days of T2M anomalies centered over Germany during DJF during ZO in shadings on the left and the middle. The average anomalies are on the right for comparison. The 500 hPa geopotential height during these dates is shown as black lines.

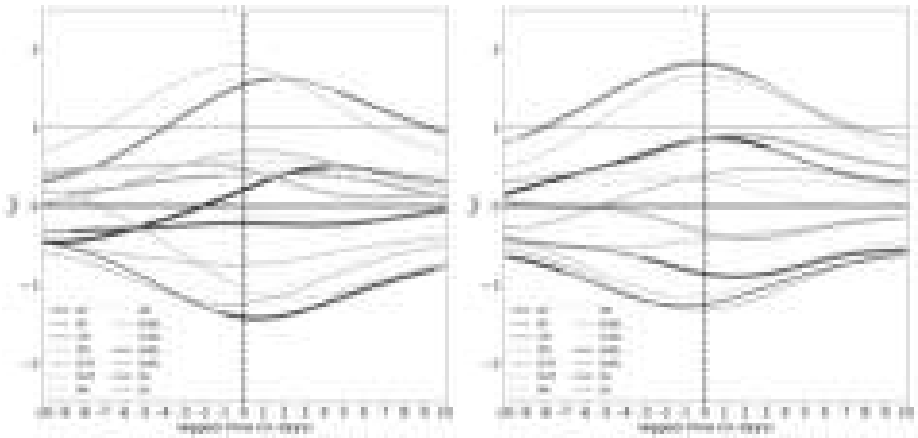

a b

Figure 4.50: 10-day lagged analysis previously and following the lower tercile days of ZO over Germany during DJF (a) and the upper tercile days (b) of T2M. The dashed line of a regime represents the timely evolution of the other two terciles. Bold dots on the solid line indicate the significance of the particular regime at this time step in comparison to the dashed line.

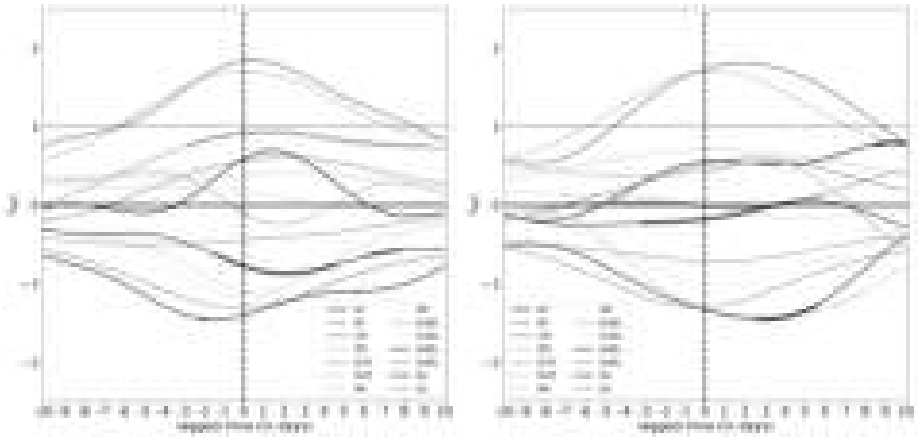

a b

Figure 4.51: 10-day lagged analysis previously and following the ten coldest (a) and warmest (b) independent days of ZO over Germany during DJF of T2M. The dashed line of a regime represents the timely evolution of the other two terciles. Bold dots on the solid line indicate the significance of the particular regime at this time step in comparison to the dashed line.

4.6 Where caution is needed when using secondary regimes

For most regimes, the secondary IWRs are a valid method to understand the variability within a regime better and make weather forecasts based on regimes more precise. However, there are examples where the secondary regimes do not perform well, and other processes are of more importance than during performing IWRs. Some examples are presented in the following section.

4.6.1 Misleading composites

The wind speed anomalies of EuBL during JJA are weak, with a slightly calm anomaly over Germany, and EuBL is the least variable regime for wind in summer (fig. 4.52). Thus, it might seem irrelevant and not worth investigating. When looking at the calmest and windiest terciles of days, the anomalies are revealed to be not very strong (fig. 4.53). Both datasets show only a mild anomaly of either calm or windy signs. The interesting flavor of EuBL is shown by comparing the Z500 flow pattern. The pattern almost looks the same for all 3 cases - calmest tercile, windiest tercile and overall average. A large block sits over Central Europe while the jet is relocated towards the Norwegian Sea, causing windy anomalies. The pressure gradient between the Z500 lines is larger for the calmest days, causing lower wind speed anomalies in the 100 m level. Over the European continent, the flow pattern for the windy and calm days is very similar, and unable to explain the observed windy anomalies since no visible pressure gradient could cause atmospheric motions of this magnitude. The windy anomalies are not confined to a small region where orography or sub-synoptic processes could be critical. Instead, the anomalies span from the Iberian Peninsula into Eastern Europe, although they are centered over Germany.
Within the lagged analysis, some significant changes are visible (figs. 4.54 panel a, 4.54, panel b). Stronger than usual, ScBL and AT precede the calm days. Less ScBL, more AR and weaker AT accompany the windy days. None of these changes are strongly projected at the Z500 level in a way that would be visible and have explanatory power for the windier days of EuBL. This is why the secondary regimes could be misleading in the case of wind speed during EuBL in JJA.
When using the extremes again, more light can be shed onto this unclear situation (fig. 4.55). During the ten windiest days for EuBL, a small, confined ridge is visible over the British Isles and a trough-like structure is located over Central Europe. The change in circulation can explain the wind speed anomalies observed due to a closer pressure gradient between a trough and a ridge. The flow configuration reminds of an amplified, eastward-shifted AR situation that is known to be windier than EuBL. However, none of these changes project significantly into other IWRs of the extreme event analysis (fig. 4.56, panel b). Only in the tercile lagged analysis does this feature seem to be visible. When assuming that EuBL events propagate eastward, being EuBL for the entire time and accompanied by stronger winds at the flanks, this could explain why there is nothing visible on the Z500 level over Europe in the tercile composite of wind speed anomalies.
The ten calmest days of EuBL over Germany occur in a weak gradient environment. The calmest anomalies occur in the German Bay. The lagged analysis shows weaker but not a significantly

weaker EuBL and no major changes in the other IWRs at time lag 0 (fig. 4.56, panel a). Towards the end of the EuBL life cycle, ScBL seems to emerge from it, which could mean that the center of EuBL slowly develops towards Scandinavia. It shows how surface impacts can be entangled with regime transitions, and this is an interesting area for further studies.
In summary, this situation shows how the flow pattern is responsible for the anomalies, with a very weak pressure gradient environment for the calm anomalies and a ridge-trough structure for the windy anomalies. The IWR analysis cannot clearly resemble the flow pattern here, especially in the case of the above-normal wind speeds. One way to resolve this situation in further research could be to use an instantaneous weather regime definition instead of a smoothed one like in this thesis. Without the five-day constraint, the windy EuBL days may fall within the AR regime, better suiting the situation but also leading to a less stable large-scale evolution and more jumping between the regimes.

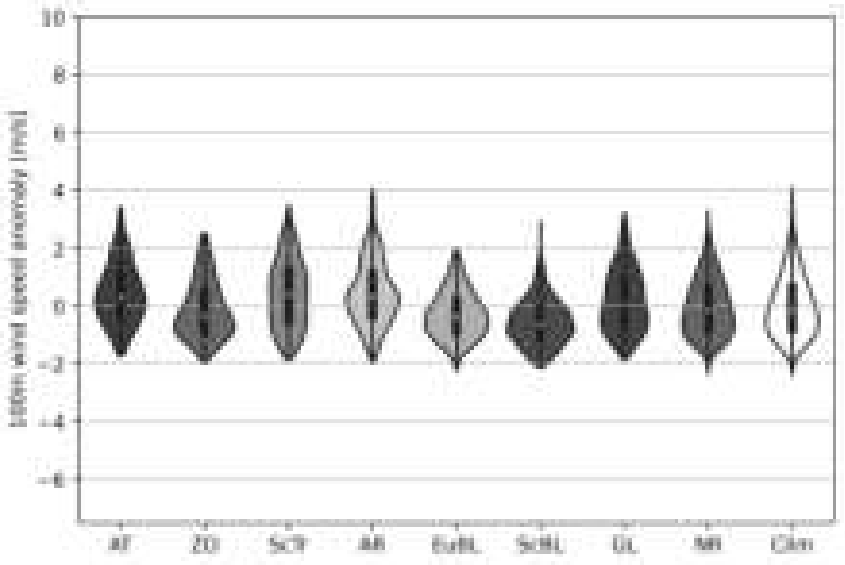

Figure 4.52: Violins showing the Wind Speed anomalies in Germany for the seven weather regimes as well as the no regime (NR) and the climatology (Clim) during JJA. The white dot marks the mean of the anomaly for the regime, the bold black bar marks the interquartile range and the thin black bar marks the 1.5 interquartile range.

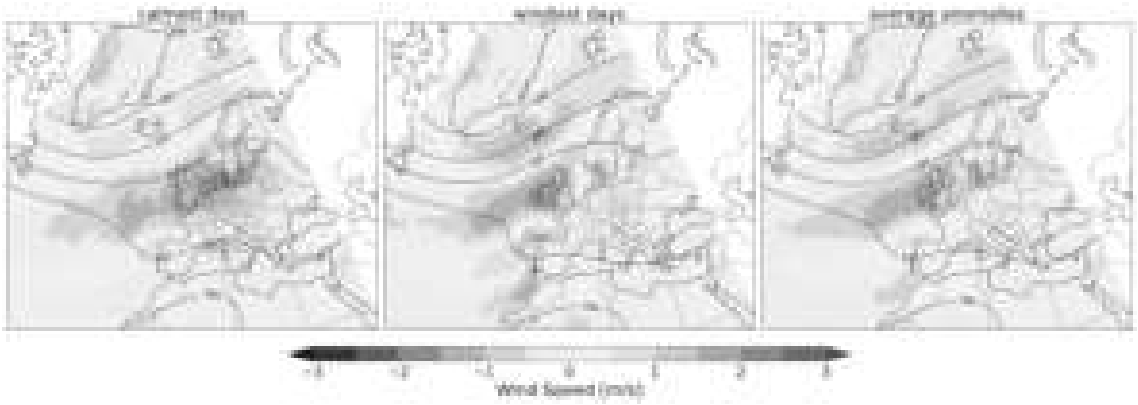

Figure 4.53: Calmest, windiest third of wind speed anomalies centered over Germany during JJA during EuBL in shadings on the left and the middle. The average anomalies are on the right for comparison. The 500 hPa geopotential height during these dates is shown as black lines.

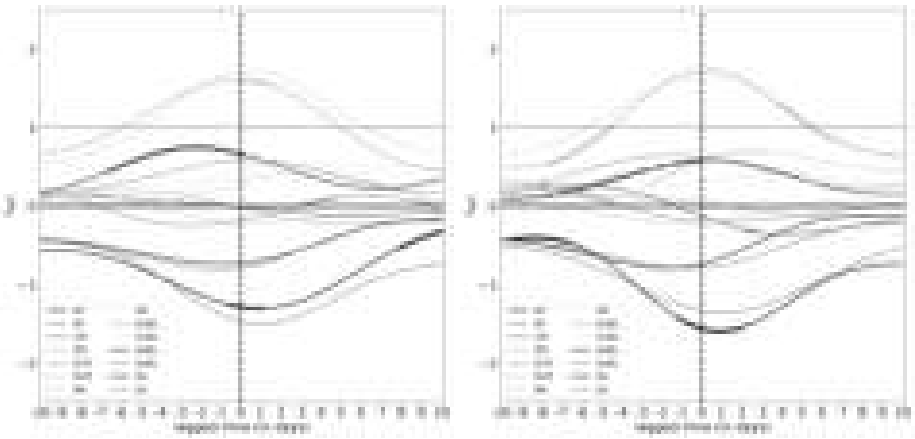

a b

Figure 4.54: 10-day lagged analysis previously and following the lower tercile days of EuBL over Germany during JJA (a) and the upper tercile days (b) of wind speed. The dashed line of a regime represents the timely evolution of the other two terciles. Bold dots on the solid line indicate the significance of the particular regime at this time step in comparison to the dashed line.

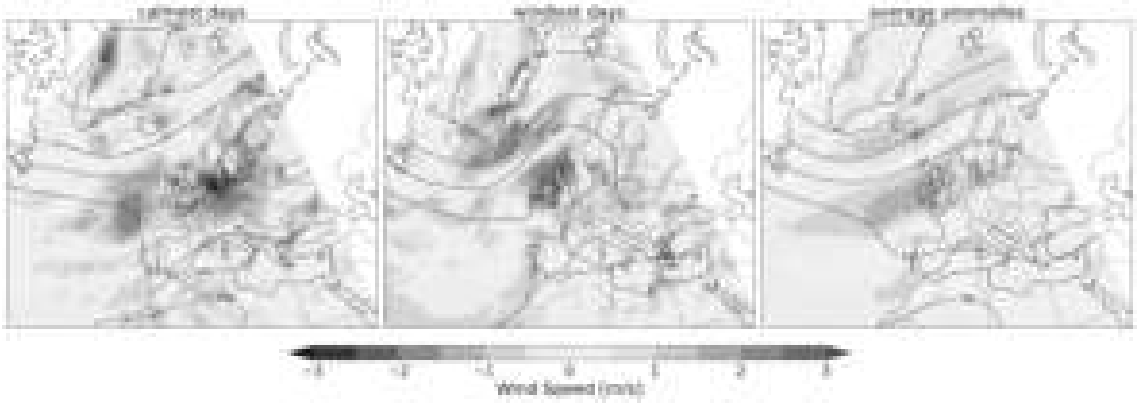

Figure 4.55: Calmest, windiest third of wind speed anomalies centered over Germany during JJA during EuBL in shadings on the left and the middle. The average anomalies are on the right for comparison. The 500 hPa geopotential height during these dates is shown as black lines.

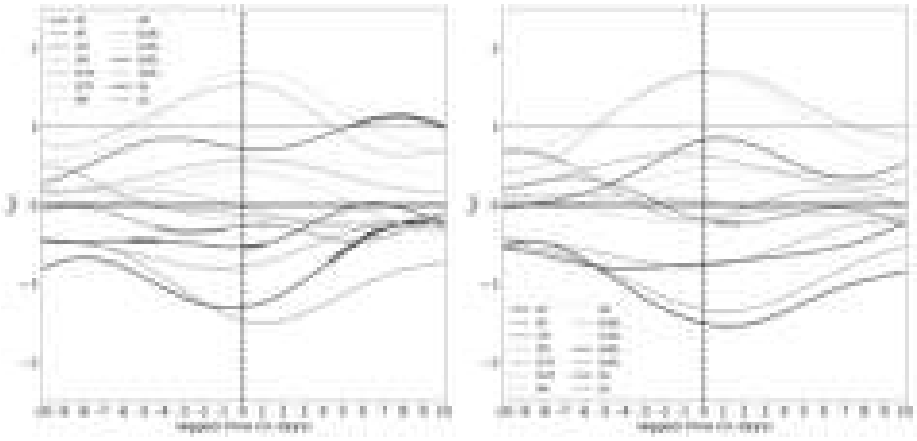

a b

Figure 4.56: 10-day lagged analysis previously and following the lower tercile days of EuBL over Germany during JJA (a) and the upper tercile days (b) of wind speed. The dashed line of a regime represents the timely evolution of the other two terciles. Bold dots on the solid line indicate the significance of the particular regime at this time step in comparison to the dashed line.

4.6.2 Preceding weather regime index

In literature, it has been found that some weather regimes preferably transform from one into another (Michel & Rivière, 2011; Teubler et al., 2023; Vautard, 1990). There are two regimes where different regime transitions distinguish between surface regime impacts. The first regime is summertime AR, which sees a strong precursing EuBL for the warmest days during JJA. The lagged analysis for warm T2M anomalies shows that clearly (fig. 4.58, panel b). About five days before the occurrence of the warm AR days, EuBL-IWR peaks with a value well above the threshold. Starting between days -9 and -8 until day -3, EuBL has the highest IWR and is the active regime. This activity marks a large difference from the other two EuBL terciles, which are usually associated with an IWR below 0.5. On day -3, AR-IWR becomes stronger, and the activity switches from EuBL to AR. The warmest AR days occur three days later in slightly earlier stages of AR. However, this time difference is not significant. What is more important is the absence of significant differences in IWR on day 0, except for the decaying EuBL. There is a significant difference in the IWRs before day 0 when EuBL is very strong and suppressing other regimes like AT and GL. At the same time, the projection into more ScBL is not surprising, given the proximity of the two. The flow pattern during warm AR days shows a large zone of high pressure stretching from southeastern Europe in the east across the North Atlantic almost to the Canadian coast (fig. 4.57). This leads to the hypothesis that AR evolves retrograde from EuBL, which travels from Europe onto the Atlantic. The retrograde evolution is supported by the findings of Teubler et al. (2023), who find that AR evolves from another blocked regime in approximately 65% of occurrences. Since EuBL is among the warm regimes in JJA and AR is a cold regime year-round, the temperature developed during EuBL might not be notable for itself, but these temperatures are anomalously warm for AR. This case includes sunny, calm and dry conditions (not shown). The other example of a precursing IWR happens during AT in JJA for cold, windy and rainy T2M anomalies (not shown). Here, GL is the precursing IWR but is of a lower magnitude than EuBL during AR. Furthermore, SOLD is not

altered significantly by GL.

The coldest anomalies for AR take some time to develop (fig. 4.58, panel a). The lagged analysis shows that the cold days occur well beyond the peak of AR. The blocked regimes of EuBL and ScBL are significantly reduced, while ScTr is enhanced, amplifying the wave pattern over Europe. Both flavors of AR are an example of the importance of the time evolution of some regimes. The warm flavor shows well how one regime transforms into another, leaving behind unusual anomalies for the following regime. The cold flavor is caused by the late occurrence together with secondary regimes.

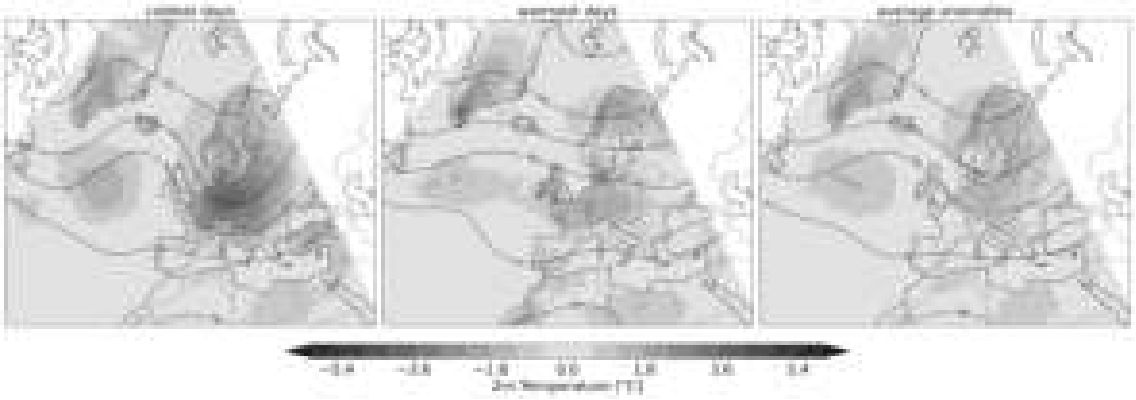

Figure 4.57: Coldest, warmest third of T2M anomalies centered over Germany during JJA during AR in shadings on the left and the middle. The average anomalies are on the right for comparison. The 500 hPa geopotential height during these dates is shown as black lines.

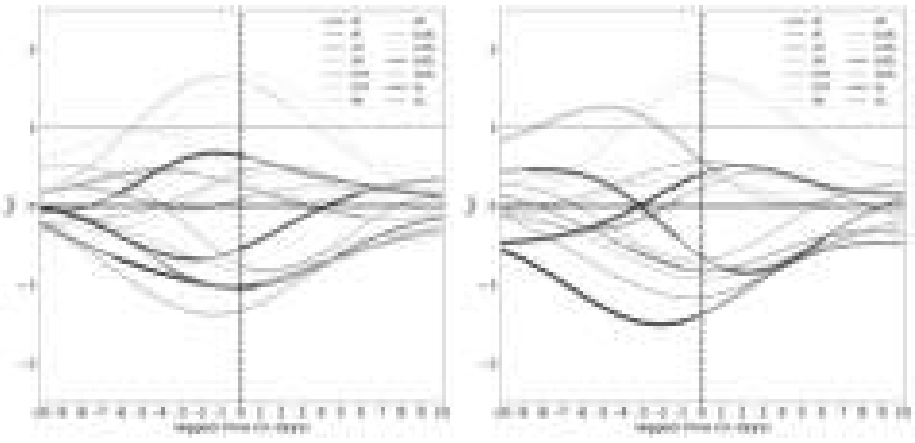

a b

Figure 4.58: 10-day lagged analysis previously and following the lower tercile days of AR over Germany during JJA (a) and the upper tercile days (b) of T2M. The dashed line of a regime represents the timely evolution of the other two terciles. Bold dots on the solid line indicate the significance of the particular regime at this time step in comparison to the dashed line.

4.6.3 Unclear cloud cover in EuBL

One example of a regime with a large variability is SOLD during EuBL in SON. On average, SOLD is above average for large European areas, except for the Mediterranean and the Norwegian coast (not shown). The anomaly is very sunny in France and Scandinavia and more neutral in Germany and Eastern Europe. The latter two are the regions where the S2N becomes small, together with a high FStD. Already, those two methods indicate high variability in that area. The violin plot confirms a large variability of SOLD (fig. 4.59). The variability is in the size of climatology, with differences in probability distribution. The probability distribution has a monopole structure for most other regimes and variables. EuBL is different in that it has an exceptionally wide distribution with a dipole structure. The central probability is below 0 at around -0.1, equal to 10% less sunshine of the possible sunshine duration. A small proportion of EuBL are the least sunniest days during SON. Conversely, a large proportion of EuBL is sunnier than usual. The probability is less for values around 0.1 and more around 0.2, balancing the cloudy anomalies. Since the violins are showing the median, it can be said that half of EuBL days are sunnier than average, and the other half is cloudier.
In the tercile plot, it reveals that for the cloudy days, the flow pattern is not changed compared to the average, but the days are much less sunny over Germany and neighboring countries, which is not visible in the average (fig. 4.60). The sunny days are accompanied by an intensified block over Central Europe and much more sunshine there. Surprisingly, this does not project into a stronger EuBL but instead into stronger ZO and understandably less ScTr (fig. 4.61, panel b). The increased ZO redirects the storm track to the north, and the blocking, with its sinking air motion, can evaporate the clouds, leading to clear skies. In the cloudy conditions, no IWR change with explanatory power is visible. It can be doubted that the slight reduction in AT and enhancement in ScTr are the drivers for more clouds due to the nearly unchanged Z500 flow pattern. One possible explanation could be radiation fog. Radiation fog develops during cool and clear nights when the air layers near the surface are cooled strongly. The wind speeds are usually low, which is given for EuBL on average in SON, and the fog emerges from condensing water vapor. Radiation fog can be observed frequently during high-pressure situations over Germany in autumn, especially in valleys. Under special circumstances like weak wind speeds and a low solar angle, the foggy conditions can last up to several days. Usually, this is the case in winter, but it can also occur during the later autumn season, such as November. In the other cases, the fog dissolves quickly as soon as the sun has warmed the atmosphere to a level where the water drops evaporate. This is why radiation fog could explain the unclear cloud cover during EuBL in SON. Even if the fog is dissolved soon after sunrise, it reduces the possible length of sunshine. By an assumed day length of 10 h, 10% of sunshine reduction as observed is equal to 1 h, which seems to be a reasonable delay of sunshine by radiation fog.
If radiation fog is the case for this unclear cloud cover, it can be verified by using (observational) cloud cover products, radiosoundings of the area or other analysis to evaluate the boundary layer stability for the given period of time.

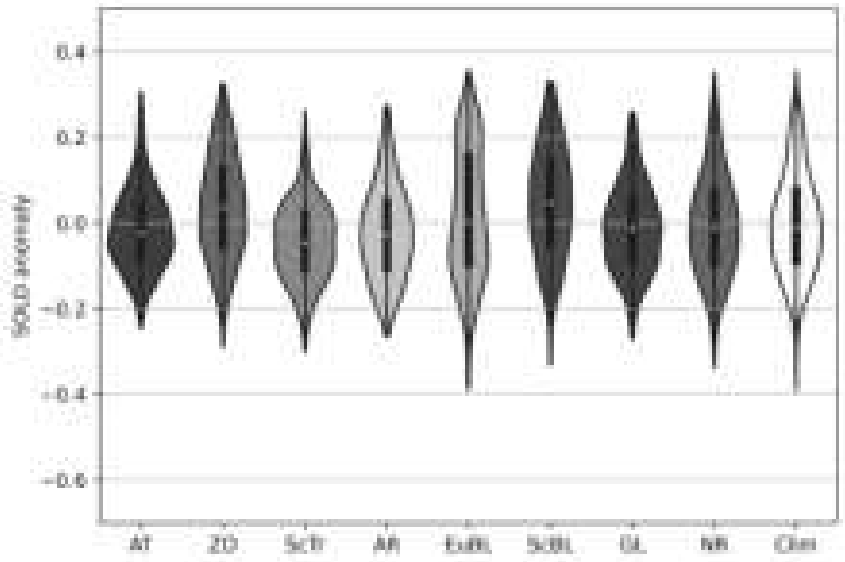

Figure 4.59: Violins showing the Wind Speed anomalies in Germany for the seven weather regimes as well as the no regime (NR) and the climatology (Clim) during SON. The white dot marks the mean of the anomaly for the regime, the bold black bar marks the interquartile range, and the thin black bar marks the 1.5 interquartile range.

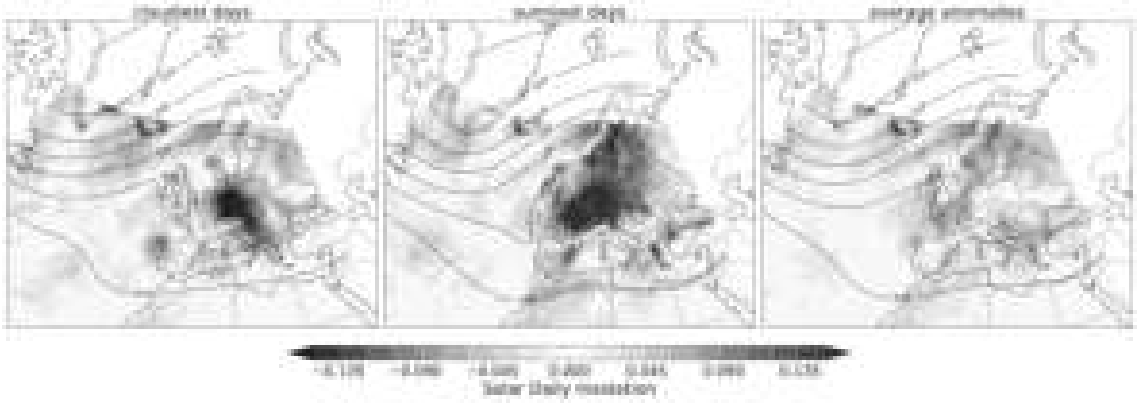

Figure 4.60: Sunniest, cloudiest third of SOLD anomalies centered over Germany during SON during EuBL in shadings on the left and the middle. The average anomalies are on the right for comparison. The 500 hPa geopotential height during these dates is shown as black lines.

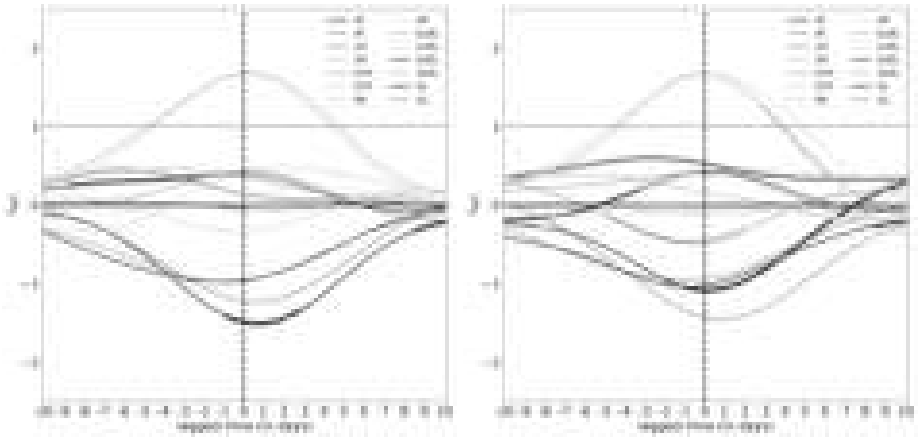

a b

Figure 4.61: 10-day lagged analysis previously and following the lower tercile days of EuBL over Germany during SON (a) and the upper tercile days (b) of wind SOLD. The dashed line of a regime represents the timely evolution of the other two terciles. Bold dots on the solid line indicate the significance of the particular regime at this time step in comparison to the dashed line.

4.6.4 Summertime precipitation

The last presented example of variability where the secondary IWR needs to be treated with caution is total precipitation in EuBL. As one expects, EuBL is a rather dry regime over Germany (fig. 4.7). The anomalies are stronger in the north than in the south. This observation also holds for Europe, with the center of abnormally dry conditions between Great Britain and Finland. There, the S2N reaches values above 1, indicating a low variability and, thus, good predictability (not shown). FStD is very low as well. In the remainder of Europe, FStD is very high, and S2N is low, indicating high variability. In fact, over Germany, EuBL is among the most variable regimes exceeded by ScBL and GL only (fig. 4.45). ScTr is among the same variability extent, but EuBL is the second driest regime, with a median well below 0, meaning that EuBL is likely to be dry. The dry tercile of EuBL occurs after the peak of EuBL, but the delay is not significant (fig. 4.63, panel a). Dry days are associated with a slightly stronger, significant projection in AR before the occurrence and changed behavior in GL, which is lower in the beginning and stronger during and after the dry days. It is unclear if that change of IWR is enough to explain the dry days. Further investigations are necessary to solve this question clearly.

The wet days are characterized by enhanced precipitation rates over southern Germany and locally reduced Z500 isobaric lines over northern Germany (fig. 4.62). The main enhancement of precipitation is at the northern side of the Alps and the medium-sized mountain ranges in the areas to the north. In the summertime, regions near the Black Forest and the Swabian Alb, as well as the southern part of Bavaria, are known to experience frequent and intense thunderstorms. These areas correspond well to the areas with high precipitation rates. This makes it more likely to explain the observed situation with convectively driven precipitation events, although using 5-day rolling mean data to reduce synoptic variability within the variables. This could mean that thunderstorms either form very frequently during summertime EuBL, leading to the low-pressure signal, or very intense thunderstorms, leading to a large signal that remains visible even if using a third of days. What

seems to be clear is that the thunderstorms need to be present for several days in a row in order to be visible in a 5-day rolling average. Here, further investigations are necessary as well, also to determine if the higher than average IWR of ScBL before the wettest EuBL days and the lower ZO plays a role in creating wet EuBL events (fig. 4.63, panel b).

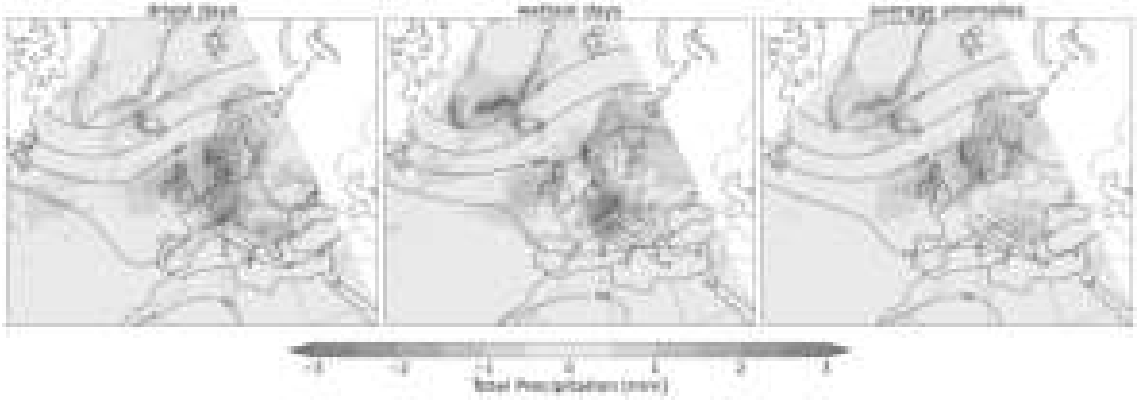

Figure 4.62: Driest, wettest third of TP anomalies centered over Germany during JJA during ScBL in shadings on the left and the middle. The average anomalies are on the right for comparison. The 500 hPa geopotential height during these dates is shown as black lines.

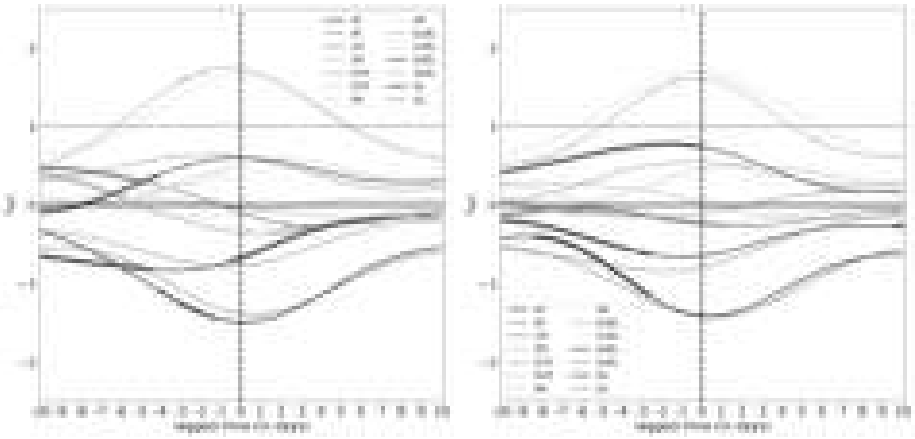

a b

Figure 4.63: 10-day lagged analysis previously and following the lower tercile days of EuBL over Germany during JJA (a) and the upper tercile days (b) of TP. The dashed line of a regime represents the timely evolution of the other two terciles. Bold dots on the solid line indicate the significance of the particular regime at this time step in comparison to the dashed line.

4.7 Guidelines of using (secondary) weather regime indices to capture weather variability

In the following section, guidelines are presented to use the (secondary) IWRs to make more precise statements of the character of a weather regime event and overview tables for winter and summer are provided (tables 4.1 4.2). When using the features, it must be remembered that the IWRs in the lagged analysis emerge from an average. On the one hand, this makes the result very robust, but on the other hand, it means that each event can behave a little differently.
There are 3 features of how the IWR of the active regime gets modified, and thus, the weather varies compared to the mean. Most regimes show a combination of at least two of them. Many regimes share some similarities of modified IWR across the variables due to the relationships between the variables. However, they are too different and benefit if each variable is reviewed separately. Also, the countries need to be evaluated separately since the impact of the different IWRs varies and is related to the distance to the acting center. For some regimes, variables, and seasons, there are situations where the IWR fails to hint at the outcome of a regime event.

1.: Stronger or weaker main IWR
In this case the driver of weather variability is the change of the IWR of the active regime. The main regime can be either stronger than usual, represented by higher IWR values, or weaker with lower than usual IWR values. In an ideal case, the strong IWR would enhance the magnitude of the average weather conditions, and the weaker value would decrease the magnitude. Stronger/weaker main IWR cases are accompanied by the change in secondary IWRs and/or a temporal shift.

2.: Shifted main IWR
The second important feature is the shift in the main IWR in relation to the onset/decay of the WR. The shift of IWR can be associated with a stronger or weaker index, but this is not always the case. On some occasions, the life cycle of the main IWR is longer or shorter than usual. In the case of a longer/shorter event the IWR rises earlier/later and/or decays later/earlier than average. This means a longer/shorter time for anomalies to evolve. On other occasions, the anomalies occur very early or late within a regime life cycle. This means that the average anomaly of a regime did not have enough time to evolve yet, or other anomalies have already superimposed it. Often, the opposite anomaly to the mean anomaly can be identified in very early or late stages of a WR. For example, cold/warm anomalies of a cyclonic/blocked regime occur in the early stages of a regime in DJF. For blocked regimes, the coldest anomalies can often be observed in the late stages of the life cycle to the time needed to develop a cold anomaly.

3.: Unchanged main IWR but changed secondary IWRs
Most regimes investigated in this Master thesis show the contribution of another regime when the weather is not of the average anomalies. For some regimes, there is a seesaw swinging between two secondary regimes and determining if the main regime sees positive or negative anomalies. A good example of that is GL with AT and AR. For other regimes and variables, the secondary regime causing the positive anomaly can differ from the one causing the negative one, especially if one or both of the other features also play a role.

4.: Non-IWR related processes
As shown in section 4.6, in some cases, other effects play an equally or more important role than the previously listed features. These features can be the transition between regimes or frequently occurring synoptic features. This adds further insecurity to the interpretation of weather regimes.

The most important contributions to the positive/negative anomalies of the different variables are presented in table 4.1 for DJF and table 4.2 for JJA. Through the coloring of the tables, it becomes easily visible that the modifying features can be identified better during DJF than during JJA. Furthermore, some general aspects can be identified:

- for some regimes the alternation between two secondary regimes or late/early occurrence shows across (almost) all variables. Examples are GL in DJF with the alternation between AR and AT and EuBL in DJF with late/early occurrences.
- for many cases the enhanced feature causing the anomaly is reduced for the case of the other anomaly and vice versa. However, the feature varies for each variable. For example ZO in DJF.
- especially GL and ZO behave in contrast in almost all cases if they play a role. If GL is stronger than usual, ZO is weaker, and vice versa. A less pronounced example is ScTr and EuBL/ScBL and AT with AR. This behavior shows the related, opposing regimes. Also, it explains why many regimes are often significantly changed at the same time.

	T2M cold	T2M warm	Wind calm	Wind windy	TP dry	TP wet	SOLD cloudy	SOLD sunny
AT 12.28%	early ZO- ScTr-	late ZO+	weak ZO- BL+	strong ZO+ BL-	weak ScTr-	strong ScTr+	ScBL-	BL+
ZO 13.55%	early BL+	late BL-	early cyl- BL+	strong cyl+ BL-	BL+ ScTr-	strong cyl+ BL-	ScTr+ ScBL-	BL+
ScTr 11.48%	ScTr- BL+	pre ZO BL-	early weak BL+	strong late cyl+ BL-	weak BL+	strong BL-	ScBL-	EuBL+
AR 9.15%	GL+ ZO- late	ZO+ GL- ScTr+	ScTr- BL+ weak	ScTr+ BL-	weak BL+	ScTr+ BL-		
EuBL 9.78%	ScBL+ ZO-	early ZO+	late	early	late	early	late	early
ScBL 7.32%	pre EuBL AR+ ZO-	AT+ AR- ZO+	AR-	AR+	strong EuBL+	weak EuBL-	early EuBL-	late EuBL+
GL 11.04%	AR+ AT- ZO-	AT+ AR- ZO+	AR+ AT- EuBL+	AT+ AR- EuBL-	AR+ AT-	cyl+ AR-	late AT+ ZO+ AR-	AR+ cyl-

Table 4.1: Overview of the main features driving a regime anomaly during DJF. The active regimes with their seasonal occurrence frequency are listed to the left, and the anomalies are on top. Abbreviations: BL stands for ScBL and EuBL together; cyl means all cyclonic regimes; late/early refers to the relative occurrence in the life cycle of the active regime; pre/post describes if the following named regime occurs notably if the following named regime occurs notably before or after the main regime. Cell color code: white cell=IWR working, yellow=IWR not so clear, red=situation unclear; if an IWR is named it is significantly different but is not considered to explain the anomalies

	T2M cold	T2M warm	Wind calm	Wind windy	TP dry	TP wet	SOLD cloudy	SOLD sunny
AT 8.99%	ScTr+ pre GL EuBL- ZO-	GL- ZO+ ScTr- EuBL+	weak BL+ ScTr-	pre GL ScTr+ BL-	BL+ ScTr-	pre GL ZO- EuBL-	ScTr+ BL- AR+	GL- BL+ ScTr-
ZO 4.16%	pre ScTr post EuBL	ScTr- AR- ScBL+	stronger	EuBl-	ScBL-	ScBL+	ScTr+ GL-	ScTr- GL+
ScTr 7.20%	AR+ GL+ ZO- EuBL-	early ZO+ GL- AR-	early ZO+ EuBL+ GL-	strong BL- GL+ ZO-	weak ZO+ EuBL+ GL-	ZO- EuBL-	strong AR+ ZO- BL-	early weak ZO+ BL+
AR 8.09%	late	pre EuBL	pre EuBL BL+ AT-	ScTr+ BL- AT+	pre EuBL ScTr-	EuBL-	ScTr+ EuBL-	pre EuBL
EuBL 13.21%	early AR+ ScTr+ ZO-	late ScBL+ ScTr-		AR+			early ZO- AR+	ScTr-
ScBL 15.90%	early ScTr+ AR+	late EuBL+ ScTr-		ZO- EuBL+	EuBL+ GL- ZO+ AR-	AT- AR+ ScTr+	AR+ ScTr+	EuBL+ ZO+ AR- ScTr-
GL 10.31%	AR+ BL- ScTr+	BL+ ScTr-	ScTr- EuBL+	ScTr+ BL-	ScTr- EuBL+	late	late	ScTr- EuBL+

Table 4.2: Overview of the main features driving a regime anomaly during JJA. The active regimes with their seasonal occurrence frequency are listed to the left, and the anomalies are on top. Abbreviations: BL stands for ScBL and EuBL together; cyl means all cyclonic regimes; late/early refers to the relative occurrence in the life cycle of the active regime; pre/post describes if the following named regime occurs notably if the following named regime occurs notably before or after the main regime. Cell color code: white cell=IWR working, yellow=IWR not so clear, red=situation unclear; if an IWR is named it is significantly different but is not considered to explain the anomalies

5 Conclusion and outlook

This thesis explores the variability in the surface impacts of European weather regimes (WRs). For the first time, a continent-wide overview of regions with low and high weather variability is provided, alongside explaining atmospheric dynamics and indications of how the variability will present itself. Previous work on the surface impact of regimes has proven valuable for the energy sector but has always focused on mean regime anomalies. Addressing only the mean anomalies leaves the gap of surface weather variability within a regime. It can lead to false assumptions when using regimes as a forecasting tool on the sub-seasonal scale. Here, several new insights are delivered by exploring variability in surface weather during regimes for the first time. This thesis clarified that significant complexity underlies the straightforward mean regime composites considered initially. Valuable insights were obtained into how this complexity can be understood and used to make better forecasts. Therefore, a 43-year-long sub-period of ECMWF's ERA5 reanalysis data set is used to evaluate the variability of weather anomalies across the European continent using different methods. Furthermore, after identifying regions, seasons, and regimes with large variability, efforts are made to understand the dynamics behind the variability and explain them simply within the regime framework using the weather regime index (IWR). The three research questions raised in the introduction (chapter 1) are answered:

1. How large is intra-regime variability in surface weather?
To answer this question, first, the mean anomalies 2 m temperature and 100 m wind speed, as well as SOLD - a measure for the incoming radiation in relation to the maximum possible at each day, are analyzed again. They agree considerably with previous studies, e.g., Cortesi et al. (2019), Grams et al. (2017), and van der Wiel, Bloomfield, et al. (2019). The main difference is the greater detail of ERA5. The precipitation anomalies during weather regimes are less studied and presented here, providing a more complete picture of the surface weather. Variability is detected and evaluated with the fractional standard deviation (FStD), signal-to-noise-ratio (S2N) and violin plots for chosen countries. The methods are applied to all seven regimes in every season and deeply analyzed for winter (DJF) and summer (JJA). It is shown that weather variability within the regimes can not be neglected due to its large ranges and spatial spread, depending on the regime and region. Some regimes, regions and variables prove to be more variable than others. In general, the absolute variability is larger in DJF than in JJA for all variables due to the larger climatology. The relative variability (variability of a WR compared to climatology) is larger in JJA than in DJF. Temperature anomalies are less variable within the meteorological variables than the anomalies of the other investigated variables. The variability within the temperature anomalies is especially low during the cyclonic regimes in winter around the North Sea, while the blocked regimes, especially Greenland blocking (GL), go along with higher variability. During JJA, the variability is larger for all regimes.

Wind speed anomalies show a more regional pattern than temperature anomalies and are also more variable in JJA than in DJF. Precipitation anomalies see the largest variabilities of all variables considered and orographic impacts. Furthermore, the seasonal difference between the regimes can be very large, for example, during European blocking and Scandinavian Blocking. SOLD sees less spatial variability and less variability for the cyclonic regimes and GL for both seasons mainly considered.

2. How can atmospheric dynamics explain intra-regime variability?
The changes in dynamics can explain the variability of a WR well. This fact is explored based on the prominent example of temperature anomalies during GL in DJF across Europe. Compared to the mean flow pattern, it changes during warm or cold anomalies, yet it is still considered a GL event. Often, one possible outcome goes along with the intensification of the average and the other with large changes in the flow pattern. Changes in the position and intensity of the ridges and troughs are the drivers of variability. A change in position can change the mean wind direction and strength and, by that, change the advection of air masses. Furthermore, radiative processes can also be altered depending on whether a region is influenced by a high-pressure system or not.

3. How can the variability be accounted for within the weather regime framework?
It is found that the changed flow pattern projects into a change of the IWR in most cases. Since the IWR measures how strong the atmosphere projects into one of the WR clusters, it is possible to make statements about a regime's true appearance (e.g., cold or warm GL). Three features can be identified: (1) changes in the strength of the main IWR. A weaker or stronger active regime is causing the anomalies. (2) A temporal shift of the main IWR compared to onset/decay, leading to a shorter or longer regime life cycle and less or more time for anomalies to evolve. The temporal shift can also mean that a certain anomaly occurs very early or late in the life cycle of a regime. Often, this is the case if a very strong and unusual opposite anomaly occurs compared to the mean anomaly. (3) the changed circulation often projects into the other, not active regimes. These changes in the IWR of the secondary regimes can describe the changed flow pattern. The secondary regime does not necessarily have to be (almost) active to explain the variability; it can also be less active than usual to provide an explanation.
Since the presented features change for regime, season and variable, each region must be considered individually. Furthermore, situations are identified where the IWR approach does not provide an easy-to-interpret picture. Here, other divers of the variability need to be considered.

This thesis does not only provide a continent-wide overview of regions with low and high weather variability for the first time together with an explanation helping to understand the variability, but this thesis also shows ways how to use information already existing within the regime framework to gain the knowledge of the true weather outcome of a regime. Together, all aspects can make WRs' weather forecasts more reliable. Situations are identified where variability is reduced, and the occurring regime brings weather close to the average, representing opportunities for very reliable weather forecasts. Situations with more variability show where a regime forecast needs to be used with more caution. The IWR analysis and its features add easy-to-understand information on the true regime impact. They thus can serve as an indicator in weather regime forecasts to make them

more precise and reliable.

This thesis also provides starting points for further research. For example, what is not investigated here is what causes the changes in the atmospheric flow patterns, leading to changed IWRs. To this stage, it remains unclear if this is just arbitrariness or if larger-scale drivers like the stratosphere, sea surface temperatures or the Madden Julian Oscillation (MJO) impact not only the occurrence frequencies of regimes but also the secondary regimes. For example, Cassou (2008) found in the context of the classical WRs that certain phases of the MJO enhance/reduce the occurrence frequencies of the NAO+/NAO- regimes by up to -40/+70% a few days after. The Atlantic ridge and Blocking regimes remain largely uninfluenced by the MJO. Also, in the classical concept of the WRs, it is found that a strong/weak stratospheric vortex favors NAO+/NAO- while Blocking is less affected (Charlton-Perez et al., 2018). Domeisen et al. (2020) found that AR and ScTr can be observed more often before a Sudden Stratospheric warming event, while AT and GL are more frequent after. This leaves room for further investigations.
Also, the exact pathways of the German cases remain open, where none of the three IWR features can explain the unusual weather. Hypotheses that seem reasonable were presented, but if they are the main cause, further case studies of these particular events are required. These cases happen less in winter and are, for the majority, unrelated to temperature anomalies. Here, the regime framework works very well, especially if the anomalies are large. The weaker signal in summer seems to be the reason for the relatively larger variability. Moreover, while IWRs can still explain unusual temperature events, many unclear situations exist for wind speed and precipitation anomalies in summer. If this is due to convective processes playing a role, it is a further point for future investigations, especially EuBL, where the IWRs fail to deliver a qualified answer.
Since most of the in-depth analysis is focused on Germany, due to time constraints, it would be interesting to repeat the analysis for other representative countries like Spain for the Iberian Peninsula, Sweden or Norway for Scandinavia and a country in southeastern Europe. This extended analysis could reveal if some regime-variable combination is exceptionally uncertain, and further analysis could deliver answers on the temporal and spatial correlations between the anomalies and features, for example, the unusual anomalies of GL in Germany and Spain. The temporal correlations between variable anomalies are also of interest to the energy sector since balancing effects are only possible if the balancing region sees high overproduction. A further point of investigation could be to combine the analysis of CFs of Grams et al. (2017) with the methods to detect variability presented here to obtain clarifications for how surface weather variability affects the output of renewables.

Bibliography

Beerli, R., & Grams, C. M. (2019). Stratospheric modulation of the large–scale circulation in the atlantic–european region and its implications for surface weather events. *Quarterly Journal of the Royal Meteorological Society*, *145*(725), 3732–3750. https://doi.org/10.1002/qj.3653

Bessec, M., & Fouquau, J. (2008). The non-linear link between electricity consumption and temperature in europe: A threshold panel approach. *Energy Economics*, *30*(5), 2705–2721. https://doi.org/10.1016/j.eneco.2008.02.003

Bieli, M., Pfahl, S., & Wernli, H. (2015). A lagrangian investigation of hot and cold temperature extremes in europe. *Quarterly Journal of the Royal Meteorological Society*, *141*(686), 98–108. https://doi.org/10.1002/qj.2339

Bloomfield, H. C., Brayshaw, D. J., Shaffrey, L. C., Coker, P. J., & Thornton, H. E. (2016). Quantifying the increasing sensitivity of power systems to climate variability. *Environmental Research Letters*, *11*(12), 124025. https://doi.org/10.1088/1748-9326/11/12/124025

Bloomfield, H. C., Brayshaw, D. J., & Charlton–Perez, A. J. (2020). Characterizing the winter meteorological drivers of the european electricity system using targeted circulation types. *Meteorological Applications*, *27*(1). https://doi.org/10.1002/met.1858

Büeler, D., Ferranti, L., Magnusson, L., Quinting, J. F., & Grams, C. M. (2021). Year-round sub-seasonal forecast skill for atlantic–european weather regimes. *Quarterly Journal of the Royal Meteorological Society*, *147*(741), 4283–4309. https://doi.org/10.1002/qj.4178

Bundesregierung, D. (2024, February 12). *So läuft der ausbau der erneuerbaren energien in deutschland*. Retrieved March 15, 2024, from https://www.bundesregierung.de/breg-de/aktuelles/ausbau-erneuerbare-energien-2225808

Cannon, D. J., Brayshaw, D. J., Methven, J., Coker, P. J., & Lenaghan, D. (2015). Using reanalysis data to quantify extreme wind power generation statistics: A 33 year case study in great britain. *Renewable Energy*, *75*, 767–778. https://doi.org/10.1016/j.renene.2014.10.024

Cassou, C. (2008). Intraseasonal interaction between the madden-julian oscillation and the north atlantic oscillation [_eprint: 18818656]. *Nature*, *455*(7212), 523–527. https://doi.org/10.1038/nature07286

Charlton-Perez, A. J., Ferranti, L., & Lee, R. W. (2018). The influence of the stratospheric state on north atlantic weather regimes. *Quarterly Journal of the Royal Meteorological Society*, *144*(713), 1140–1151. https://doi.org/10.1002/qj.3280

Commission, E. (2019). *The european green deal - striving to be the first climate-neutral continent*. Retrieved February 21, 2024, from https://commission.europa.eu/strategy-and-policy/priorities-2019-2024/european-green-deal_en

Cortesi, N., Torralba, V., González-Reviriego, N., Soret, A., & Doblas-Reyes, F. J. (2019). Characterization of european wind speed variability using weather regimes. *Climate Dynamics*, *53*(7), 4961–4976. https://doi.org/10.1007/s00382-019-04839-5

Domeisen, D. I. V., Grams, C. M., & Papritz, L. (2020). The role of north atlantic–european weather regimes in the surface impact of sudden stratospheric warming events. *Weather and Climate Dynamics*, *1*(2), 373–388. https://doi.org/10.5194/wcd-1-373-2020

Dorrington, J. C. (2021). *On the variability and forced response of atmospheric regime systems* [Doctoral dissertation, University of Oxford].

Dulière, V., Zhang, Y., & Salathé, E. P. (2011). Extreme precipitation and temperature over the u.s. pacific northwest: A comparison between observations, reanalysis data, and regional models*. *Journal of Climate*, *24*(7), 1950–1964. https://doi.org/10.1175/2010JCLI3224.1

ECMWF. (2023, August 23). *Fact sheet: Reanalysis*. Retrieved February 21, 2024, from https://www.ecmwf.int/en/about/media-centre/focus/2023/fact-sheet-reanalysis

Garrido-Perez, J. M., Ordóñez, C., Barriopedro, D., García-Herrera, R., & Paredes, D. (2020). Impact of weather regimes on wind power variability in western europe. *Applied Energy*, *264*, 114731. https://doi.org/10.1016/j.apenergy.2020.114731

Grams, C. M., Beerli, R., Pfenninger, S., Staffell, I., & Wernli, H. (2017). Balancing europe's wind power output through spatial deployment informed by weather regimes [_eprint: 28781614]. *Nature climate change*, *7*(8), 557–562. https://doi.org/10.1038/NCLIMATE3338

Grams, C. M., Ferranti, L., & Magnusson, L. (2020, November). *How to make use of weather regimes in extended-range predictions for europe* (Newsletter No. 165). Retrieved February 20, 2024, from https://www.ecmwf.int/en/newsletter/165/meteorology/how-make-use-weather-regimes-extended-range-predictions-europe

Hauser, S., Teubler, F., Riemer, M., Knippertz, P., & Grams, C. M. (2022, August 8). *Towards a diagnostic framework unifying different perspectives on blocking dynamics: Insight into a major blocking in the north atlantic-european region* (preprint). Dynamical processes in midlatitudes. https://doi.org/10.5194/wcd-2022-44

Hersbach, H., Bell, B., Berrisford, P., Hirahara, S., Horányi, A., Muñoz–Sabater, J., Nicolas, J., Peubey, C., Radu, R., Schepers, D., Simmons, A., Soci, C., Abdalla, S., Abellan, X., Balsamo, G., Bechtold, P., Biavati, G., Bidlot, J., Bonavita, M., … Thépaut, J.-N. (2020). The ERA5 global reanalysis. *Quarterly Journal of the Royal Meteorological Society*, *146*(730), 1999–2049. https://doi.org/10.1002/qj.3803

Hertig, E., & Jacobeit, J. (2014). Variability of weather regimes in the north atlantic-european area: Past and future. *Atmospheric Science Letters*, *15*(4), 314–320. https://doi.org/10.1002/asl2.505

Kautz, L.-A., Martius, O., Pfahl, S., Pinto, J. G., Ramos, A. M., Sousa, P. M., & Woollings, T. (2022). Atmospheric blocking and weather extremes over the euro-atlantic sector – a review. *Weather and Climate Dynamics*, *3*(1), 305–336. https://doi.org/10.5194/wcd-3-305-2022

Lavers, D. A., Simmons, A., Vamborg, F., & Rodwell, M. J. (2022). An evaluation of ERA5 precipitation for climate monitoring. *Quarterly Journal of the Royal Meteorological Society*, *148*(748), 3152–3165. https://doi.org/10.1002/qj.4351

Lee, J. C. K., Lee, R. W., Woolnough, S. J., & Boxall, L. J. (2020). The links between the madden-julian oscillation and european weather regimes. *Theoretical and Applied Climatology*, *141*(1), 567–586. https://doi.org/10.1007/s00704-020-03223-2

Lee, S. H., Tippett, M. K., & Polvani, L. M. (2023). A new year-round weather regime classification for north america. *Journal of Climate*, *36*(20), 7091–7108. https://doi.org/10.1175/JCLI-D-23-0214.1

Li, B., Basu, S., Watson, S. J., & Russchenberg, H. W. J. (2021). A brief climatology of dunkelflaute events over and surrounding the north and baltic sea areas. *Energies*, *14*(20), 6508. https://doi.org/10.3390/en14206508

Madonna, E., Li, C., Grams, C. M., & Woollings, T. (2017). The link between eddy-driven jet variability and weather regimes in the north atlantic-european sector. *Quarterly Journal of the Royal Meteorological Society*, *143*(708), 2960–2972. https://doi.org/10.1002/qj.3155

Messori, G., & Dorrington, J. (2023). A joint perspective on north american and euro-atlantic weather regimes. *Geophysical Research Letters*, *50*(21), e2023GL104696. https://doi.org/10.1029/2023GL104696

Michel, C., & Rivière, G. (2011). The link between rossby wave breakings and weather regime transitions. *Journal of the Atmospheric Sciences*, *68*(8), 1730–1748. https://doi.org/10.1175/2011JAS3635.1

Michelangeli, P.-A., Vautard, R., & Legras, B. (1995). Weather regimes: Recurrence and quasi stationarity. *Journal of the Atmospheric Sciences*, *52*(8), 1237–1256. https://doi.org/10.1175/1520-0469(1995)052<1237:WRRAQS>2.0.CO;2

Mockert, F., Grams, C. M., Brown, T., & Neumann, F. (2023). Meteorological conditions during dunkelflauten in germany: Characteristics, the role of weather regimes and impacts on demand.

Molina, M. O., Gutiérrez, C., & Sánchez, E. (2021). Comparison of ERA5 surface wind speed climatologies over europe with observations from the HadISD dataset. *International Journal of Climatology*, *41*(10), 4864–4878. https://doi.org/10.1002/joc.7103

Mühlemann, D., Folini, D., Pfenninger, S., Wild, M., & Wohland, J. (2022). Meteorologically–informed spatial planning of european PV deployment to reduce multiday generation variability. *Earth's Future*, *10*(7). https://doi.org/10.1029/2022EF002673

NCAR, C. D. G. (2024). *Atmospheric reanalysis: Overview & comparison tables*. Retrieved February 21, 2024, from https://climatedataguide.ucar.edu/climate-data/atmospheric-reanalysis-overview-comparison-tables

Osman, M., Beerli, R., Büeler, D., & Grams, C. M. (2023). Multi-model assessment of sub-seasonal predictive skill for year-round atlantic–european weather regimes. *Quarterly Journal of the Royal Meteorological Society*, *149*(755), 2386–2408. https://doi.org/10.1002/qj.4512

Otero, N., Martius, O., Allen, S., Bloomfield, H., & Schaefli, B. (2022). Characterizing renewable energy compound events across europe using a logistic regression-based approach. *Meteorological Applications*, *29*(5), e2089. https://doi.org/10.1002/met.2089

Pasquier, J. T., Pfahl, S., & Grams, C. M. (2019). Modulation of atmospheric river occurrence and associated precipitation extremes in the north atlantic region by european weather regimes. *Geophysical Research Letters*, *46*(2), 1014–1023. https://doi.org/10.1029/2018GL081194

Pfahl, S., & Wernli, H. (2012). Quantifying the relevance of atmospheric blocking for co-located temperature extremes in the northern hemisphere on (sub-)daily time scales. *Geophysical Research Letters*, *39*(12), n/a–n/a. https://doi.org/10.1029/2012GL052261

Plaut, G., & Simonnet, E. (2001). Large-scale circulation classification, weather regimes, and local climate over france, the alps and western europe. *Climate Research*, *17*, 303–324. https://doi.org/10.3354/cr017303

Raynaud, D., Hingray, B., François, B., & Creutin, J. (2018). Energy droughts from variable renewable energy sources in european climates. *Renewable Energy*, *125*, 578–589. https://doi.org/10.1016/j.renene.2018.02.130

Robertson, A. W., & Ghil, M. (1999). Large-scale weather regimes and local climate over the western united states. *Journal of Climate*, *12*(6), 1796–1813. https://doi.org/10.1175/1520-0442(1999)012<1796:LSWRAL>2.0.CO;2

Staffell, I., & Pfenninger, S. (2018). The increasing impact of weather on electricity supply and demand. *Energy*, *145*, 65–78. https://doi.org/10.1016/j.energy.2017.12.051

Teubler, F., Riemer, M., Polster, C., Grams, C. M., Hauser, S., & Wirth, V. (2023). Similarity and variability of blocked weather-regime dynamics in the atlantic–european region. *Weather and Climate Dynamics*, *4*(2), 265–285. https://doi.org/10.5194/wcd-4-265-2023

Ullmann, A., Fontaine, B., & Roucou, P. (2014). Euro-atlantic weather regimes and mediterranean rainfall patterns: Present-day variability and expected changes under CMIP5 projections. *International Journal of Climatology*, *34*(8), 2634–2650. https://doi.org/10.1002/joc.3864

van der Wiel, K., Stoop, L. P., van Zuijlen, B., Blackport, R., van den Broek, M. A., & Selten, F. M. (2019). Meteorological conditions leading to extreme low variable renewable energy production and extreme high energy shortfall. *Renewable and Sustainable Energy Reviews*, *111*, 261–275. https://doi.org/10.1016/j.rser.2019.04.065

van der Wiel, K., Bloomfield, H. C., Lee, R. W., Stoop, L. P., Blackport, R., Screen, J. A., & Selten, F. M. (2019). The influence of weather regimes on european renewable energy production and demand. *Environmental Research Letters*, *14*(9), 094010. https://doi.org/10.1088/1748-9326/ab38d3

Vautard, R. (1990). Multiple weather regimes over the north atlantic: Analysis of precursors and successors. *Monthly Weather Review*, *118*(10), 2056–2081. https://doi.org/10.1175/1520-0493(1990)118<2056:MWROTN>2.0.CO;2

Velikou, K., Lazoglou, G., Tolika, K., & Anagnostopoulou, C. (2022). Reliability of the ERA5 in replicating mean and extreme temperatures across europe. *Water*, *14*(4), 543. https://doi.org/10.3390/w14040543

White, C. J., Carlsen, H., Robertson, A. W., Klein, R. J., Lazo, J. K., Kumar, A., Vitart, F., Coughlan De Perez, E., Ray, A. J., Murray, V., Bharwani, S., MacLeod, D., James, R., Fleming, L., Morse, A. P., Eggen, B., Graham, R., Kjellström, E., Becker, E., … Zebiak, S. E. (2017). Potential applications of subseasonal-to-seasonal (s2s) predictions. *Meteorological Applications*, *24*(3), 315–325. https://doi.org/10.1002/met.1654

Yiou, P., Goubanova, K., Li, Z. X., & Nogaj, M. (2008). Weather regime dependence of extreme value statistics for summer temperature and precipitation. *Nonlinear Processes in Geophysics*, (15), 365–378.

Yiou, P., & Nogaj, M. (2004). Extreme climatic events and weather regimes over the north atlantic: When and where? *Geophysical Research Letters*, *31*(7), n/a–n/a. https://doi.org/10.1029/2003GL019119

Appendix

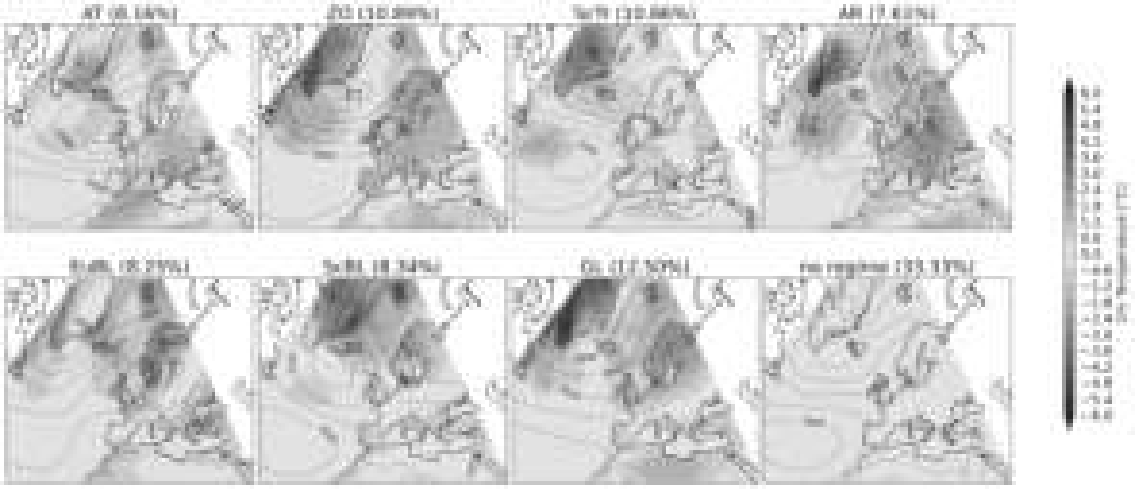

Figure 1: T2M anomalies in [°C] during the seven different weather regimes and the no regime in shadings during MAM over Europe and the North Atlantic together with mean sea level pressure lines in black and units in hectopascal. The occurrence frequency of the regimes is given in brackets.

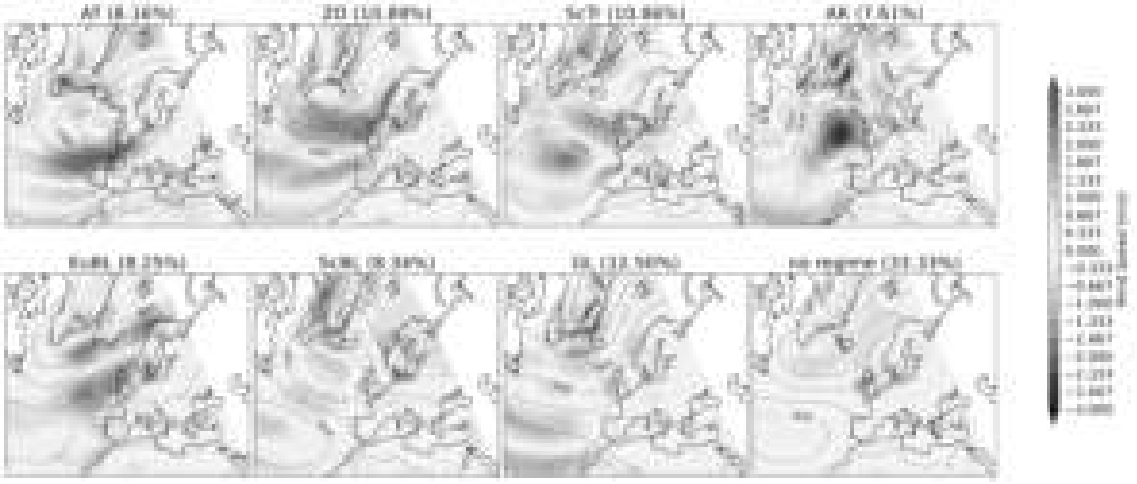

Figure 2: 100 m wind speed anomalies in [m/s] during the seven different weather regimes and the no regime in shadings during MAM over Europe and the North Atlantic together with mean sea level pressure lines in black and units in hectopascal. The occurrence frequency of the regimes is given in brackets.

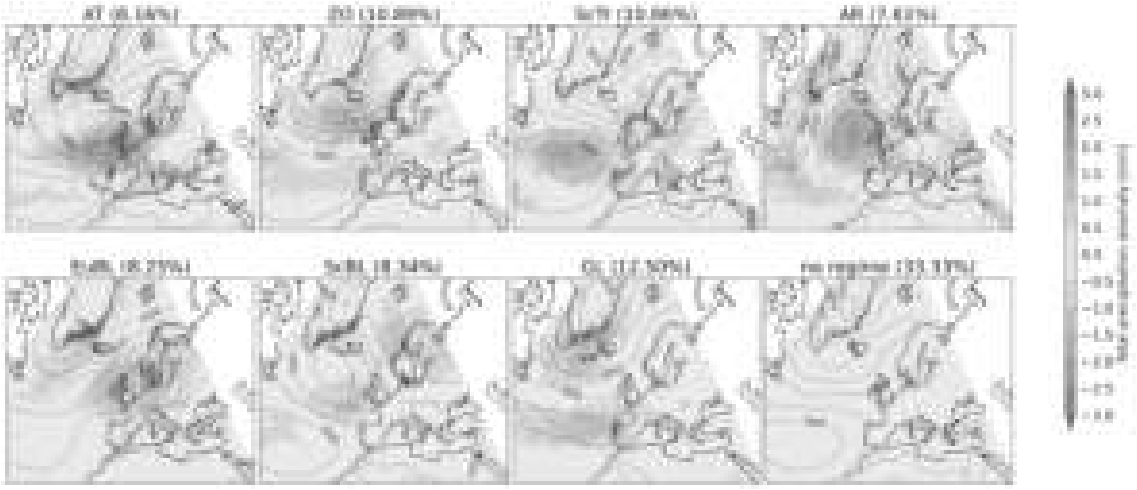

Figure 3: Anomalies in TP in [mm] during the seven different weather regimes and the no regime in shadings during MAM over Europe and the North Atlantic together with mean sea level pressure lines in black and units in hectopascal. The occurrence frequency of the regimes is given in brackets.

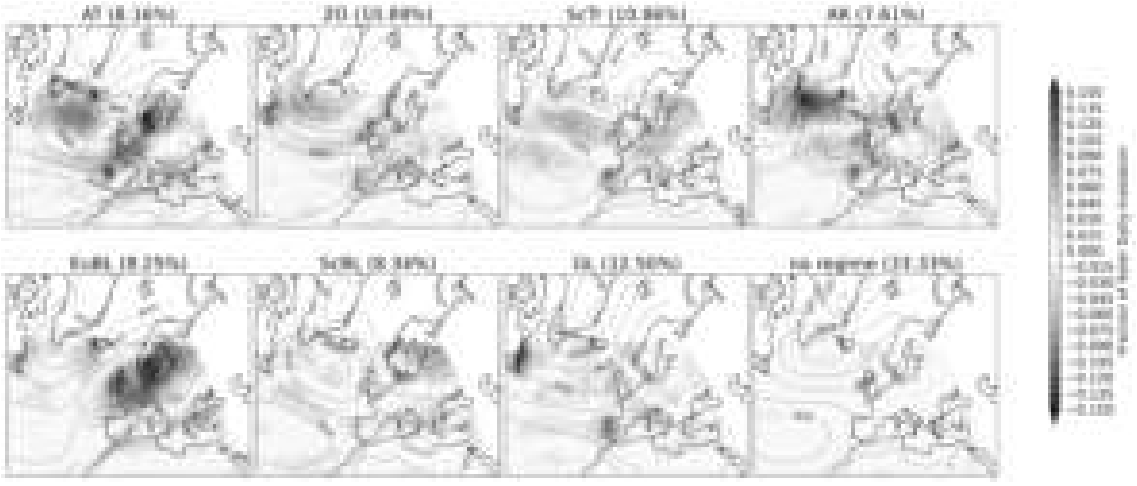

Figure 4: Fraction of SOLD anomalies during the seven different weather regimes and the no regime in shadings during MAM over Europe and the North Atlantic together with mean sea level pressure lines in black and units in hectopascal. The occurrence frequency of the regimes is given in brackets.

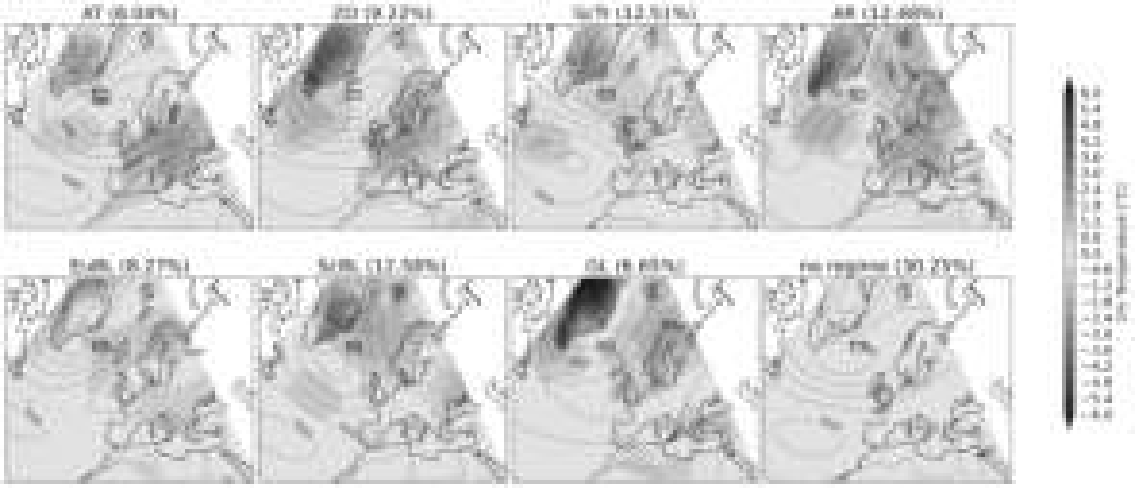

Figure 5: T2M anomalies in [°C] during the seven different weather regimes and the no regime in shadings during SON over Europe and the North Atlantic together with mean sea level pressure lines in black and units in hectopascal. The occurrence frequency of the regimes is given in brackets.

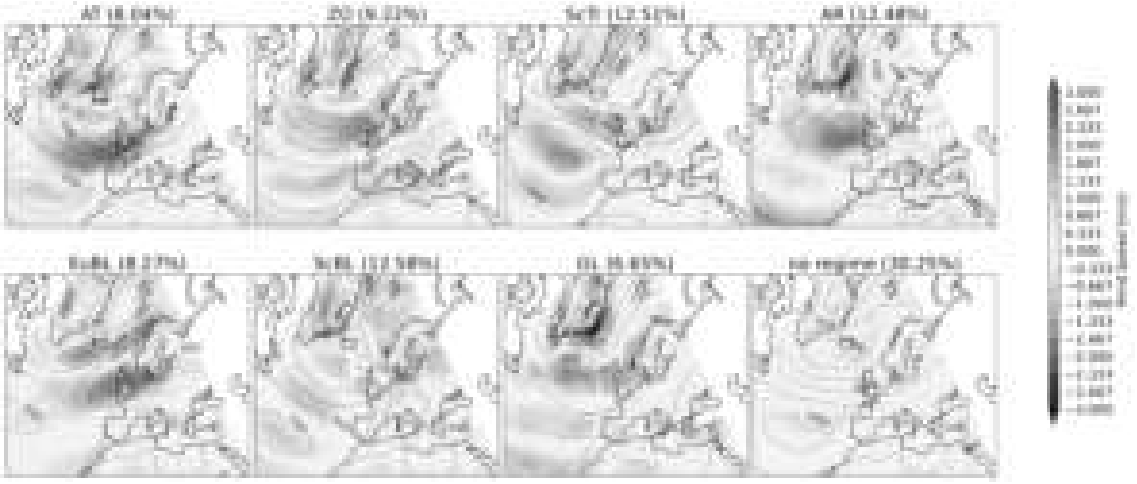

Figure 6: 100 m wind speed anomalies in [m/s] during the seven different weather regimes and the no regime in shadings during SON over Europe and the North Atlantic together with mean sea level pressure lines in black and units in hectopascal. The occurrence frequency of the regimes is given in brackets.

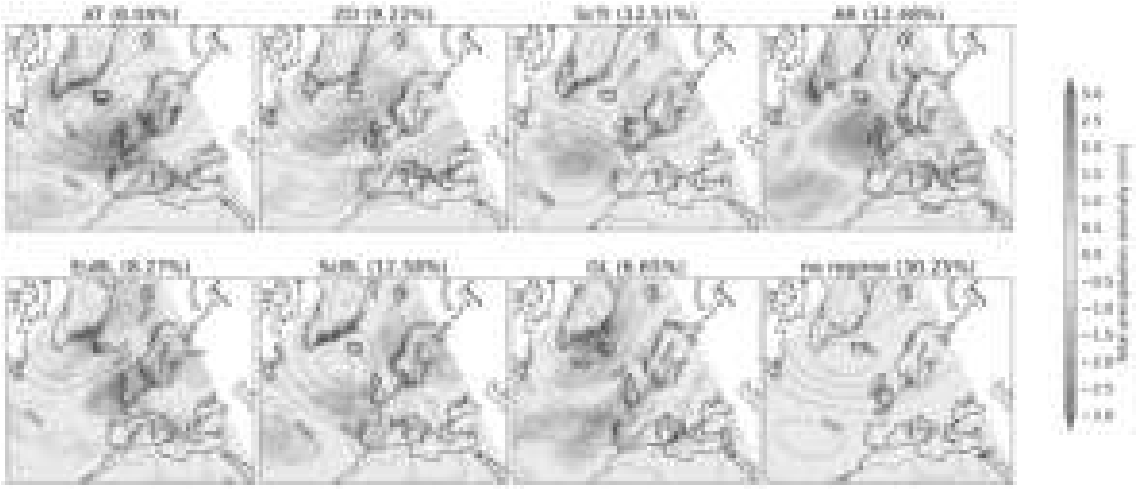

Figure 7: Anomalies in TP in [mm] during the seven different weather regimes and the no regime in shadings during SON over Europe and the North Atlantic together with mean sea level pressure lines in black and units in hectopascal. The occurrence frequency of the regimes is given in brackets.

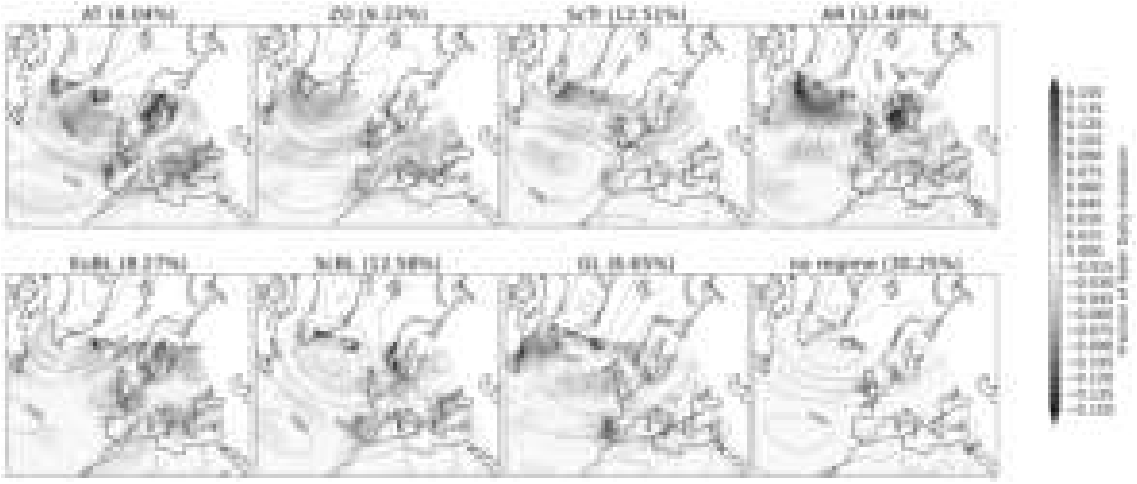

Figure 8: Fraction of SOLD anomalies during the seven different weather regimes and the no regime in shadings during SON over Europe and the North Atlantic together with mean sea level pressure lines in black and units in hectopascal. The occurrence frequency of the regimes is given in brackets.

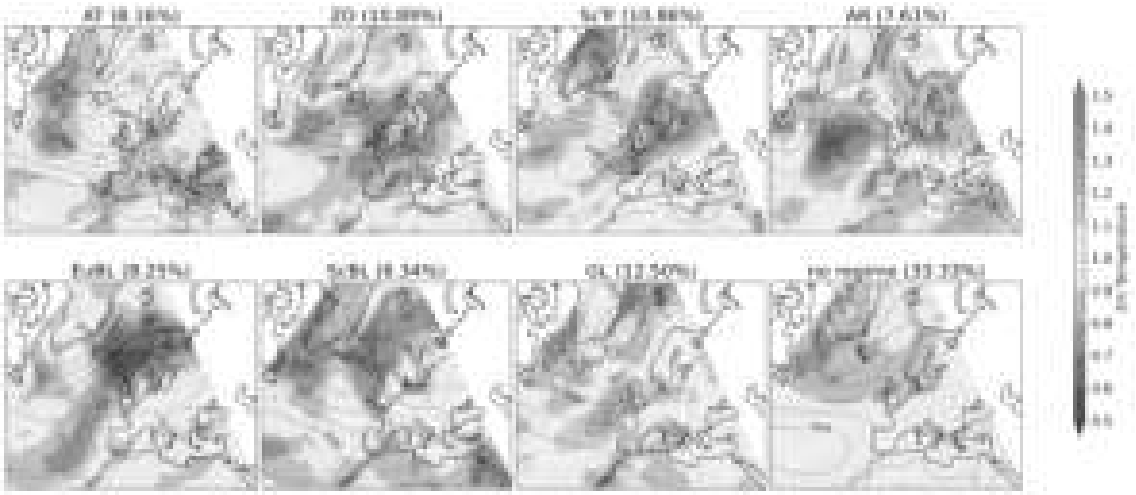

Figure 9: Fractional standard deviation of T2M anomalies during the seven different weather regimes and the no regime in shadings during MAM over Europe and the North Atlantic together with mean sea level pressure lines in black and units in hectopascal.

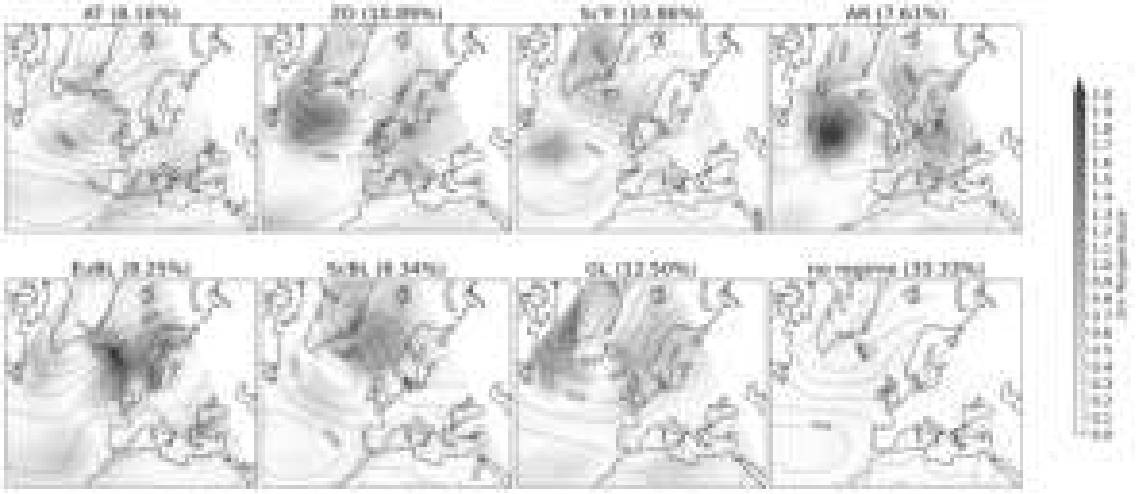

Figure 10: Absolute values of the signal to noise ratio of T2M anomalies during the seven different weather regimes and the no regime in shadings during MAM over Europe and the North Atlantic together with mean sea level pressure lines in black and units in hectopascal. The red line indicates values above 1.

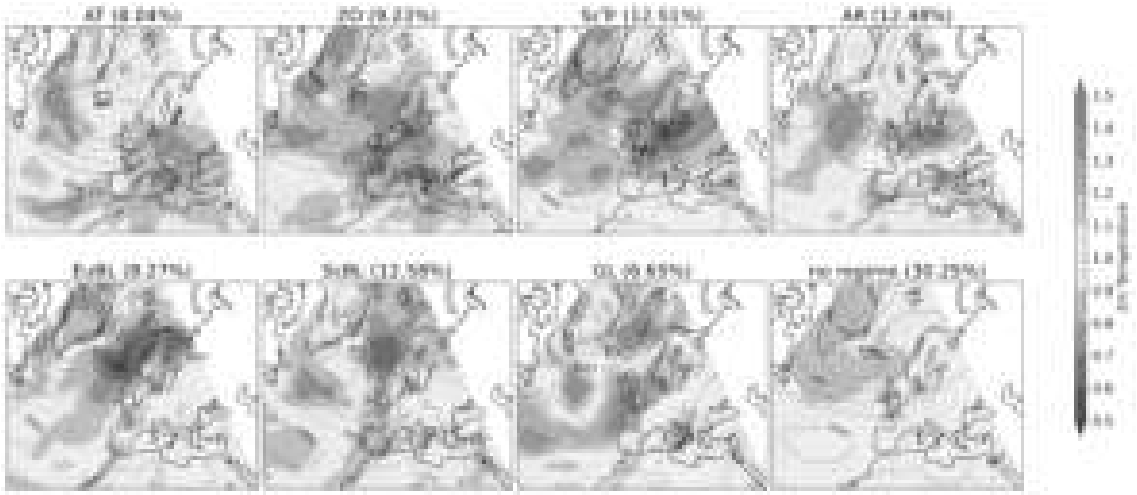

Figure 11: Fractional standard deviation of T2M anomalies during the seven different weather regimes and the no regime in shadings during SON over Europe and the North Atlantic together with mean sea level pressure lines in black and units in hectopascal.

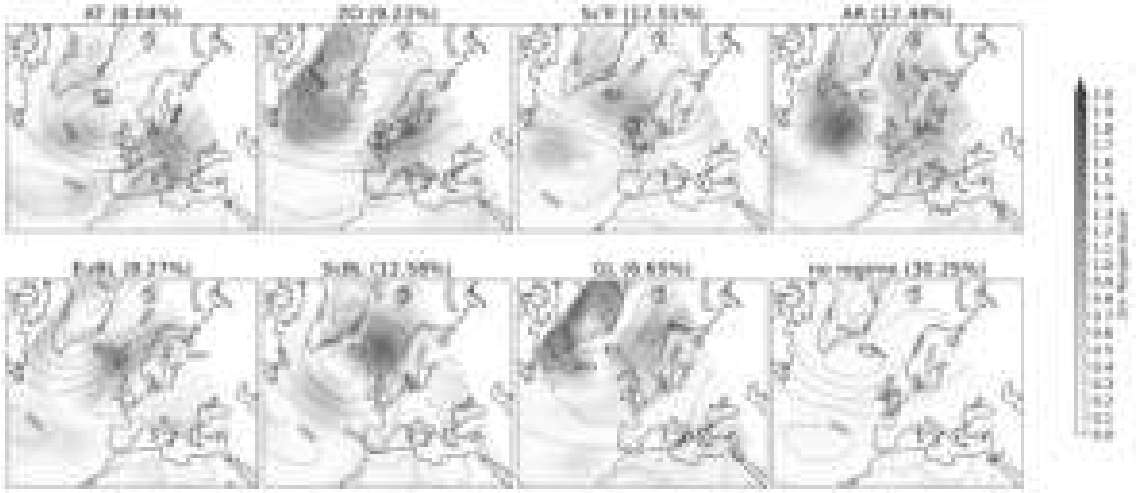

Figure 12: Absolute values of the signal to noise ratio of T2M anomalies during the seven different weather regimes and the no regime in shadings during SON over Europe and the North Atlantic together with mean sea level pressure lines in black and units in hectopascal. The red line indicates values above 1.

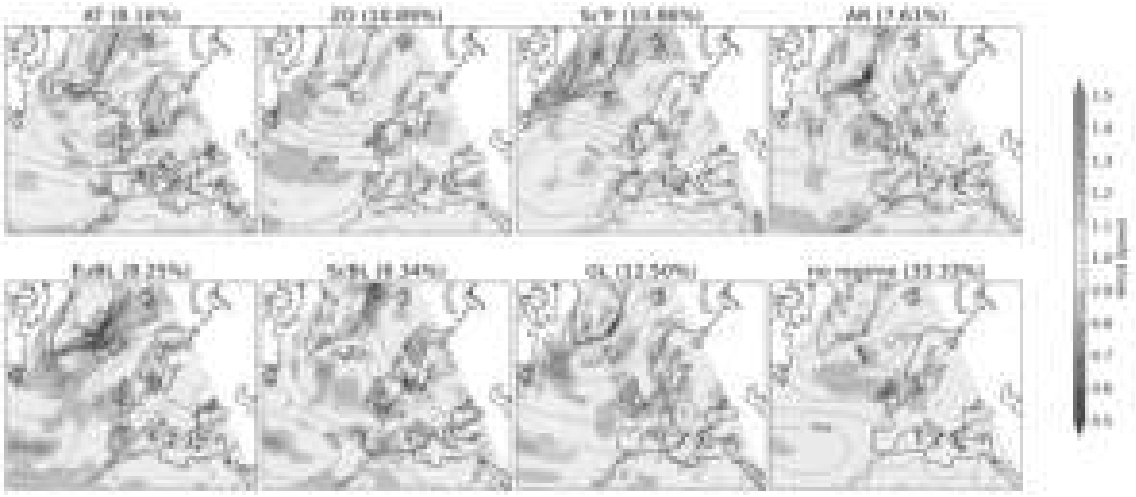

Figure 13: Fractional standard deviation of 100 m wind speed anomalies during the seven different weather regimes and the no regime in shadings during MAM over Europe and the North Atlantic together with mean sea level pressure lines in black and units in hectopascal.

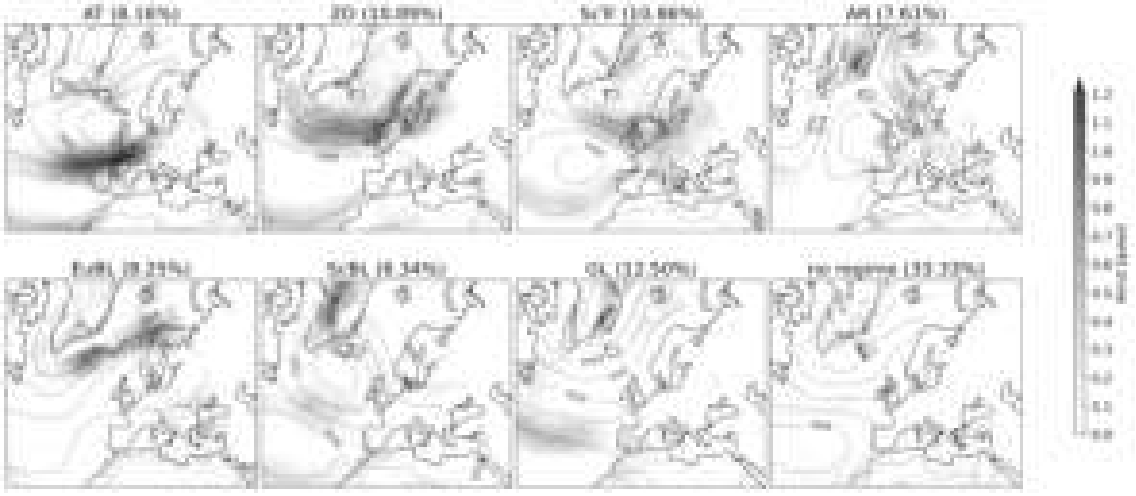

Figure 14: Absolute values of the signal to noise ratio of 100 m wind speed anomalies during the seven different weather regimes and the no regime in shadings during MAM over Europe and the North Atlantic together with mean sea level pressure lines in black and units in hectopascal. The red line indicates values above 1.

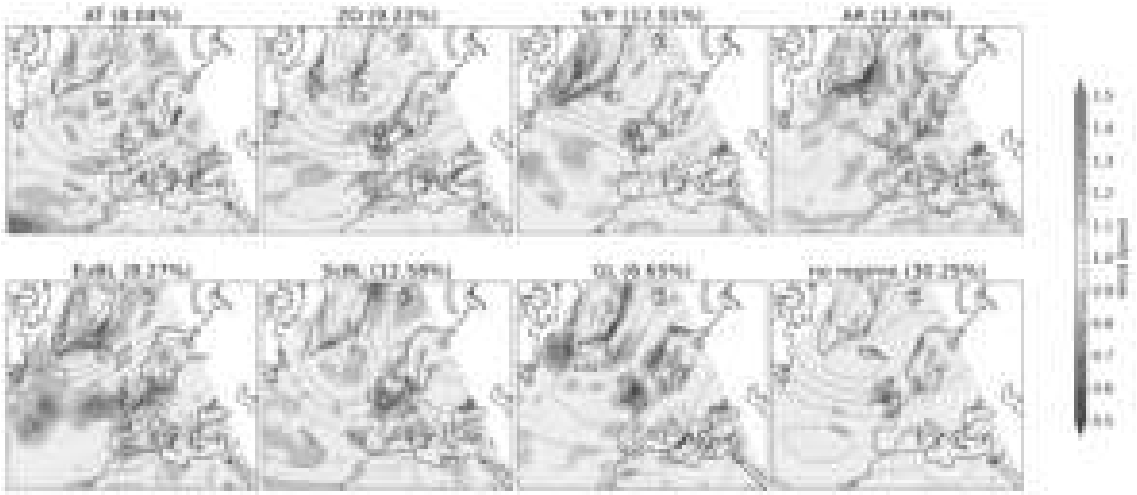

Figure 15: Fractional standard deviation of 100 m wind speed anomalies during the seven different weather regimes and the no regime in shadings during SON over Europe and the North Atlantic together with mean sea level pressure lines in black and units in hectopascal.

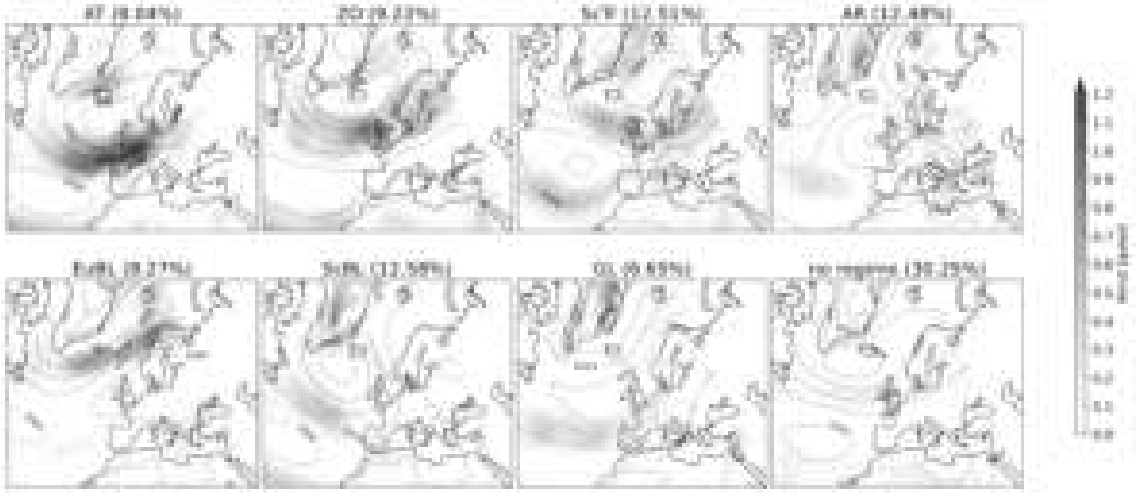

Figure 16: Absolute values of the signal to noise ratio of 100 m wind speed anomalies during the seven different weather regimes and the no regime in shadings during SON over Europe and the North Atlantic together with mean sea level pressure lines in black and units in hectopascal. The red line indicates values above 1.

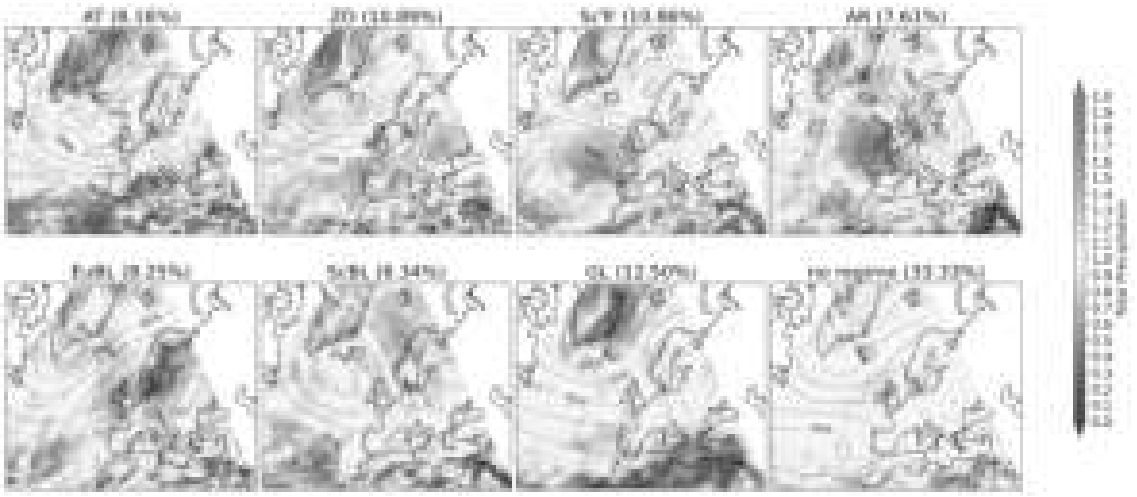

Figure 17: Fractional standard deviation of TP anomalies during the seven different weather regimes and the no regime in shadings during MAM over Europe and the North Atlantic together with mean sea level pressure lines in black and units in hectopascal.

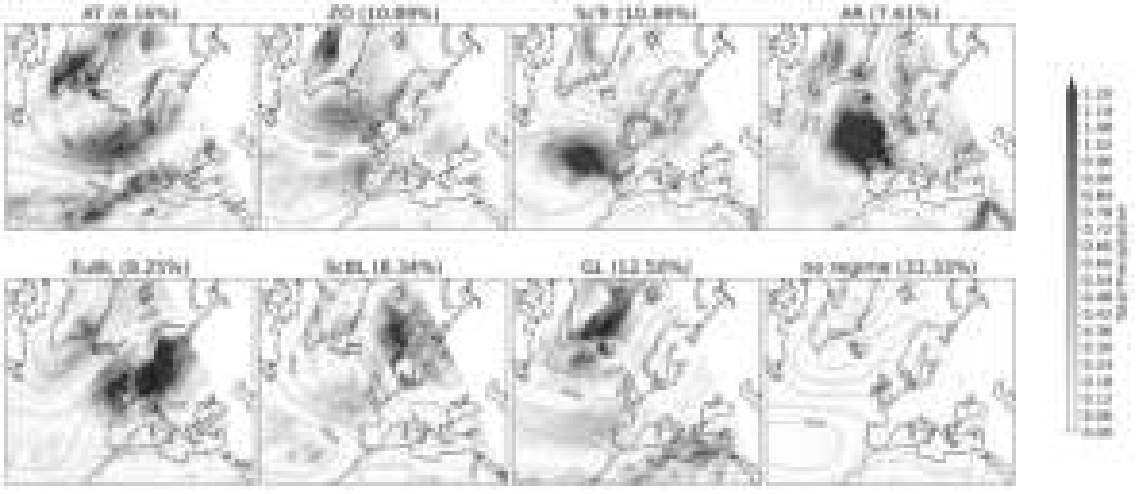

Figure 18: Absolute values of the signal to noise ratio of TP anomalies during the seven different weather regimes and the no regime in shadings during MAM over Europe and the North Atlantic together with mean sea level pressure lines in black and units in hectopascal. The red line indicates values above 1.

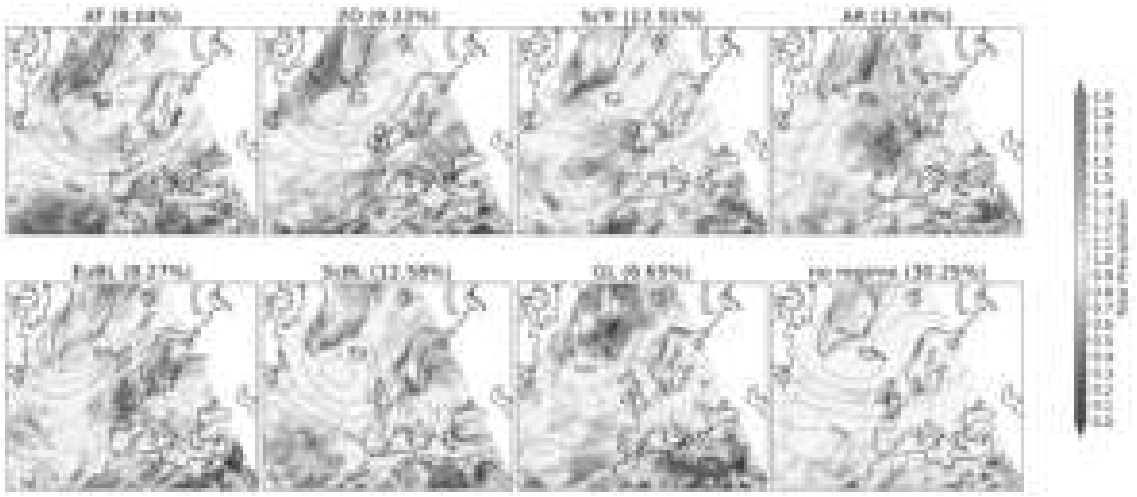

Figure 19: Fractional standard deviation of TP anomalies during the seven different weather regimes and the no regime in shadings during SON over Europe and the North Atlantic together with mean sea level pressure lines in black and units in hectopascal.

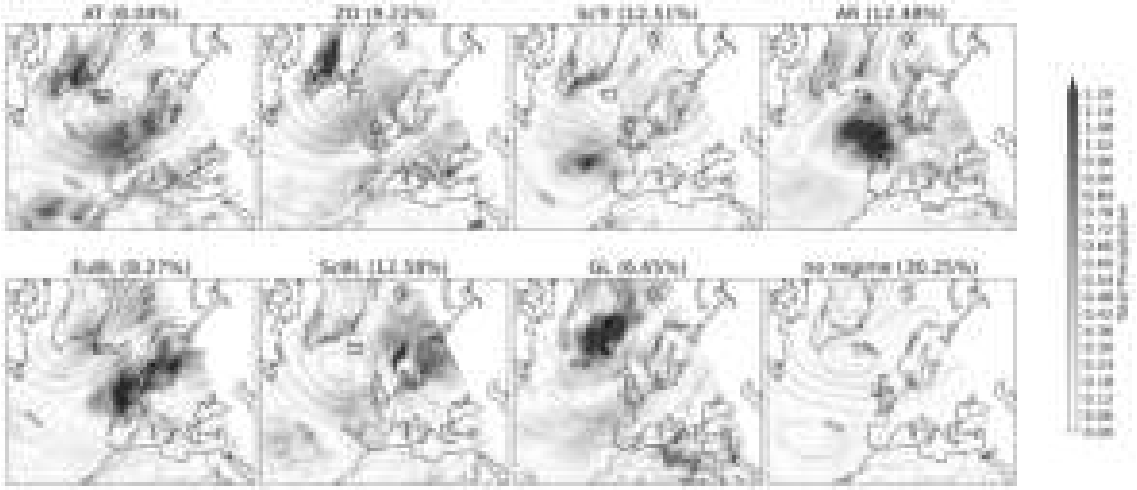

Figure 20: Absolute values of the signal to noise ratio of TP anomalies during the seven different weather regimes and the no regime in shadings during SON over Europe and the North Atlantic together with mean sea level pressure lines in black and units in hectopascal. The red line indicates values above 1.

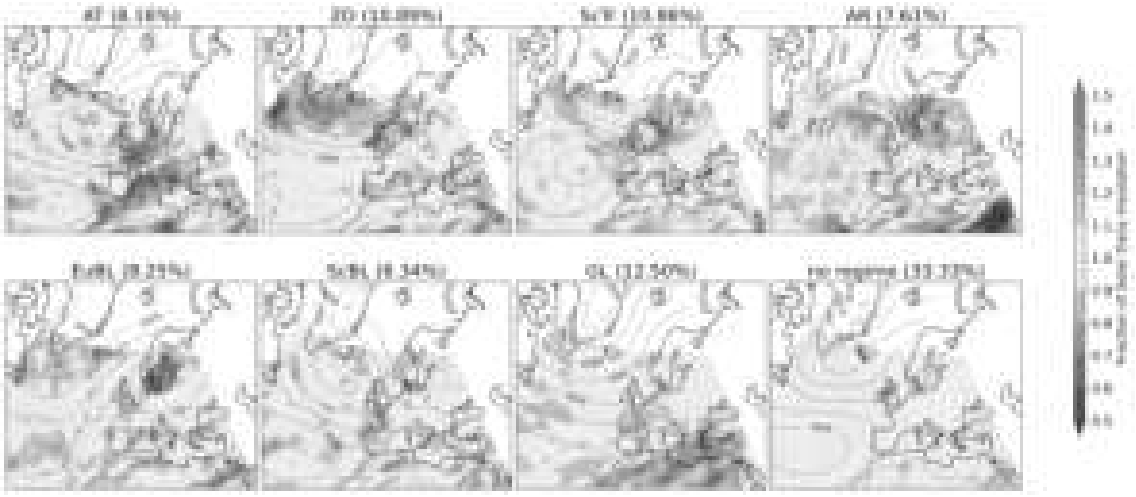

Figure 21: Fractional standard deviation of SOLD anomalies during the seven different weather regimes and the no regime in shadings during MAM over Europe and the North Atlantic together with mean sea level pressure lines in black and units in hectopascal.

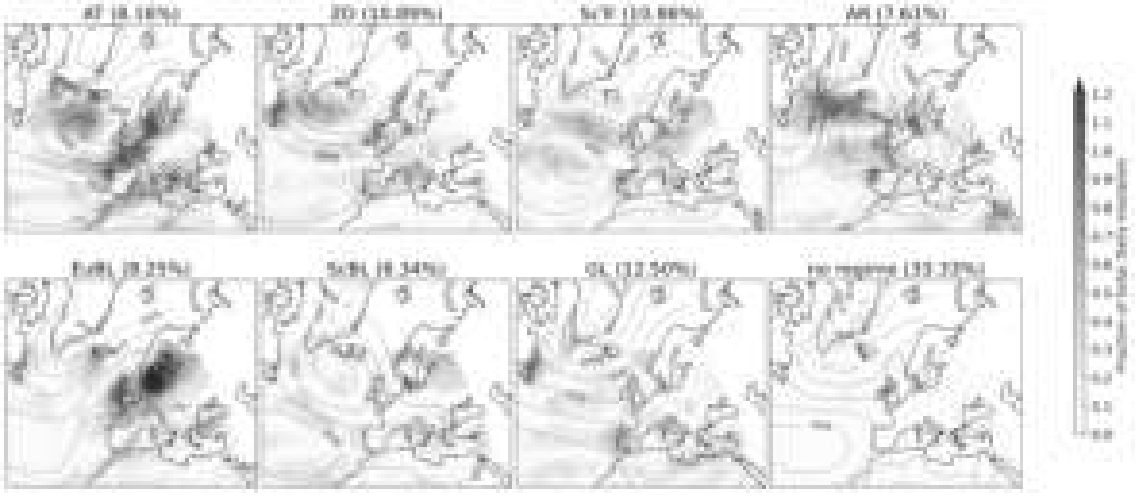

Figure 22: Absolute values of the signal to noise ratio of SOLD anomalies during the seven different weather regimes and the no regime in shadings during MAM over Europe and the North Atlantic together with mean sea level pressure lines in black and units in hectopascal. The red line indicates values above 1.

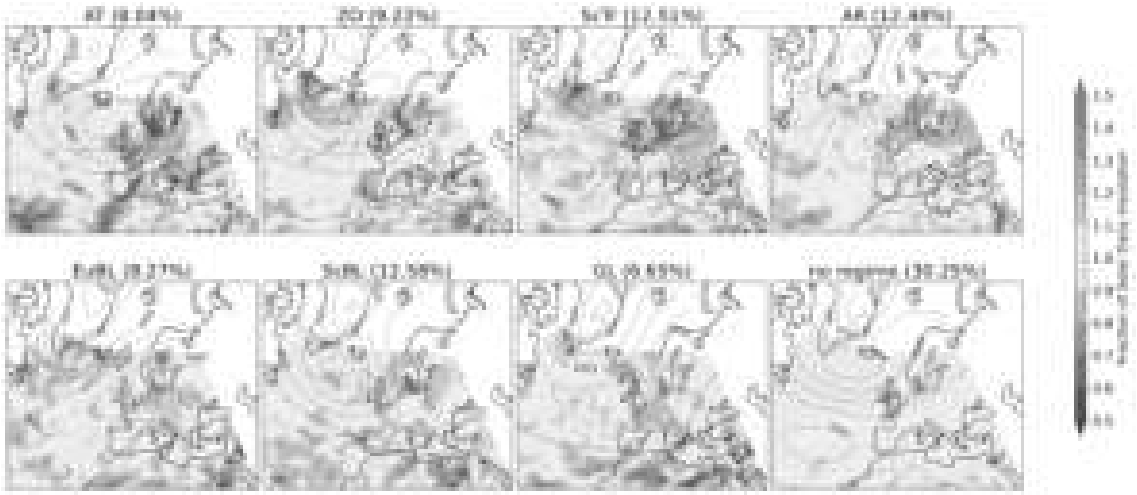

Figure 23: Fractional standard deviation of SOLD anomalies during the seven different weather regimes and the no regime in shadings during SON over Europe and the North Atlantic together with mean sea level pressure lines in black and units in hectopascal.

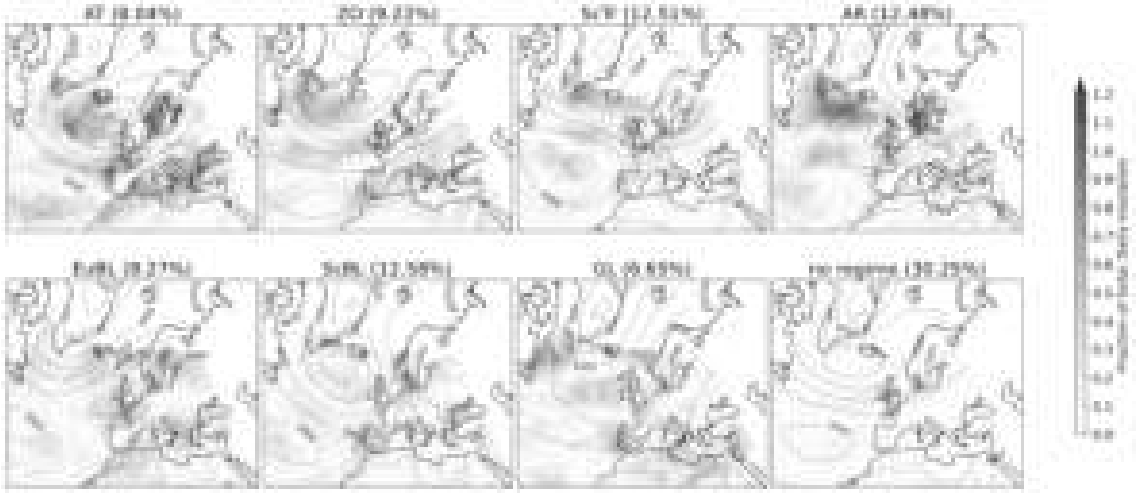

Figure 24: Absolute values of the signal to noise ratio of SOLD anomalies during the seven different weather regimes and the no regime in shadings during SON over Europe and the North Atlantic together with mean sea level pressure lines in black and units in hectopascal. The red line indicates values above 1.

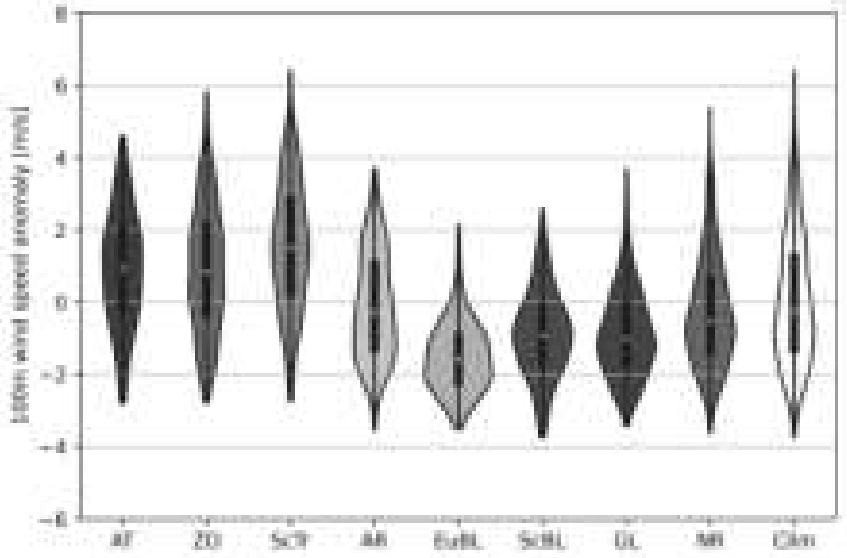

Figure 25: Violins showing the wind speed anomalies in Germany for the seven weather regimes as well as the no regime (NR) and the climatology (Clim) during DJF. The white dot marks the mean of the anomaly for the regime, the bold black bar marks the interquartile range, and the thin black bar marks the 1.5 interquartile range.

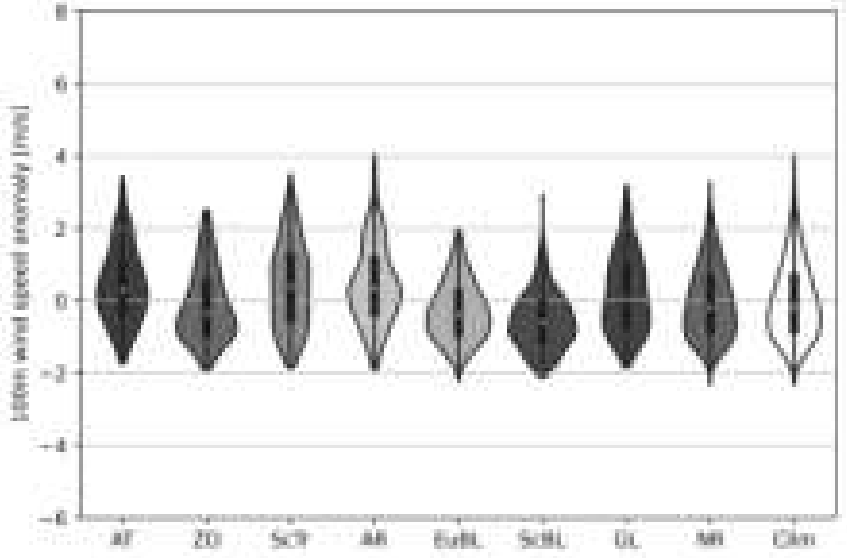

Figure 26: Violins showing the wind speed anomalies in Germany for the seven weather regimes as well as the no regime (NR) and the climatology (Clim) during JJA. The white dot marks the mean of the anomaly for the regime, the bold black bar marks the interquartile range, and the thin black bar marks the 1.5 interquartile range.

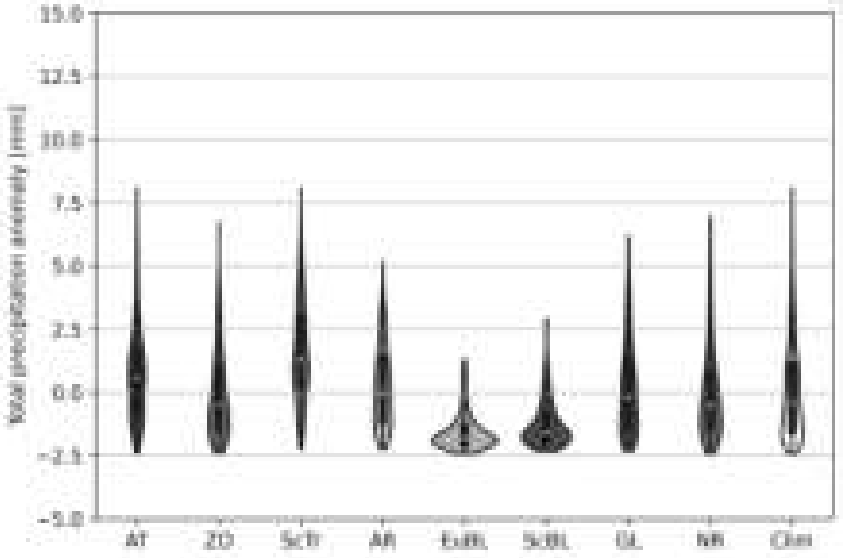

Figure 27: Violins showing the TP anomalies in Germany for the seven weather regimes as well as the no regime (NR) and the climatology (Clim) during DJF. The white dot marks the mean of the anomaly for the regime, the bold black bar marks the interquartile range, and the thin black bar marks the 1.5 interquartile range.

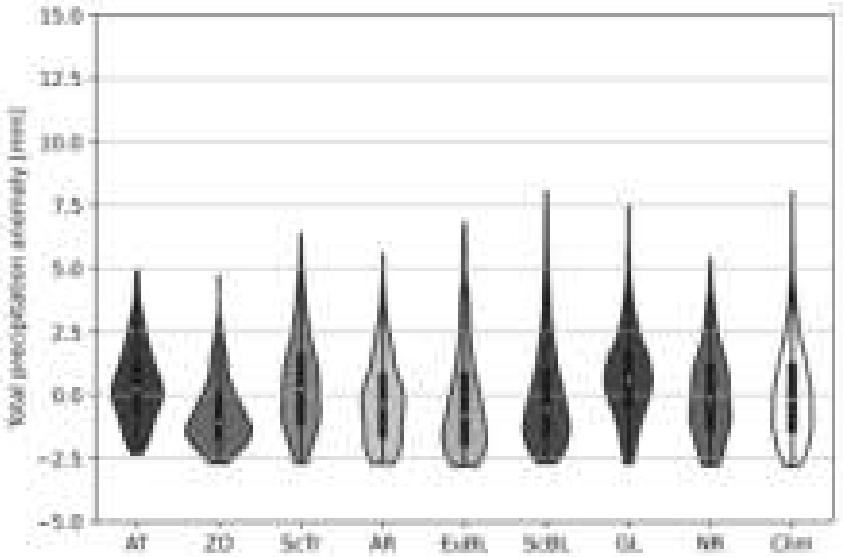

Figure 28: Violins showing the TP anomalies in Germany for the seven weather regimes as well as the no regime (NR) and the climatology (Clim) during JJA. The white dot marks the mean of the anomaly for the regime, the bold black bar marks the interquartile range, and the thin black bar marks the 1.5 interquartile range.

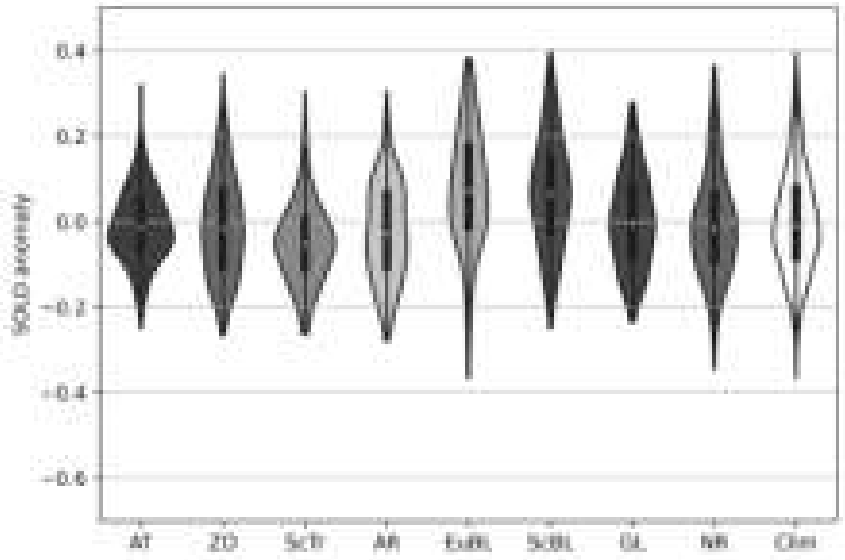

Figure 29: Violins showing the SOLD anomalies in Germany for the seven weather regimes as well as the no regime (NR) and the climatology (Clim) during DJF. The white dot marks the mean of the anomaly for the regime, the bold black bar marks the interquartile range, and the thin black bar marks the 1.5 interquartile range.

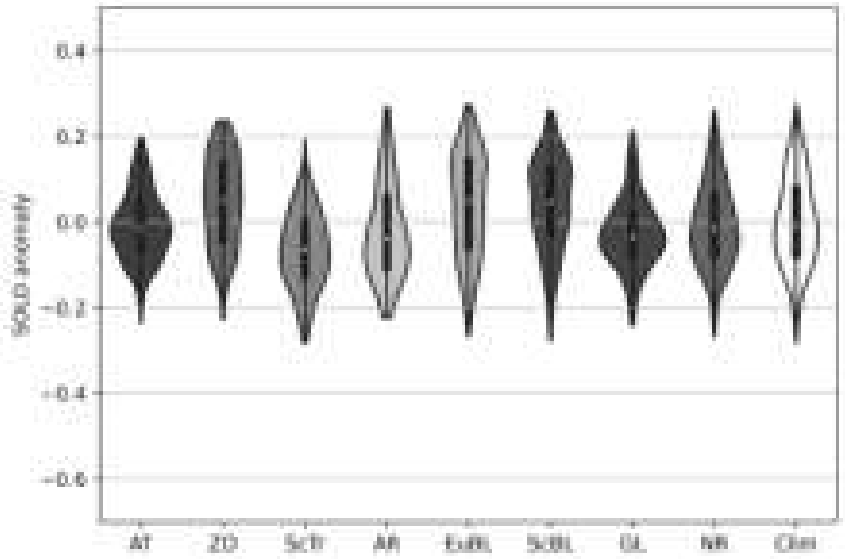

Figure 30: Violins showing the SOLD anomalies in Germany for the seven weather regimes as well as the no regime (NR) and the climatology (Clim) during JJA. The white dot marks the mean of the anomaly for the regime, the bold black bar marks the interquartile range, and the thin black bar marks the 1.5 interquartile range.

regime	AT	ZO	ScTr	AR	EuBL	ScBL	GL	NR	Clim
T2M median	3.01	3.068	1.200	-1.89	-1.43	-2.48	-2.34	0.02	0.18
T2M max	8.20	8.17	7.56	3.95	5.52	6.64	6.57	9.29	9.29
T2M min	-8.86	-8.34	-5.81	-9.32	-13.35	-14.32	-13.19	-13.65	-14.32
T2M range	17.06	16.51	13.37	13.27	18.87	20.96	19.76	22.94	23.61
T2M diff (%)	27.76	30.07	43.36	43.79	20.09	11.23	16.31	2.84	27.52
Wind median	0.93	0.84	1.49	-0.28	-1.61	-0.92	-1.03	-0.54	-0.25
Wind max	4.58	5.82	6.39	3.69	2.15	2.57	3.70	5.37	6.39
Wind min	-2.80	-2.79	-2.74	-3.54	-3.52	-3.74	-3.42	-3.63	-3.74
Wind range	7.38	8.61	9.13	7.24	5.67	6.32	7.11	8.99	10.13
Wind diff (%)	27.10	15.02	9.86	28.55	44.03	37.64	29.78	11.24	27.43
TP median	0.57	-0.49	1.28	-0.01	-1.81	-1.593	-0.20	-0.52	-0.41
TP max	8.06	6.74	8.07	5.17	1.29	2.891	6.16	6.96	8.07
TP min	-2.39	-2.39	-2.23	-2.23	-2.42	-2.32	-2.31	-2.42	-2.42
TP range	10.45	9.12	10.31	7.40	3.71	5.22	8.47	9.376	10.49
TP diff (%)	0.46	13.06	1.78	29.52	64.66	50.30	19.34	10.65	25.59
SOLD median	-0.02	-0.02	-0.05	-0.03	0.07	0.06	-0.00	-0.02	-0.01
SOLD max	0.32	0.35	0.30	0.30	0.38	0.40	0.28	0.36	0.40
SOLD min	-0.25	-0.27	-0.26	-0.28	-0.37	-0.25	-0.23	-0.35	-0.37
SOLD range	0.57	0.61	0.57	0.58	0.75	0.64	0.51	0.71	0.76
SOLD diff (%)	25.49	19.58	25.49	23.52	1.71	15.38	32.59	6.83	∅ 20.537

Table 1: Overview of the variability ranges of all seven weather regimes, the no regime (NR) and the climatology (Clim) for the four investigated variables of T2M, wind speed, TP and SOLD for Germany in DJF. The median, the maximum (max), the minimum (min) values are given and the absolute range between maximum and minimum is calculated as well as the reduction of range (diff %) compared to the range of the climatology. The value in that line for the climatology gives the average reduction of range for the seven weather regimes.

regime	**AT**	**ZO**	**ScTr**	**AR**	**EuBL**	**ScBL**	**GL**	**NR**	**Clim**
T2M median	0.093	1.33	-1.57	-1.62	0.99	1.43	-0.92	-0.40	-0.00
T2M max	6.21	6.46	4.27	5.32	8.43	7.30	5.27	6.56	8.43
T2M min	-4.26	-5.45	-5.36	-6.02	-5.16	-4.52	-5.73	-5.47	-6.02
T2M diff	10.47	11.91	9.63	11.35	13.59	11.71	11.00	12.03	14.45
T2M diff (%)	27.54	17.61	33.40	21.48	6.00	19.00	23.91	16.78	21.28
Wind median	0.31	-0.36	0.38	0.33	-0.38	-0.62	0.05	-0.18	-0.18
Wind max	3.42	2.51	3.48	4.05	1.94	2.91	3.19	3.29	4.05
Wind min	-1.71	-1.91	-1.85	-1.90	-2.20	-2.12	-1.84	-2.31	-2.31
Wind diff	5.13	4.41	5.33	5.95	4.14	5.03	5.03	5.60	6.36
Wind diff (%)	19.35	30.58	16.12	6.50	34.85	20.89	20.95	11.91	21.32
TP median	0.23	-1.07	0.24	-0.40	-0.80	-0.58	0.61	-0.14	-0.19
TP max	4.88	4.69	6.38	5.57	6.78	8.01	7.42	5.36	8.01
TP min	-2.33	-2.69	-2.69	-2.72	-2.80	-2.68	-2.70	-2.78	-2.80
TP diff	7.21	7.38	9.07	8.28	9.58	10.69	10.13	8.14	10.82
TP diff (%)	33.35	31.75	16.12	23.40	11.38	1.15	6.38	24.78	17.65
SOLD median	-0.02	0.05	-0.07	-0.04	0.05	0.05	-0.04	-0.02	-0.01
SOLD max	0.20	0.24	0.19	0.27	0.27	0.26	0.21	0.26	0.27
SOLD min	-0.24	-0.23	-0.28	-0.22	-0.26	-0.28	-0.24	-0.27	-0.28
SOLD diff	0.43	0.46	0.47	0.49	0.54	0.54	0.45	0.53	0.55
SOLD diff (%)	22.02	16.43	14.80	11.19	3.07	3.43	18.23	4.69	12.74

Table 2: Overview of the variability ranges of all seven weather regimes, the no regime (NR) and the climatology (Clim) for the four investigated variables of T2M, wind speed, TP and SOLD for Germany in JJA. The median, the maximum (max), the minimum (min) values are given and the absolute range between maximum and minimum is calculated as well as the reduction of range (diff %) compared to the range of the climatology. The value in that line for the climatology gives the average reduction of range for the seven weather regimes.

Erklärung

Ich versichere wahrheitsgemäß, die Arbeit selbstständig verfasst, alle benutzten Hilfsmittel vollständig und genau angegeben und alles kenntlich gemacht zu haben, was aus Arbeiten anderer unverändert oder mit Abänderungen entnommen wurde sowie die Satzung des KIT zur Sicherung guter wissenschaftlicher Praxis in der jeweils gültigen Fassung beachtet zu haben.

Karlsruhe, den 24.04.2024

(Judith Gerighausen)

Acknowledgement

First of all, I would like to thank Jun. Prof. Dr. Christian Grams for the opportunity to write my master's thesis in his working group. I would also like to thank him for the support I received after he left the KIT. Furthermore, I would like to thank my supervisors, Dr. Joshua Dorrington and Dr. Marisol Osman, who were always there to help me with advice and knowledge when I faced problems and questions. Without them, I would not have been able to finish my thesis. I want to thank all three of them for the many insightful and fruitful discussions on the topic of the thesis. I am very grateful to Josh, who helped me with his knowledge of Python and for his advice and commitment in the final phase of the thesis.

Next, I would also like to thank EnBW Energie Baden-Württemberg AG for the insights into the daily business of a large company heavily involved in the renewable energy sector.

Thanks to Prof. Dr. Peter Knippertz and Prof. Dr. Joaquim Pinto for supporting and correcting my master's thesis, even though the topic is outside their expertise.

I would also like to thank all the team members of the former young investigator group "Large-scale Dynamics and Predictability" at the IMKTRO as well as the head, Dr. Julian Quinting, and team members of the new young investigator group "Meteorological Data Science" for the warm welcome and the discussions, feedback and advice.

Last, I want to thank my parents for their tireless support throughout my entire studies.